

STEADY-STATE FLUORESCENCE ANISOTROPY AND NEUTRAL
LIPID, PHOSPHOLIPID, AND CERAMIDE COMPOSITION
OF NORMAL AND HEREDITARY LYSOSOMAL β -GLUCOSIDASE
DEFICIENT CULTURED HUMAN SKIN FIBROBLASTS

by

Ravi/Salgia

A Dissertation Submitted to the Faculty of the Graduate School
of Loyola University of Chicago in Partial Fulfillment
of the Requirements for the Degree of
Doctor of Philosophy
May, 1985

TABLE OF CONTENTS

	Page
ACKNOWLEDGMENTS	v
VITA	vi
LIST OF TABLES	vii
LIST OF ILLUSTRATIONS	ix
LIST OF ABBREVIATIONS AND SYMBOLS	xi
 Chapter	
I. INTRODUCTION	1
II. REVIEW OF RELATED LITERATURE	7
Gaucher Disease	7
Clinical Disease	7
Pathology and Pathogenesis	9
Diagnosis	10
Properties of β -Glucosidase	11
Lipid Abnormalities	14
Treatment	15
Membrane Fluidity	16
Concept of Membrane Fluidity	16
Techniques of Determining Membrane Fluidity.	21
NMR	21
ESR	22
Raman Spectroscopy	22
Fluorescence Spectroscopy	23
Steady-State Fluorescence Anisotropy	25
Theory	25
Fluidity Probes	30
Perylene	30
DPH	31
DPH in Biological Membranes	34
Abnormalities in Cultured Human	
Skin Fibroblasts	38
Lipid Composition of Cultured Human Skin	
Fibroblasts	41

TABLE OF CONTENTS.--Continued

Chapter	Page
III. MATERIALS AND METHODS	46
Cell Culture	46
Fluorescence Labeling of Cells	47
Fluorescence Anisotropy Measurements	48
Monensin Treatment and (³ H) Acetate Labeling of Fibroblasts	50
Lipid Isolation and Quantitation	50
Fatty Acid Analysis of Phospholipids and Cholesterol Ester	54
Hydrogenation	58
IV. RESULTS	60
Fluorescence of DPH Incorporation into Cells	60
Fluorescence Anisotropy of Normal and Diseased Cells	77
Neutral Lipid Content of Normal and Diseased Cells	84
Phospholipid Content of Normal and Diseased Cells	89
Ceramide Content of Normal and Diseased Cells	93
Effect of Monensin on Normal Fibroblast Lipids	93
Phospholipid and Cholesterol Ester Fatty Acid Analysis	98
Membrane Fluidity and Correlation with Various Lipid Ratios	107
V. DISCUSSION	110
Relevance of Membrane Fluidity	110
DPH Incorporation	110
Fluorescence Anisotropy	111
Cholesterol/Phospholipid and Cholesterol/ Sphingomyelin Ratios	113
Temperature Scans and Arrhenius Plots	116
Relevance of Neutral Lipid, Phospholipid, and Ceramide Composition of Fibroblasts	120
Neutral Lipid Composition	120
Phospholipid Composition	121
Ceramide Composition	123
Effects of Monensin	124
Fatty Acid Composition	125

TABLE OF CONTENTS.--Continued

Chapter	Page
VI. SUMMARY	128
BIBLIOGRAPHY	131

ACKNOWLEDGMENTS

The author wishes to thank Dr. Abraham Rosenberg, Department of Biochemistry and Biophysics, for his continuous patience, assistance and guidance in directing this work. Special note of gratitude is also expressed to Dr. Mariko Saito for considerable assistance and helpful criticism of the project involved. Gratitude is also expressed to the committee members for helpful guidance and assistance in completing this work.

Thanks are also expressed to all the members in the laboratory, including Dr. Mitsuo Saito, Dr. Robert Durrie, Mike Hogan and Gisela Kindel for assistance and constructive criticism. The assistance of Russell Beckley in performing the ceramide analysis is gratefully acknowledged. The careful typing/word processing of this dissertation by Joan Allman is also gratefully acknowledged.

Finally, the author wishes to thank his parents and family for their continuous patience, understanding and support while completing this dissertation.

VITA

Ravi Salgia, son of Dr. and Mrs. K. M. Salgia, was born in Indore, India on June 1, 1960. He was graduated from Maine Township High School South in Illinois in June, 1977, where he was the recipient of several awards in science, mathematics and language. From 1977 to 1981 he attended Loyola University of Chicago and graduated summa cum laude with a Bachelor of Arts degree in Chemistry and Bachelor of Science degree in Mathematics and Biology including awards in mathematics and chemistry. In August, 1981, he was admitted to Loyola University of Chicago, Stritch School of Medicine, as a candidate for combined M.D.-Ph.D. degree and received a Medical Science Fellowship Award in support of his graduate studies. He began research training in the laboratory of Dr. Abraham Rosenberg in June of 1982.

LIST OF TABLES

Table		Page
1.	Gaucher Disease--Clinical Subtypes	8
2.	Fluorescence Polarization (25°C) of Cultured Human Skin Fibroblasts from Various Diseases . .	40
3.	Neutral Lipid Composition of Cultured Human Skin Fibroblasts	42
4.	Phospholipid Composition of Cultured Human Skin Fibroblasts	43
5.	Glycosphingolipid and Ceramide Composition of Cultured Human Skin Fibroblasts	44
6.	Conditions for Gas Liquid Chromatography Using a Perkin-Elmer Model 990 G-C	57
7.	Fluorescence Polarization (P), Anisotropy (r_S), Membrane Viscosity (η), Limiting Anisotropy (r_∞), and Order Parameter (S) of Normal and Gaucher Diseased Fibroblasts at 25°C	78
8.	Slope, Ordinate Intercept, and Correlation Coefficient Derived from Arrhenius Plots of Log (Fluorescence Anisotropy) versus [Temperature (°K)] ⁻¹	85
9.	Neutral Lipid Composition of Normal and Gaucher Diseased Fibroblasts	88
10.	Phospholipid Composition of Normal and Gaucher Diseased Fibroblasts	92
11.	Ceramide Composition of Normal and Gaucher Diseased Fibroblasts	96
12.	Effect of Monensin on Normal Fibroblast (GM 3440) Lipids	97

LIST OF TABLES.--Continued

Table		Page
13.	Fatty Acid Composition of Phosphatidylcholine of Fibroblasts	99
14.	Fatty Acid Composition of Phosphatidylethanolamine of Fibroblasts	101
15.	Fatty Acid Composition of Sphingomyelin of Fibroblasts	102
16.	Fatty Acid Composition of Phosphatidylserine of Fibroblasts	104
17.	Fatty Acid Composition of Phosphatidylinositol of Fibroblasts	105
18.	Fatty Acid Composition of Cholesterol Ester of Fibroblasts	106
19.	Fluorescence Anisotropy Values with the Relevant Lipid Ratios	108
20.	Passaging of Fibroblasts and Its Effect on Fluorescence Anisotropy	117

LIST OF ILLUSTRATIONS

Figure		Page
1.	Schematic representation of hydrolysis of glucosylceramide into glucose and ceramide by β -Glucosidase	12
2.	Schematic representation of a cholesterol molecule with a phospholipid in a lipid bilayer	19
3.	Schematic representation of various parameters utilized in fluorescence polarization	26
4.	(a) The molecular structure of perylene. (b) The disk-like shape assumed for perylene	32
5.	The molecular structure of DPH with the rod-like shape	32
6.	The absorption and fluorescence spectrum of DPH in various organic solvents	33
7.	Time course study of fluorescence anisotropy of Normal, NmlF, and Gaucher, InG 1247, fibroblasts .	61
8.	Relative fluorescence intensity versus time of incubation with DPH for normal, NmlF, and Gaucher, InG 1247, fibroblasts	62
9.	Emission spectra of DPH in normal infant fibroblasts (GM 302A).	63
10.	Excitation spectra of DPH in normal infant fibroblasts (GM 302A)	65
11.	Emission spectra of DPH in type 1 infant Gaucher fibroblasts (GM 4394)	67
12.	Emission spectra of DPH in type 2 infant Gaucher fibroblasts (InG 1247)	69
13.	Emission spectra of DPH in type 3 juvenile Gaucher fibroblasts (JuvG)	71
14.	Emission spectra of DPH in normal adult fibroblasts (GM 3440)	73

LIST OF ILLUSTRATIONS.--Continued

Figure		Page
15.	Emission spectra of DPH in type 1 adult Gaucher fibroblasts (AdG 1470)	75
16.	Temperature dependence of anisotropy of DPH in normal infant and Gaucher diseased fibroblasts--type 2 and type 3	80
17.	Temperature dependence of anisotropy of DPH in normal adult and type 1 adult Gaucher diseased fibroblasts	81
18.	Arrhenius plots of DPH in normal infant and Gaucher diseased fibroblasts--type 2 and type 3	82
19.	Arrhenius plots of DPH in normal adult and type 1 Gaucher diseased fibroblasts	83
20.	HPTLC chromatogram of neutral lipids isolated from fibroblasts	86
21.	HPTLC chromatogram of phospholipids isolated from fibroblasts	90
22.	HPTLC chromatogram of ceramide containing lipid fraction, isolated from fibroblasts	94

LIST OF ABBREVIATIONS AND SYMBOLS

ACAT	acyl coenzyme A:cholesterol O-acyltransferase
AdG 119a	type 1 adult Gaucher disease fibroblast cell line
AdG 1470	type 1 adult Gaucher disease fibroblast cell line
C/PL	cholesterol/phospholipid ratio
CPM	counts per minute
C/SPM	cholesterol/sphingomyelin ratio
$C_{(r_s)}$	parameter relating to molecular shape and the location of the transition dipoles of the fluorophore
DPH	1,6-diphenyl-1,3,5-hexatriene
DPM	disintegrations per minute
D_w	wobbling diffusion constant
ESR	electron spin resonance
$\bar{\eta}$	apparent microviscosity
F	total fluorescence intensity
GbO _{se3} Cer	globotriaosylceramide or trihexosylceramide
GbO _{se4} Cer	globotetraosylceramide or tetrahexosylceramide
GD _{1a}	disialosylgangliotetraosylceramide
GD ₃	disialosyllactosylceramide
GlcCer	glucosylceramide
GM ₁	sialosylgangliotetraosylceramide
GM ₃	sialosyllactosylceramide
GM ₂	sialosylgangliotriaosylceramide

LIST OF ABBREVIATIONS AND SYMBOLS.--Continued

GM 302A	normal infant fibroblast cell line
GM 877	type 2 infant Gaucher disease fibroblast cell line
GM 3440	normal adult fibroblast cell line
GM 4394	type 1 infant Gaucher disease fibroblast cell line
GRSL	mouse thymus derived ascitic leukemia
HMG-CoA	3-hydroxy-3-methylglutaryl coenzyme A
HPTLC	high performance thin-layer chromatography
I_{\parallel}	emission intensity parallel to analyzer
I_{\perp}	emission intensity perpendicular to analyzer
$I_{h,v}/I_{h,h}$	transmission efficiency correction factor of the emission monochromator
$I_{v,h}$	fluorescence intensity with polarizers horizontal
$I_{v,v}$	fluorescence intensity with polarizers parallel
InG 1247	type 2 infant Gaucher disease fibroblast cell line
JuvG	type 3 juvenile Gaucher disease fibroblast cell line
LacCer	lactosylceramide
LM cells	transformed murine fibroblast cell line
M_r	molecular weight
NBD-phospholipid	1-acyl-2-N-4-nitrobenzeno-2-oxa-1,3-diazole-amino-caproyl phospholipid
Nm1F	normal adult fibroblast cell line
NMR	nuclear magnetic resonance
P	steady-state fluorescence polarization
PBS	phosphate buffered saline
PC	phosphatidylcholine

LIST OF ABBREVIATIONS AND SYMBOLS.--Continued

PE	phosphatidylethanolamine
ϕ	apparent rotational relaxation time
PI	phosphatidylinositol
PS	phosphatidylserine
r_f	dynamic part of r_s
r_s	steady-state fluorescence anisotropy
r_0	limiting value of r_s at infinite viscosity
r_∞	static part of r_s or limiting fluorescence anisotropy
S	order parameter
σ	experimentally determined value used in evaluating D_w
SD	standard deviation
SEM	standard error of mean
SPM	sphingomyelin
SPM/PC	sphingomyelin/phosphatidylcholine ratio
SPM/PL	sphingomyelin/phospholipid ratio
T	absolute temperature ($^{\circ}$ K)
τ	excited state lifetime of the fluorescent probe
θ_c	half angle of cone
TNBS	2,4,6-trinitrobenzene sulfonate

CHAPTER I

INTRODUCTION

Hereditary lysosomal β -glucosidase deficiency (Gaucher disease), an autosomal recessive disorder, is characterized by accumulation of the neutral glycosphingolipid glucosylceramide in the reticuloendothelial system--especially spleen, liver and the bone marrow (Brady & Barranger, 1983). This lipid abnormality arises due to a deficiency of the specific catabolic lysosomal enzyme glucosylceramide: β -glucosidase (glucocerebrosidase) (Brady et al., 1965). Clinically, Gaucher disease can be subclassified into three types: type 1 (adult non-neuronopathic form), type 2 (infantile neuronopathic form) and type 3 (juvenile subacute neuronopathic form) (Desnick, 1982).

Although the lipid accumulated in the reticuloendothelial system for all three types of Gaucher disease is glucosylceramide, the lipid content in cultured human skin fibroblasts from subjects with Gaucher disease is somewhat different. In cultured fibroblasts, there is not an increased amount of glucosylceramide, but there is a higher quantity of the ganglioside sialosylgangliotriaosylceramide (GM₂) in type 2 Gaucher disease as compared to normal, and sialosylgangliotetraosylceramide (GM₁), and disialosylgangliotetraosylceramide (GD_{1a}) in type 1 Gaucher disease (Saito & Rosenberg, 1984a,b). At this moment, however, it is not known if there are any other lipid

abnormalities in cultured human skin fibroblasts from Gaucher disease.

Since there is alteration of lipid composition in Gaucher disease, it might be suspected that there may be alteration in membrane fluidity of diseased fibroblast membranes. This alteration in membrane fluidity could possibly have a significant role in the pathogenesis and pathology of Gaucher disease. Therefore, it is important to understand membrane structure in terms of membrane fluidity.

Fluidity specifically refers to properties of the hydrophobic region of the membrane--in particular the physical state of the fatty acyl chains comprising the bilayer structure (Stubbs & Smith, 1984). Phenomena relevant to fluidity encompass unsaturation and acyl chain length of fatty acids, lateral and rotational mobility of phospholipids, changes in the frequency of trans-gauche isomerization of contiguous methylene groups (C-C bonds) in the phospholipid acyl chains, changes in the swinging motion of the phospholipid fatty acyl chains, changes in phospholipid headgroup conformation, changes in interaction of cholesterol with other lipids, and changes in the interaction of proteins with lipids (Houslay & Stanley, 1982).

There are both chemical and physical effectors which can be natural modulators of membrane lipid fluidity. The main chemical modulators are cholesterol content as compared with phospholipids, the degree of unsaturation of phospholipid acyl chains, the content of sphingomyelin as compared with phosphatidylcholine, and the content of membrane proteins as compared with lipids. The physical effectors of lipid fluidity are temperature, pressure, pH, membrane potential and Ca^{2+} concentration (Shinitzky & Yuli, 1982).

There are several techniques for investigating fluidity of biological membranes--including nuclear magnetic resonance (NMR), electron spin resonance (ESR), and steady-state fluorescence polarization. NMR is useful in determining motional characteristics of each C-H bond along the acyl chain. ESR gives information on degree of disorder in membranes. Steady-state fluorescence polarization gives information regarding overall motion of acyl chains adjacent to the fluorescent probe (Stubbs & Smith, 1984). Fluorescence polarization has several advantages over ESR and NMR in that it can be readily applied to complex systems such as biological membranes, the polarized signal is highly sensitive and reproducible, and the data obtained are promptly interpretable. It is to be noted, however, that the common steady-state approach is an overall average of all membranes involved and does not reflect only one aspect of the membranes (Shinitzky & Barenholz, 1978).

A considerable number of fluorescent probes are available for fluidity measurements; however, 1,6-diphenyl-1,3,5-hexatriene (DPH) is the most efficient probe for investigating membrane fluidity of biological systems. DPH is a hydrophobic, rigid, elongated molecule with cylindrical symmetry (Zannoni et al., 1983). It aligns normally with its long axis parallel to the lipid chains in the middle of the membrane bilayer (Lentz et al., 1976a,b). It has no fluorescence signal when in an aqueous environment; however, when incorporated into the lipid bilayer, it displays a sharp fluorescence signal (Shinitzky & Barenholz, 1974). It is to be noted, again, that DPH can only give some average value of fluidity in the heterogenous lipid

domains present in cell membranes (Shinitzky & Barenholz, 1978).

Owing to its many useful and well-defined properties, DPH has been used to evaluate membrane fluidity, via fluorescence polarization, of a variety of cell membranes. In particular, it has been used on cultured human skin fibroblasts from subjects with various diseases with interesting results. Using DPH as a probe in whole cells or plasma membranes of familial hypercholesterolemia (Haggerty et al., 1978), and Duchenne dystrophy plasma membranes (Shaw et al., 1983), it has been shown that there is an increased fluidity of membranes as compared to matched controls; whereas, whole cells or plasma membranes of cultured fibroblasts from Huntington's disease do not exhibit any significant difference in membrane fluidity from controls (Lakowicz & Sheppard, 1981; Schroeder et al., 1984). Even though this technique of determining membrane fluidity has not been used considerably in various diseases with membrane lipid abnormalities in cultured human skin fibroblasts, it has a useful potential in investigating inherited metabolic disorders-- especially Gaucher disease.

It is known that glycosphingolipids are altered in Gaucher disease; however, since glycosphingolipids make up only approximately 3 percent of total cell membrane lipids (Dawson et al., 1972), they possibly do not contribute significantly to the average membrane fluidity. The major contributors to the lipid fluidity in membranes seem to be cholesterol and phospholipids (Borochoy et al., 1977; Cooper et al., 1977, 1978; Shinitzky & Barenholz, 1978; Van Blitterswijk et al., 1981). It is not known at present whether the content of neutral lipids and phospholipids are also altered along with glycosphingolipids

in cultured skin fibroblasts from subjects with Gaucher disease.

It is known that cholesterol and phospholipids may be altered in red blood cells of patients with Gaucher disease (Balint et al., 1963). Along with this, there is evidence that phospholipid content may be abnormal in Gaucher fibroblasts. When glucosyl (³H) ceramide (labeled in sphingosine as well as fatty acid moiety) was administered to normal human fibroblasts, it was catabolized, and subsequently, (³H) labeled products were found in phospholipids--especially sphingomyelin, phosphatidylcholine and phosphatidylethanolamine; whereas, in Gaucher cells, this process is greatly reduced (Barton & Rosenberg 1974).

Any neutral lipid or phospholipid abnormality in Gaucher disease would imply that even though there is only a deficiency of one enzyme, namely β -glucocerebrosidase, leading to decreased catabolism of glucosylceramide, the metabolic consequences are more widely felt, affecting a variety of membrane lipids. Such a finding has not been reported and would be of great interest.

The objective of this dissertation is to evaluate the effect of hereditary lysosomal β -glucosidase deficiency in cultured human skin fibroblasts on membrane fluidity and correlate this with changes in lipid composition. Membrane fluidity in Gaucher disease and in normal controls has been evaluated via the technique of steady-state fluorescence anisotropy using the fluorescent hydrocarbon probe 1,6-diphenyl-1,3,5-hexatriene. In addition, neutral lipid and phospholipid composition of fibroblasts were evaluated and correlated with membrane fluidity measurements. Attention has been given to cholesterol,

sphingomyelin and phosphatidylcholine content of normal and diseased fibroblasts and their fatty acid composition. The amount of ceramide has also been determined in normal and Gaucher diseased fibroblasts. The effect of monensin on fibroblast lipids was also investigated and correlated in terms of Gaucher disease lipid abnormalities.

CHAPTER II

REVIEW OF RELATED LITERATURE

Gaucher Disease

Clinical Disease

Gaucher disease is an autosomal recessive lysosomal disorder characterized by deficiency of β -glucocerebrosidase activity with accumulation of neutral glycosphingolipid glucosylceramide in the reticuloendothelial system and possibly brain. Clinically, Gaucher disease can be classified into three major types as shown in Table 1 (Desnick et al., 1982). Type 1, chronic nonneuronopathic or "adult" form of the disease is the most prevalent (1/2000 in United States Ashkenazi Jews) among patients with Gaucher disease. These patients usually exhibit signs of hepatosplenomegaly along with symptoms of thrombocytopenia, anemia, and bone involvement. Of the three types of the disease, type 1 is probably least in degree of severity. However, in each individual patient, the severity of the disease varies greatly along with the age of the individual (Brady & Barranger, 1983).

Type 2 Gaucher disease, also known as acute neuronopathic or "infantile" form of the disease is the most severe in its presentation. It is usually apparent before six months of age and fatal by two years. Not only is there massive hepatosplenomegaly but the nervous system is heavily involved--exhibiting muscular hypertonicity

TABLE 1.--Gaucher Disease--Clinical Subtypes

Clinical Features	Type 1-Non-Neuronopathic	Type 2-Acute Neuronopathic	Type 3-Subacute Neuronopathic
Clinical onset	Childhood/adulthood	Infancy	Childhood
Hepatosplenomegaly	+	+	+
Hematologic complications Secondary to hypersplenism	+	+	+
Skeletal deterioration	+	+	+
Neurodegenerative course	-	+++	++
Death	Variable	By 2 yr	2nd-4th decade
Ethnic predilection	Ashkenazi Jewish	Panethnic	Swedish

Adapted from Desnick et al., (1982).

and persistent retroflexion of the head. This form of the disease is not restricted to Jewish individuals but is pan-ethnic (Brady & Barranger, 1983).

Type 3 Gaucher disease, also known as subacute neuronopathic or "juvenile" form of the disease is also characterized by hepatosplenomegaly and neurologic involvement. The neurologic damage, however, occurs later in life and is usually fatal (Brady & Barranger, 1983). The ethnic predilection seems to be of non-Jewish individuals involving Swedish people in particular Norrbottnian types (Svennerholm et al., 1982).

Pathology and Pathogenesis

One of the pathognemonics for Gaucher disease is the presence of Gaucher cells in the reticuloendothelial system. These are large macrophage like cells, having a "wrinkled tissue paper" appearance (Brady & Barranger, 1983). Along with the presence of Gaucher cells in the reticuloendothelial system, there is a considerable hepatosplenomegaly encountered in this disease. Along with this, there is a frequent skeletal involvement in patients with types 1 and 3 Gaucher disease. In types 2 and 3 Gaucher disease, there is extensive neurologic involvements. The cranial nerves and brainstem are heavily involved. There is minimal storage of glucocerebroside in ganglion cells, but there is loss of neurons, neuronophagia, and deposition of this neutral glycolipid in periadventitial cells.

It seems logical to conclude that most of the pathology that arises in Gaucher disease is due to an accumulation of glucosylceramide

in the reticuloendothelial system. It seems, however, that there is some accumulation of glucosylsphingosine in the brains of patients with Gaucher disease leading to the acute severity of type 2 and type 3 disease (Nilsson & Svennerholm, 1982). This then could be similar to Krabbe's disease in which there is a deficiency of the enzyme galactocerebroside: β -galactosidase leading to an increased amount of galactosylceramide and the toxic galactosphingosine (Suzuki & Suzuki, 1983). The involvement of glucosylsphingosine in the pathogenesis of Gaucher disease is a very preliminary finding and would have to be reconfirmed.

Diagnosis

There are several ways to arrive at the diagnosis of Gaucher disease once it is suspected in a particular patient. Not only is there hepatosplenomegaly and Gaucher cells in the bone marrow aspirates but there is elevation of serum nontartrate-inhibitable acid phosphatase. The most sensitive method of establishing the diagnosis is the measurement of the enzyme β -glucosidase in tissues obtained from liver biopsies, cultured amniotic fluid cells, white blood cell preparations or cultured skin fibroblasts (Brady & Barranger, 1983).

There are various methodologies, utilizing various substrates and activators, available to assay the activity of β -glucosidase. The two most widely used substrates are radioactively labeled glucosylceramide and the artificial fluorogenic substrate 4-methylumbelliferyl- β -glucoside. The labeled glucosylceramide is the best method for diagnosis of the disease; however, 4-methylumbelliferyl- β -glucoside

is an inexpensive and efficient way to measure the β -glucosidase activity (Daniels & Glew, 1982). There are several activators for this enzyme which can be used in the assay of β -glucosidase activity--including negatively charged phospholipids, gangliosides, sodium taurocholate, Triton X-100, oleic acid and cutscum (Mueller & Rosenberg, 1977, 1979; Wenger & Olson, 1981; ; Saito et al., 1982; Vaccaro et al., 1983). It should be noted that there is reduced activity of β -glucosidase in samples obtained from patients with Gaucher disease as compared to matched controls. Currently, there is no way to distinguish the clinical severity of the disease from the enzyme activity data (Mueller & Rosenberg, 1979; Wenger & Olson, 1981).

Properties of β -Glucosidase

The reaction catalyzed by β -glucosidase for cleaving glucosylceramide into glucose and ceramide is as shown in Figure 1. The structural gene for β -glucosidase has been assigned to chromosome 1 using somatic cell hybridization techniques (Shafit-Zagardo et al., 1981). Using artificial substrate 4-methylumbelliferyl- β -D-glucoside, two major β -glucosidases have been identified--"acid" and "neutral" β -glucosidase (Shafit-Zagardo et al., 1980). In cultured human skin fibroblasts, there is only the "acid" form of β -glucosidase present in the lysosomes. Also, in the various Gaucher subtypes only the acid isozyme is deficient in fibroblasts and other organs (Desnick, 1982). This acid form of β -glucosidase is a lysosomal membrane-bound enzyme or is very hydrophobic requiring detergents for optimum activity (Mueller & Rosenberg, 1979; Desnick, 1982; Desnick et al., 1982).

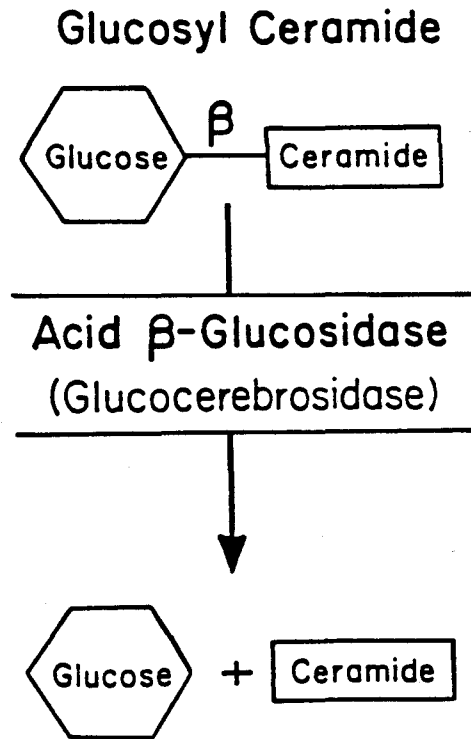


Fig. 1. Schematic representation of hydrolysis of glucosylceramide into glucose and ceramide by β -Glucosidase. Adapted from Desnick (1982).

Using an antibody raised against placental glucocerebrosidase, cultured skin fibroblasts have been identified to have two major isozymes with molecular weights (M_r) of 63,000 and 56,000 and a minor component with M_r of 61,000 (Ginns et al., 1982). In type 1 Gaucher disease, the major β -glucosidase isozyme exhibits M_r of 56,000 with minor bands occurring at M_r of 63,000 and 61,000. There is cross-reacting material to M_r of 63,000 in type 3 disease; whereas, there is no crossreacting material found in type 2 Gaucher fibroblasts (Ginns et al., 1983).

There seems to be no difference in the pH optima, and K_m values of β -glucosidase in Gaucher fibroblasts (all three types) as compared to normal cells. However, the V_{max} for β -glucosidase from Gaucher fibroblasts is decreased as compared to normals (Desnick et al., 1982; Saito et al., 1982). Based on inhibitor and activator studies, the active site of the enzyme has been proposed to have three components (Gatt et al., 1982):

1. Catalytic site--which recognizes β -glucosyl moiety of its substrates and conduritol β -epoxide (an irreversible inhibitor of the enzyme).
2. Substrate binding site--which binds the aglycon moiety of inhibitors and substrates.
3. Hydrophobic site--which can bind lipids and other hydrophobic molecules such as phosphatidylserine, glucosylsphingosine and taurocholate.

Ho and O'Brien (1971) and Peters et al. (1977) have also identified a heat stable, soluble, acidic glycoprotein devoid of β -glu-

cosidase activity as an activator protein for β -glucosidase.

Lipid Abnormalities

Glucosylceramide--consisting of sphingosine, a long-chain fatty acid, and glucose--is considerably elevated in the reticuloendothelial system of patients with Gaucher disease. The amount of glucocerebroside in normal human spleens varies between 60-280 μ g/gram wet weight (Brady & Barranger, 1983). The values in Gaucher spleens are considerably raised ranging from 3-40.5 mg per gram wet weight. Along with increased glucosylceramide, there are increased amounts of GM₃ but not lactosylceramide in the spleen (Kuske & Rosenberg, 1972). The amount of glucosylceramide in brain of Gaucher disease patients is somewhat variable. In type 2 disease, there are increased amounts of glucosylceramide in gray matter (Sudo, 1977); this lipid is also increased in plasma in Gaucher disease (Vance et al., 1969). However, there may not be any increased amounts of glycolipids in brains from types 1 and 3 patients.

The accumulated glucosylceramide in the reticuloendothelial system arises from several sources. Erythrocytes, which contain glucosylceramide (GlcCer), lactosylceramide (LacCer), trihexosylceramide and globoside, are catabolized via the reticuloendothelial system; thereby, originating a source for GlcCer. The turnover of leukocytes is the major source of GlcCer along with LacCer (Suzuki, 1982). Also, it seems probable that this lipid could also arise from normal cellular turnover (Brady & Barranger, 1983).

Unlike the accumulation of above mentioned lipids in the

reticuloendothelial system, cultured human skin fibroblasts from Gaucher disease have a different lipid accumulation as compared to normal fibroblasts. There is a higher quantity of the ganglioside sialosylgangliosylceramide (GM₂) in type 2 Gaucher disease as compared to normal, and sialosylgangliosylceramide (GM₁) and disialosylgangliosylceramide (GD_{1a}) in type 1 Gaucher disease (Saito & Rosenberg, 1984a,b). Along with this, there is evidence that phospholipid content may be abnormal in Gaucher fibroblasts. When glucosyl (3H) ceramide (labeled in sphingosine as well as fatty acid moiety) was administered to normal human fibroblasts, it was catabolized, and subsequently, (3H) labeled products were found in phospholipids--especially sphingomyelin, phosphatidylcholine and phosphatidylethanolamine; whereas, in Gaucher cells, this process was greatly reduced (Barton & Rosenberg, 1974). Cholesterol levels in a Gaucher fibroblast cell line has been determined and there seems to be no difference as compared with normal cells (Warren et al., 1976).

There also seems to be an indication that erythrocyte neutral lipid and phospholipids may be altered in Gaucher disease. Balint et al. (1963) have shown that there is probably a decreased amount of cholesterol, cephalins (PS & PE), and sphingomyelin in an adult patient with Gaucher disease as compared to normal adult erythrocyte lipids.

Treatment

Recently, a bone-marrow transplant was performed in a patient with type 3 Gaucher disease with no change in clinical status post-

transplantation. The plasma glucocerebroside concentration, however, returned to normal implying that the enzymatic abnormality in hemato-poietic cells in Gaucher disease may be correctable by bone-marrow transplantation (Rappeport & Ginns, 1984).

Several trials of enzyme replacement via placental β -glucosidase infusion have also been tried but to no avail since the enzyme was not taken up by the appropriate macrophage. Thus, the only treatment available for Gaucher disease is in the form of supportive treatment (Brady & Barranger, 1983).

Membrane Fluidity

Concept of Membrane Fluidity

Fluidity specifically refers to the physical state or dynamics of the fatty acyl chains comprising the membrane bilayer (Chapman, 1983; Stubbs & Smith, 1983). Phenomena relevant to fluidity encompass unsaturation and acyl chain length of fatty acids, lateral and rotational mobility of phospholipids, changes in the frequency of trans-gauche isomerization of C-C bonds of methylene groups in the phospholipid acyl chains, changes in the swinging motion of the phospholipid fatty acyl chains, changes in phospholipid headgroup conformation, changes in interaction of cholesterol with membrane lipids, and changes in the interaction of proteins with lipids (Shinitzky & Barenholz, 1978; Houslay & Stanley, 1982; Chapman, 1983; Stubbs & Smith, 1983).

The extent of unsaturation and chain length of fatty acids is an important determinant of biomembrane fluidity. The exact correlation with membrane fluidity to the unsaturation and fatty acyl

chain length seems varied and complex depending on the number, position, and type of the double bonds, the nature of membrane under investigation and the method used to probe the membrane physical state (Stubbs, 1983). Using model membranes it has been concluded that the effect of increasing the unsaturation results in only a slight increase in acyl chain mobility (Stubbs & Smith, 1984). A decrease in double bond index/saturated fatty acid ratio, defined as:

$$\frac{(\text{number unsaturated mol} \times \text{no. double bonds})}{(\text{number saturated mol})}$$

has been used as a chemical measure of membrane fluidity (Farias et al., 1975). This assumption is valid when other parameters such as cholesterol/phospholipid ratio remain constant and the fatty acid double bonds of compared membranes have the same cis structure (Castuma & Brenner, 1983). Studies with biological membranes show that a significant change in level of unsaturation and chain length does not necessarily lead to changes in fluidity as measured with fluorescent or ESR probes (Gilmore et al., 1979a,b; Herring et al., 1980; Stubbs et al., 1980; Stubbs & Smith, 1984).

Various head groups, lateral and rotational mobility, trans-gauche isomerization, and fatty acyl chain swinging motions of phospholipids are relevant to membrane fluidity. Similar to the data for unsaturation and fatty acyl chain length mentioned previously, the influence of the phospholipid head groups on the motion of the acyl chain (and thus fluidity) in cell membranes is complex and varied (Gilmore et al., 1976b; Stubbs, 1983). Although it is clear that the head group region has an influence on acyl chain motion, it is

difficult to assess its importance in biological membranes due to the fact that the phospholipids in membranes have differing fatty acid composition (Stubbs, 1983). With respect to the lateral and rotational mobility, trans-gauche isomerization and fatty acyl chain swinging motions of phospholipids, it is known that they all can influence the membrane fluidity; however, the fluorescence method utilized in this dissertation cannot discern the effects of these parameters (Stubbs, 1983; Stubbs & Smith, 1984).

Cholesterol is a principal modulator of membrane fluidity. This lipid has rigid, planar, wedge-shaped structure which orients perpendicular to the membrane bilayer, with the hydroxyl group in the vicinity of the fatty acyl carbonyls, as shown in Figure 2 (Houslay & Stanley, 1982; Stubbs, 1983). Cholesterol has the ability to condense phospholipid bilayers (Kitajima & Thompson, 1977). A variety of physical techniques have demonstrated that cholesterol has a small fluidizing effect below the phase transition temperature (gel phase) of phospholipids and a large rigidizing effect above this temperature (Oldfield & Chapman, 1972; Kawato et al., 1978; Chapman, 1983). Presence of large amounts of cholesterol prevents lipid chain crystallization and removes phase transition characteristics (Chapman, 1983). In general, therefore, the effect of cholesterol in biological membranes is to decrease fluidity (Kawato et al., 1978; Hildenbrand & Nicolau, 1979). The cholesterol/phospholipid ratio has been used to represent the amount of order (rigidity, inverse of fluidity) in membranes (Shinitzky & Barenholz, 1978; Van Blitterswijk et al., 1981; Houslay & Stanley, 1982).

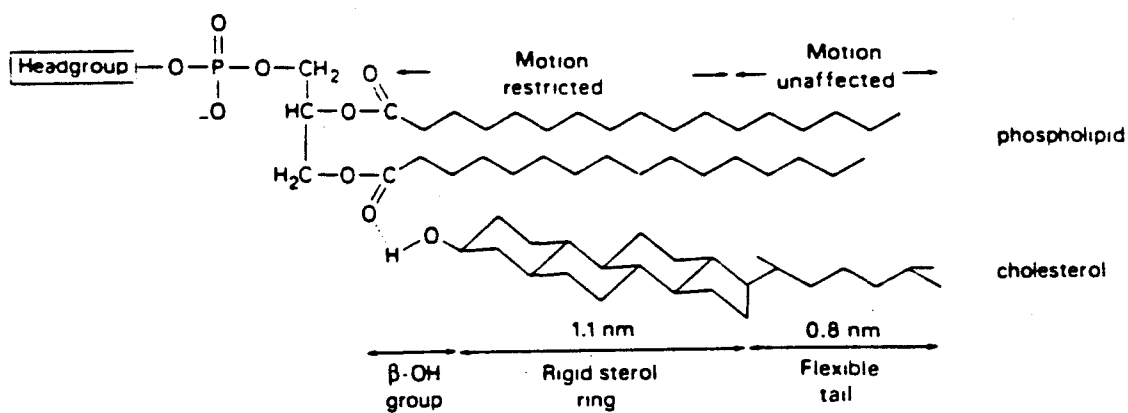


Fig. 2. Schematic representation of a cholesterol molecule with a phospholipid in a lipid bilayer. Adapted from Houslay and Stanley (1982).

Proteins also have translational and rotational movements in the membrane. This has been investigated on the bacterial protein rhodopsin; where it was shown by electron spin resonance that proteins have specific rotational diffusion rates (Barrion et al., 1977) and, by fluorescence photobleaching recovery, that proteins have a specific lateral diffusion rates as well. The estimation of the contribution of membrane proteins to membrane fluidity depends on the type of membrane involved and the method used to determine membrane fluidity. In contrast to electron spin resonance and fluorescence photobleaching recovery, steady-state fluorescence anisotropy of proteins using the probe diphenylhexatriene gives virtually no contribution to fluidity in lymphoid, liver, hepatoma, and erythrocyte membranes (Van Blitterswijk et al., 1981).

Along with nature of fatty acyl composition, cholesterol, phospholipid structures, and proteins there are various physical effectors of lipid fluidity including pressure, pH, membrane potential, Ca^{2+} concentration and temperature (Shinitzky & Yuli, 1982). Of these, temperature plays an important role in membrane fluidity; and it can be generally stated that fluidity increases with increasing temperature and this corresponds to an overall increase in molecular motion throughout the membrane bilayer.

With respect to the effect of temperature on membrane fluidity, one can observe various phases of lipids as the temperature is varied in biological membranes (phase transition). This phase transition occurs at characteristic temperatures for a particular phospholipid species. Phase transition detects lipid phase separations in the

biological membranes, where lipid phase separation can be defined as spontaneous coexistence of membrane domains with different composition (Grant, 1983). The two phases for phospholipids are: crystalline-solid state where the acyl chains of phospholipid are fully extended parallel to the bilayer with their C-C bonds in the all-trans position, and liquid-crystalline (fluid) state in which there are rotational isomers about the C-C bonds of the fatty acyl chains (Houslay & Stanley, 1982).

At the lipid phase transition temperature the bilayer changes from solid to the fluid state. The nature of the headgroup, the length of the fatty acyl chain, and the number, position and type of double bonds in the acyl chain of a phospholipid determine its phase transition temperature (Houslay & Stanley, 1982; Chapman, 1983). It should also be noted, however, that since cholesterol increases the rigidity of fluid-state lipid bilayers and increases the fluidity of solid-state lipid bilayers, it may tend to cancel or dampen the lipid phase transition in biological membranes (Oldfield & Chapman, 1972; Houslay & Stanley, 1982; Chapman, 1983). As a theoretical consideration, the evidence for lateral phase separation comes from studies showing non-linear Arrhenius plots of the temperature dependence of fluorescence anisotropy (Shinitzky & Yuli, 1982; Stubbs, 1983).

Techniques for Determining Membrane Fluidity

NMR

Nuclear magnetic resonance (NMR) studies of membrane structure employ the (^2H) NMR method with high field superconducting magnets to

investigate the organization of polar headgroups and backbone and hydrocarbon chain regions in phospholipids and glycolipids (Smith & Oldfield, 1984). With the deuterated species of interest incorporated into the membrane, motional characteristics of C-H bond can be determined by this technique. From this, it has been possible to obtain an order profile for phospholipid acyl chains (Seelig & Seelig, 1977). The drawback of performing NMR studies is the expensive apparatus required and the need to synthesize specially deuterated lipids in relatively large amounts. Also the calculations and assumptions in deriving the rate of motion are very complex and may be less reliable than those obtained in fluorescence studies (Stubbs, 1983).

ESR

Electron spin resonance of a nitroxide probe in the membrane bilayer can give information on relaxation (mobility) of the probe, orientation of the probe with respect to its environment, concentration of the label in a given phase, order of the system, and the lateral diffusion of the probe in the plane of the bilayer (Jain & Wagner, 1980). Much of the information on membrane structure has arisen from ESR studies. The theory behind ESR is similar to that of NMR and has been reviewed extensively elsewhere (Cantor & Schimmel, 1980). One of the major drawbacks for this technique is similar to that of NMR in which the equipment is expensive. Also, one needs to synthesize spin-labeled probes, and the probe perturbs the system.

Raman Spectroscopy

Raman spectroscopy is a relatively new technique for deter-

mining acyl chain motions in membranes by looking at the vibrational states of C-C bonds. Even though it is a non-perturbing technique which has provided information on model lipid bilayers, interference from bonds in the phosphate and protein regions occurs with biological membranes (Stubbs, 1983). It is still in its infancy stages and much more experimentation is needed in order for this to be a major tool in membrane fluidity investigations of biological membranes.

Fluorescence Spectroscopy

Fluorescence spectroscopy is based on the phenomenon that when a fluorophore is excited by light, the fluorophore absorbs the energy and emits photons of lower energy. This phenomenon then can be adapted to give information on the orientation or range and rate of motion of the fluorophore and its adjacent environment. There are several fluorescence techniques which give information on lipid rotational motion including fluorescence photobleaching recovery and fluorescence anisotropy.

In fluorescence photobleaching recovery, membrane lipids are labeled with a fluorescent compound and a small area of labeled cell is exposed to a laser pulse. The time dependence of fluorescence recovery in the bleached area is followed over time and from it lateral diffusion constants can be obtained (Golan et al., 1983; Stubbs, 1983). This has been used to determine lateral diffusion of proteins as well as lipids and the way lipid-protein interaction may occur (Golan et al., 1984; Spiegel et al., 1984).

Fluorescence anisotropy techniques can include both time-

resolved decay and steady-state anisotropy measurements. Time-resolved fluorescence anisotropy decay gives information on the range of acyl motion and the rate of motion. Investigators using the fluorescent probe DPH, a rod shaped molecule which aligns parallel to the acyl chains in the middle of the membrane bilayer, have assumed the range of acyl chain motion to be contained within a volume approximating to a cone which has an half angle (θ_c) (Kawato et al., 1977; Kinoshita et al., 1977; Kawato et al., 1978)--also known as "wobbling-in-cone" model. From the half angle, one can determine the order parameter (S):

$$S = [1/2 \cos \theta_c (1 + \cos \theta_c)]^2.$$

The rate of probe motion is described as the wobbling diffusion constant (D_w), which is obtained from the apparent rotational relaxation time (ϕ): $D_w = \sigma/\phi$, where σ has been experimentally determined (Kawato et al., 1978; Stubbs et al., 1984).

Steady-state fluorescence anisotropy gives information on rate of rotational diffusion of the probe as well as range of motion of the probe (Van Blitterswijk et al., 1981; Stubbs & Smith, 1984). Steady-state fluorescence measurements give information on the microviscosity as well as the order parameter in relation to decay measurements--to be discussed in the next section in considerable detail. Fluidity parameters of lipids in biomembranes are usually determined via this method and the information obtained is an overall average of all lipid domains present in cell membranes. Fluorescence anisotropy measurements have several advantages over ESR and NMR in that it can be readily applied to complex systems such as biological mem-

branes, the polarized signal is highly sensitive and reproducible, and the data obtained are promptly interpretable (Shinitzky & Barenholz, 1978). Whereas, fluorescence anisotropy decay measurements take longer and require complex apparatus and analysis (Stubbs, 1983).

Steady-State Fluorescence Anisotropy

Theory

When a fluorophore is incorporated into biomembranes and it is excited by a continuous source of plane polarized light (along z-axis in figure 3), the steady state fluorescence anisotropy (r_s) and polarization (P) can be determined by the emission intensities through an analyzer oriented parallel ($I_{||}$) and perpendicular (I_{\perp}) to the direction of polarization of the excitation light. Generally, the emission is detected at a right angle to the excitation, and the direction of polarization of $I_{||}$ is along z-axis and I_{\perp} is along y-axis in the figure. From this, the values for fluorescence polarization and anisotropy can be calculated as:

$$P = \frac{I_{||} - I_{\perp}}{I_{||} + I_{\perp}} \quad (1)$$

$$r_s = \frac{I_{||} - I_{\perp}}{I_{||} + 2I_{\perp}} = \frac{2P}{3 - P} \quad (2),$$

where the range of P is $-1/3 < P < 1/2$ and r_s is $-1/5 < r_s < 2/5$. The total fluorescence intensity (F) can be calculated as:

$$F = I_{||} + 2I_{\perp} \quad (3).$$

From the steady-state fluorescence anisotropy determinations of the membrane in question, there are two ways to evaluate and interpret membrane fluidity. One interpretation is that the anisotropy reflects

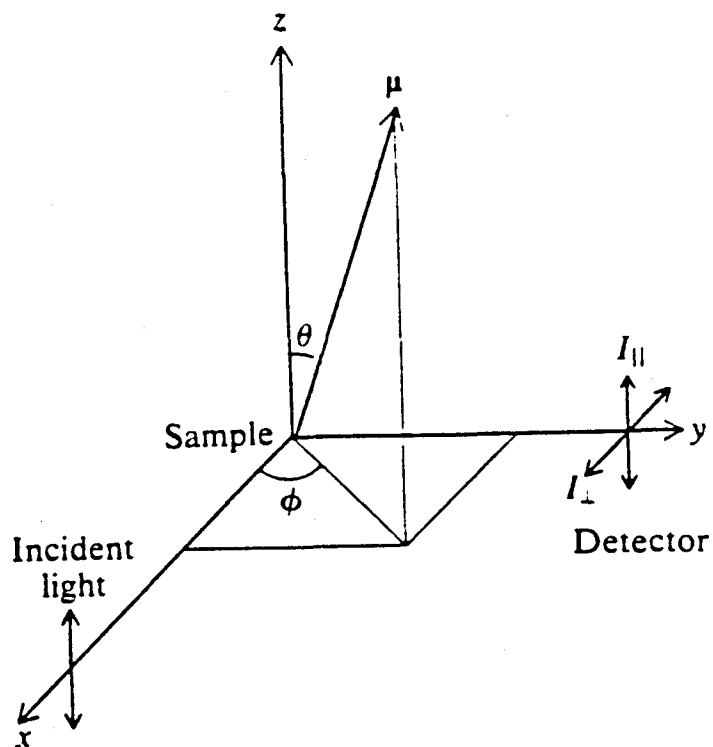


Fig. 3. Schematic representation of various parameters utilized in fluorescence polarization. Adapted from Cantor and Schimmel (1980).

the rate of rotational diffusion of the probe, or microviscosity. Note that the average fluidity of the membranes can then be calculated as the reciprocal of the apparent microviscosity ($\bar{\eta}$). The apparent microviscosity of the membrane interior is estimated by comparing the fluorescence anisotropy in the system with that observed in a macroscopic isotropic system (reference mineral oil) and applying the classical hydrodynamic system of Perrin to yield the Perrin equation:

$$\bar{\eta} = C_{(r_s)} T \tau \left(\frac{r_0}{r_s} - 1 \right)^{-1} \quad (4),$$

where $C_{(r_s)}$ is a parameter which relates to the molecular shape and the location of the transition dipoles of the fluorophore as expressed in the determined anisotropy (r_s) values, T is the absolute temperature, τ is the excited state lifetime of the probe, and r_0 is the limiting value of r_s at infinite viscosity. The units for $\bar{\eta}$ is dyne-cm⁻² which is defined as 1 P (poise) (Shinitzky & Barenholz, 1978).

The values for $C_{(r_s)}$, r_0 and τ can be determined for the individual probe in question. However, the values for DPH, a widely used and efficient probe, have been determined to yield $r_0 = 0.362$ and $C_{(r)} T \tau$ remains relatively constant in liposomes and model membranes yielding a value of 2.4 poise for temperatures between 0-40°C (Shinitzky & Barenholz, 1978). From this, an approximate value of $\bar{\eta}$ can be calculated for DPH in membranes to yield:

$$\bar{\eta} = \frac{2.4 r_s}{0.362 - r_s} = \frac{2P}{0.46 - P} \quad (5).$$

It can be seen from this modified empirical Perrin equation that as the value of anisotropy increases, the apparent microviscosity increases and, thus, the fluidity decreases.

From the microviscosity, phase transitions and thus phase separation in lipids can be determined by the Arrhenius plot of $\log \bar{\eta}$ versus $1/T$. If there are any phase separations of lipid domains, the Arrhenius plot will be non-linear; whereas, if there is a straight line in the Arrhenius plot, it implies that there are no phase transitions of the lipid under investigation and thus the steady-state fluorescence polarization technique cannot detect phase separations of lipid domains (Shinitzky & Barenholz, 1978).

One of the major assumptions in the Perrin type calculations for apparent microviscosity is that the probe is localized in an isotropic medium; whereas, membranes have an anisotropic environment. Although the apparent microviscosity calculated may not be absolute, it is useful in comparing membrane fluidities. The second interpretation of the steady-state fluorescence anisotropy data comes from time-resolved fluorescence polarization decay measurements. From this, it was interpreted that it is mainly the degree to which the fluorophore rotations are restricted by the molecular packing of the lipids (a static factor), rather than its rotational rate (a dynamic factor), which determines the steady-state fluorescence anisotropy in lipid membranes. Thus, r_s can be resolved into a static part r_∞ (proportional to the square of lipid order parameter), and a dynamic parameter r_f (related to the rotational relaxation time of the fluorophore--which in turn is proportional to the microviscosity) (Van Blitterswijk et al., 1981; Pottel et al., 1983). As an equation,

$$r_s = r_f + r_\infty \quad (6).$$

Also, for the probe DPH, the limiting fluorescence anisotropy, r_∞ ,

is proportional to the square of the lipid order parameter, S

$$r_{\infty}/r_0 = S^2 \quad , \quad 0 < S < 1 \quad (7)$$

where r_0 is the fluorescence anisotropy value in the absence of a rotational motion of the probe and is 0.362 for DPH in biological membranes.

From experimental data for the steady state fluorescence anisotropy (r_s) and the limiting fluorescence anisotropy (r_{∞}) of a variety of artificial and biological membranes, an empirical relationship can be arrived:

$$r_{\infty} = \frac{4}{3}(r_s) - 0.10 \quad (8)$$

in the region $0.13 < r_s < 0.28$ --which is the value for most biological membranes. From equations 7 and 8, the order parameter can be calculated

$$S_{DPH} = \left(\frac{4}{3} \frac{r_s}{r_0} - 0.28 \right)^{1/2} \quad (9).$$

As can be seen from equation (9), as the anisotropy increases, so does the order parameter.

It is believed by Van Blitterswijk et al. (1981) that the structural order of membrane lipids is related to the degree of molecular packing. Lipid fluidity may then be defined as the reciprocal of the lipid structural order parameter (S_{DPH}) rather than apparent microviscosity. The physical state of the biological membrane can thus be suitably described by the order parameter (Pottel et al., 1983). In this theory, also, lateral phase separation can be determined by the non-linear Arrhenius plots of the steady-state fluorescence anisotropy versus the temperature (Stubbs, 1983).

Although the apparent microviscosity is not in an absolute scale and the lipid order parameter (S_{DPH}) only takes into account the static component of r_s , both of these parameters can be considered to define the inverse of lipid fluidity. It is not certain at this point which interpretation of steady-state fluorescence anisotropy data is appropriate; however, they both imply that an increase in steady-state anisotropy value of the membrane is due to a decrease in membrane fluidity (Castuma & Brenner, 1983).

Fluidity Probes

There are several probes utilized in studying membrane fluidity. Of the many examples, fluorescent probes can be divided into two major classes. The first class includes fluorescent compounds which can incorporate spontaneously into a well defined lipid region of membranes--thus, directly reflecting the membrane fluidity from its fluorescence anisotropy values. The other class includes fluorescent dyes which are covalently attached to fatty acids or phospholipids (Shinitzky & Barenholz, 1978). Examples of the first class include 1,6-diphenyl-1,3,5-hexatriene (DPH) and perylene; whereas, examples of the latter class include parinaric acid and its phospholipid derivatives, 1-acyl-2-N-4-nitrobenzeno-2-oxa-1,3-diazole-amino-caproyl phospholipid (NBD-phospholipid), and DL-12-(9-anthroyl) stearic acid. In the context of membrane fluidity, the most efficient probes are perylene and DPH and thus shall be discussed in some detail.

Perylene

Perylene is a flat aromatic molecule with an approximate shape

of a disk with a diameter of 0.8 nm, as shown in Figure 4 (Zannoni et al., 1983). The absorption and emission spectrum of perylene overlap somewhat and exhibit a good mirror symmetry. It is a stable fluorophore with a considerably shorter fluorescence decay time of $\tau_0 = 7.2\text{ns}$; whereas τ_0 for DPH = 11.4 ns. Also, the excited state lifetime of perylene is much more sensitive to temperature or fluidity changes --thus, this probe is used similar to DPH in high fluidity systems (Shinitzky & Barenholz, 1978).

DPH

DPH is one of the most useful and efficient probes for studying membrane fluidity. It is a rigid, rod shaped molecule, approximately 1.3 nm long, with cylindrical symmetry, as shown in Fig. 5 (Zannoni et al., 1983). DPH absorbs light in near uv and emits with very high quantum yield in the blue region of visible spectrum. The absorption spectrum of DPH in various organic solvents is shown in Figure 6. It can be noted that the absorption spectrum changes as the polarity of the solvent changes. The absorption maximum occurs around 355 nm with an extinction coefficient of $80,000\text{ M}^{-1}\text{cm}^{-1}$ (Shinitzky & Barenholz, 1978). In contrast to the absorption spectrum, the emission spectrum of DPH changes very little with a change in solvent. Particularly, the emission maximum is relatively insensitive to changes in polarity, viscosity and temperature (Zannoni et al., 1983). The absorption and emission spectra do not show a good "mirror symmetry." This probe in membranes has a high and constant value of r_0 of 0.362 and a fluorescence decay time of $\tau_0 = 11.4\text{ ns}$.



Fig. 4. (a) The molecular structure of perylene. (b) The disk-like shape assumed for perylene. Adapted from Zannoni et al. (1983).

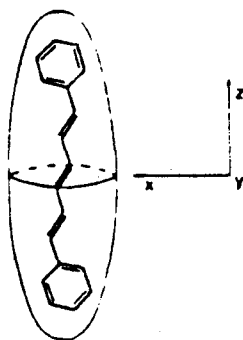


Fig. 5. The molecular structure of DPH with the rod-like shape. Adapted from Zannoni et al. (1983).

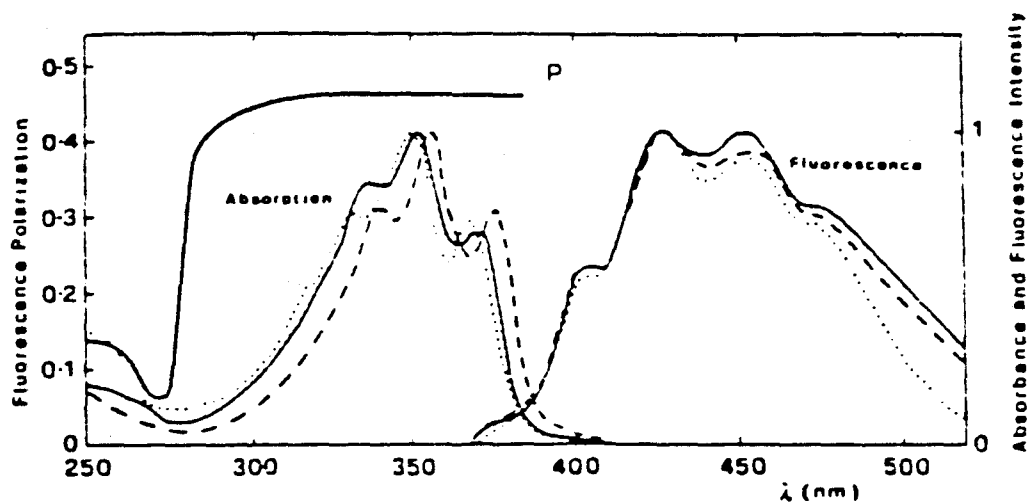


Fig. 6. The absorption and fluorescence spectrum of DPH in various organic solvents: ethanol (—); dioxane (---); hexane (···). Also shown is the polarization of fluorescence as a function of wavelength determined in polypropylene glycol at $T = -50^{\circ}\text{C}$. Adapted from Zannoni et al. (1983).

There are certain favorable properties of DPH which allow it to be an excellent membrane fluidity probe. It has no fluorescence signal when in an aqueous environment; however, when incorporated into the lipid bilayer, it displays a sharp fluorescence signal (Shinitzky & Barenholz, 1974, 1978). Its high extinction coefficient and fluorescence quantum yield allow the detection of a fluorescence signal even at very low concentration (approximately $1\mu\text{M}$). The separated absorption and emission reduce the possibility of energy transfer between DPH molecules and facilitate the elimination of excitation light scattering. The rod like shape aligns itself normally with the long axis parallel to the lipid chains (Lentz et al., 1976a,b).

One of the more debated questions regarding the probe DPH is its location in the membrane bilayer. Owing to its property that DPH in bilayers is similar to that in apolar organic solvents, and it is relatively insoluble in water implies that DPH is located in the hydrocarbon region of the bilayer. The orientation of the long axis of DPH is believed to be parallel to that of the lipid chains (Lentz et al., 1976a,b; Thulburn, 1981; Zannoni et al., 1983). Once DPH has been incorporated into the bilayer, it partitions equally well into fluid or solid lipid domains (Lentz et al., 1976a,b). The derived fluidity represents the weight average of all lipid domains (Shinitzky & Barenholz, 1978).

DPH in Biological Membranes

DPH has been extensively used as a probe in model membranes such as liposomes and micelles as well as biological membranes. With

respect to the biological membranes, DPH has been used both in isolated cell membranes and in intact cells. When DPH is introduced into various membrane lipids of intact cells, the dye is dissolved in the surface membrane lipid layer within minutes (Shinitzky & Barenholz, 1978). The fluorescence of the labeled cells is initially confined to the plasma membrane; however, with time the probe molecules partition into the cell inner membranes until an equilibrium distribution is reached. Pagano et al. (1977) have shown using autoradiographic methods that DPH, when incubated with intact fibroblasts locates itself not only on the cell surface membrane but also in the cytoplasmic regions. It should be noted, however, in this method the labeled cells are treated with cross-linking agents and ethanol, and the exposure time is days or weeks. The conditions are non-physiological and thus may increase the rate of partitioning of the probe. Also, Bouchy et al. (1981) have analyzed the evolution of DPH fluorescence polarization following incubation in living cells. They found a decrease of r_s and r_∞ with time, a decrease not present in isolated plasma membranes. This is also questionable since Haggerty et al. (1977) found no difference between plasma membrane and cell microviscosity using fibroblasts. However, it is important to note that the fluidity of the whole cell gives physiologically important information which may be used in comparing disease states with normal controls. One can also determine the lipid fluidity in plasma membranes of intact cells by selective quenching (Grunberger et al., 1982).

As stated previously, the steady-state fluorescence anisotropy using DPH has been measured in diseased states and there are several

lipid abnormalities which correlate with an altered anisotropy values. It is known that the cholesterol/phospholipid ratio is related to the inverse of fluidity. In red cells of patients with liver disease, the cholesterol/phospholipid (mol/mol) ratio is increased to 1.0-1.6 from normal values of 0.9-1.0 with the concomitant decrease in membrane fluidity in the diseased state (Cooper et al., 1972, 1978; Owen et al., 1982). As another example, the cholesterol/phospholipid ratio is decreased in mouse thymus derived ascitic leukemic (GRSL) cells as compared to normal thymocytes (GRSL = 0.22-0.30, normal thymocyte = 0.37). This is correlated with the increased fluidity observed in the GRSL cells ($\bar{\eta}_{GRSL} = 1.73P$, $\bar{\eta}_{thymocyte} = 3.24P$) (Van Blitterswijk et al., 1977). Also, the cholesterol/phospholipid ratio is significantly elevated (0.52 ± 0.045 versus 0.129 ± 0.012) in cord mononuclear leukocytes as compared to adult cells and this is again correlated with increased microviscosity values (polarization values of 0.339 ± 0.030 versus 0.186 ± 0.019) (Neufeld & Carbo, 1984).

Another factor important in fluorescence anisotropy values is the sphingomyelin to phosphatidylcholine ratio. There is an increase in the phosphatidylcholine/sphingomyelin (mol/mol) ratio in sheep red blood cells treated with EGTA as compared to non-treated red blood cells (0.14 ± 0.01 versus 0.030 ± 0.005); this increase in phosphatidylcholine/sphingomyelin ratio is concomitant with an increase in lipid fluidity ($(r_o/r_s - 1)^{-1}$ values at 25°C of 2.22 ± 0.004 versus 2.58 ± 0.004). In this study, however, there was no increase in the ratio of cholesterol/phospholipid noted (Borochoy et al., 1977). Also, the microviscosity of erythrocyte membranes from patients with

abetalipoproteinemia was increased compared to normal erythrocytes (\bar{n} acanthocyte = 4.01 - 4.14, \bar{n} normal = 3.2 \pm 0.1P) which then is explained in terms of an excess amount of sphingomyelin in acanthocyte membranes with a concomitant increase in the sphingomyelin/phosphatidylcholine ratio (0.84 \pm 0.08 in normals, 1.45-1.61 in acanthocytes) (Cooper et al., 1977). Van Blitterswijk et al. (1981) have also stated that sphingomyelin/total phospholipid ratio is an important determinant in fluidity of membranes. They show that for certain membranes, cholesterol/phospholipid ratios remain constant but there is an altered structural order parameter; and this could be due to an altered sphingomyelin/phospholipid ratio. The authors stipulate that the sphingomyelin/phospholipid ratio is directly proportional to the order parameter (and thus inversely to fluidity).

It is interesting to note that cholesterol/sphingomyelin ratio may also be important since it has been theoretically proposed that cholesterol tightly associates with sphingomyelin (Patton, 1970). The existence of a strong preferential interaction between cholesterol and sphingomyelin has been proven in artificial membranes (Barenholz & Thompson, 1980). At this moment, the exact ratio of cholesterol/sphingomyelin has not been correlated with any fluidity change, but the literature does point to it (Barenholz et al., 1981; Barenholz & Thompson, 1980; Van Blitterswijk et al., 1981).

When cholesterol/phospholipid ratio and sphingomyelin/phosphatidylcholine ratio are constant but there is an altered membrane fluidity, the double bond index/saturated fatty acid ratio can be correlated with the changes in fluidity. A decrease in this ratio

leads one to conclude that there might be a decrease in lipid bilayer fluidity (Farias et al., 1975). As an example, this has been done with liver microsomal membranes from guinea-pigs on a fat-free diet in which there was a decrease in membrane fluidity with no change in cholesterol/phospholipid ratio. However, there was a decrease in the double bond index/saturated fatty acid ratio corresponding to the decreased membrane fluidity.

It is known that certain organisms can adapt to changes in their environmental temperature by altering their lipid composition and a constant lipid fluidity is maintained--termed homeoviscous adaptation. Cultured cells have a limited ability to exhibit the property of homeoviscous adaptation. A transformed murine fibroblast cell line, LM cells, grown in a defined synthetic medium with supplements of choline or its analogues N,N'-dimethylethanolamine or N-monomethyl-ethanolamine, was able to maintain plasma membrane fluidity constant by altering the degree of saturation of acyl chains in all classes of phospholipids. Only an ethanolamine supplement caused a decrease in the fluidity of the plasma membrane; again, alterations in the fatty acid composition of phospholipids was seen (Schroeder, 1978). This method of supplementation cannot be used to assess any changes in fluidity but it is a useful means of manipulating membrane lipid composition and testing for the sensitivity of membrane probes to changes in their lipid environment (Houslay & Stanley, 1982).

Abnormalities in Cultured Human Skin Fibroblasts

Owing to its many useful and well defined properties, DPH

has been used to evaluate membrane fluidity, via fluorescence anisotropy, of a variety of cell membranes. In particular, it has been used on cultured human skin fibroblasts from subjects with various diseases with interesting results. This information is summarized in Table 2.

As shown in Table 2, there is decreased polarization value in fibroblasts obtained from homozygous familial hypercholesterolemia as compared to controls in both the intact cells and plasma membranes. It is interesting to note that there is no difference in the polarization values of intact fibroblasts as compared with plasma membranes. Shaw et al. (1983) have shown that the difference or no difference observed between the total cell membrane fluidity and plasma membrane fluidity could be due to the way a plasma membrane is prepared. They seem to suggest that the method of membrane preparation is an essential step in determining membrane fluidity. Using a sucrose-step gradient, they have isolated plasma membranes from fibroblasts obtained from normal subjects as well as fibroblasts from subjects with Duchenne muscular dystrophy; and on these isolated membranes, membrane fluidity measurements using DPH revealed an increased fluidity of membranes as compared to matched controls. Fluidity in Huntington disease fibroblasts has also been evaluated and there is no difference observed between controls and diseased membranes--either in intact cells, plasma membranes, microsomes or mitochondrial membranes. Even though this technique of determining membrane fluidity has been used only in a few disease states using cultured human skin fibroblasts, it has a

TABLE 2.--Fluorescence Polarization (25°C) of Cultured Human Skin Fibroblasts from Various Diseases

Fluorescence Polarization				
Description of Various Cell Lines	Intact Cells	Plasma Membranes	Other Organelles	Ref.
1. a. Normal Control				
Caucasion (n=2)	0.242 \pm 0.003	0.242 \pm 0.013		Haggerty et al. (1978)
Negro (n=4)	0.238 \pm 0.005	0.259 \pm 0.011		
b. Homozygous familial hypercholesterolemia (n=4)	0.206 \pm 0.006	0.208 \pm 0.011		
2. a. Control, 22°C (n=9)		0.306 \pm 0.016		Shaw et al. (1983)
b. Duchenne dystrophy fibroblasts, 22°C (n=9)		0.289 \pm 0.008		
3.*** a. Control (n=10)	0.2639 \pm 0.0085			Beverstock & Pearson (1981)
b. Huntington fibroblasts (n=11)	0.2625 \pm 0.0179			
4.*** a. Control (n=9,8,8)		0.299 \pm 0.010	0.308 \pm 0.010*	Schroeder (1984)
			0.266 \pm 0.011**	
b. Huntington fibroblasts (n=9,8,8)		0.301 \pm 0.006	0.313 \pm 0.007* 0.278 \pm 0.012**	

Values represent mean \pm standard deviation.

*microsomes; **mitochondria; ***mean \pm standard error of mean.

very useful potential in investigating inherited metabolic disorders --especially Gaucher disease.

Lipid Composition of Cultured Human Skin Fibroblasts

It is important to know the composition of lipids in fibroblasts in order to correlate this with the membrane fluidity measurements. The amount of neutral lipids have been determined in normal human cultured skin fibroblasts and the major constituents seem to be cholesterol, cholesterol esters, and triglycerides. Some of these values are summarized in Table 3 (Chatterjee et al., 1976).

Along with neutral lipids, one of the major lipid classes found in fibroblasts are the glycerophospholipids. In normal human fibroblasts, there seem to be several important phospholipids including sphingomyelin, phosphatidylcholine, phosphatidylinositol, phosphatidylserine, phosphatidylethanolamine, and some disphosphatidylglycerol and lysophosphatidylcholine (Chatterjee et al., 1976; Malkiewicz-Wasowicz et al., 1977; Schroeder et al., 1984). The results of a typical phospholipid analysis in cultured fibroblasts is presented in Table 4 (Schroeder et al., 1984).

Along with neutral lipids and phospholipids, fibroblasts also contain glycosphingolipids. Glycosphingolipids make up approximately 3 percent of total membrane lipids (Dawson et al., 1972). Glycosphingolipids can be divided up into neutral glycosphingolipids and acidic glycosphingolipids (gangliosides). Neutral glycosphingolipids in human fibroblasts consist of glucosylceramide (GlcCer), lactosylceramide (LacCer), globotriaosylceramide or trihexosylceramide

TABLE 3.--Neutral Lipid Composition of Cultured Human
Skin Fibroblasts

Neutral Lipid	μg lipid/mg of Protein
Cholesterol	30
Cholesterol Ester	18
Triglyceride	34

Data adapted from Chatterjee et al. (1976)

TABLE 4.--Phospholipid Composition of Cultured Human Skin Fibroblasts

Phospholipid	Composition (mole %)
Phosphatidylcholine	50 \pm 5
Phosphatidylethanolamine	19 \pm 3
Phosphatidylinositol + Phosphatidylserine	10 \pm 1
Sphingomyelin + Lysophosphatidylcholine	10 \pm 1
Cardiolipin	6 \pm 1

Data adapted from Schroeder et al. (1984). Number of samples was 4, values represent the mean \pm SEM.

TABLE 5.--Glycosphingolipid and Ceramide Composition of Cultured Human Skin Fibroblasts

Glycosphingolipid	nanomol/mg of protein	Ref.
Neutral Glycosphingolipid		
GlcCer	1.11 \pm 0.48	Saito & Rosenberg (1984a)
LacCer	0.41 \pm 0.17	
GbOse ₃ Cer	2.50 \pm 0.56	
GbOse ₄ Cer	1.40 \pm 0.29	
Gangliosides		
GM ₃	3.13 \pm 0.32	
GM ₂	1.10 \pm 0.16	
GM ₁	0.26 \pm 0.03	
GD ₃	0.71 \pm 0.24	
GD _{1a}	0.47 \pm 0.18	
Ceramide	5*	Chen et al. (1981)

*Concentration of ceramide expressed as μ g/mg of protein. Values represent the mean \pm SD.

(GbOse₃Cer) and globotetraosylceramide or tetrahexosylceramide (GbOse₄Cer). Gangliosides in fibroblasts consist of sialosyl lactosyl ceramide (GM₃), sialosyl gangliotriaosyl ceramide (GM₂), sialosyl gangliotetraosyl ceramide (GM₁), disialosyl lactosyl ceramide (GD₃), and disialosyl gangliotetraosyl ceramide (GD_{1a}) (Saito & Rosenberg, 1984a). The actual amount is represented in Table 5. Ceramide also is a constituent of cultured human fibroblasts and it has been determined that its concentration is approximately 5µg ceramide/mg of protein (Chen et al., 1981).

The lipid composition of cultured human fibroblasts may be altered by a disease process (due to an enzymopathy), such as Gaucher disease, or it may be altered by culturing the cells in the presence of chemical modulators. Monensin, a carboxylic monovalent cationophore, is such a chemical which can modify membrane lipid structure. It has been shown that monensin decreases activity of lysosomal enzymes by increasing the pH (Tartakoff, 1983) and may influence glycosphingolipid biosynthesis in the Golgi apparatus (Saito et al., 1984). Using monensin, Saito et al. (1984) have shown that there is increased accumulation of the neutral glycosphingolipids GlcCer and LacCer in normal cultured human skin fibroblasts; and this accumulation is increased in Gaucher diseased fibroblasts which then may be explained in terms of cation regulation. At this time, however, the effects of monensin on neutral lipids, phospholipids, and ceramide is not known.

CHAPTER III

MATERIALS AND METHODS

Cell Culture

Normal cultured human skin fibroblasts (Human Genetic Mutant Cell Repository GM 3440 [adult], GM 302A [infant]), type 1 Gaucher disease fibroblasts (GM 4394 [infant non-neuronopathic]), and type 2 Gaucher disease fibroblasts (GM 877 [infant neuronopathic]) were obtained from the Institute for Medical Research (Camden, N.J.). Other fibroblasts were obtained from Dr. David Wenger, University of Colorado Medical Center, Dr. A Beaudet, Baylor College of Medicine and Dr. A. Milunsky, E. K. Shriver Center (Waltham, Mass.)--type 1 Gaucher fibroblasts (AdG 1470, AdG 119a [adult non-neuronopathic]), type 2 Gaucher fibroblasts (InG 1247 [infant neuronopathic]), and type 3 Gaucher fibroblasts (JuvG [juvenile neuronopathic]). One normal adult fibroblast cell line was established from biopsy in our laboratory (Nm1F) (Barton & Rosenberg, 1974; Mueller & Rosenberg, 1977; Saito et al., 1984).

All cell culture was performed according to well established methods using 10 ml of growth medium containing 88% Dulbecco's modified Eagle's medium (GIBCO), 10% heat inactivated fetal calf serum (GIBCO, heated at 56°C for 30 min), and 2% penicillin-streptomycin (5000 I.U. and 5 mg/ml, respectively, Flow Laboratories) in 75-cm² plastic

tissue culture flasks (Falcon) at 37°C in a 5% CO₂ atmosphere in air. Change of media was performed every 5–6 days until the cells were confluent. Approximate time for confluency is 10–14 days after seeding of fibroblasts. Unless otherwise noted, fibroblasts were between the fifth and nineteenth passage in this study. Total cell protein was determined by the method of Hartree (1972).

Fluorescence Labeling of Cells

The fluorescent hydrocarbon 1,6-diphenyl-1,3,5-hexatriene (DPH, Aldrich) was used as a probe for monitoring the degree of fluidity of normal and diseased fibroblasts. Labeling of fibroblast membranes was done according to the modified procedures of (Shinitzky & Barenholz, 1974; Shinitzky & Inbar, 1974; Fuchs et al., 1975; Haggerty et al., 1978; Van Hoeven et al., 1979) where 2mM DPH in tetrahydrofuran was diluted 100-fold with vigorously stirred calcium and magnesium free phosphate buffered saline (PBS, pH 7.2) and was further stirred for 30 minutes under a nitrogen stream to evaporate the tetrahydrofuran. Confluent fibroblasts, in 75 cm² flasks, were then incubated with 10 ml of 20µM DPH for 1 hour; whereas, the controls were incubated with 10 ml of PBS for the same period of time at 37°C. After incubation, the cells were detached from the flask substratum, via trypsin (type III from bovine pancreas, Sigma) treatment (0.05% in PBS for 5 min), and the trypsin activity was neutralized by the growth media. The cells were recovered by centrifugation (500 xg, 5 min) and suspended in 2 ml of PBS and approximately 50 µl of it was taken to be counted in a hemocytometer (ultra plane Spotlite counting chamber,

S/P). The cells were again centrifuged and resuspended in PBS, using the appropriate volumes to get the same cell numbers for labeled and unlabeled cells ($\approx 1-5 \times 10^6$ cells/ml). These were then immediately used for fluorescence measurements.

For some of these cells, trypan blue exclusion test was also performed to check the viability of the fibroblasts. After the labeling of cells and collecting the suspension, 0.1ml of 0.01% trypan blue in PBS was added to the 1 ml suspension of cells and incubated for 1-5 min and the cells were counted with a hemocytometer. The percentage of viable cells is calculated as:

$$\% \text{ viable cells} = 100 \left[1 - \frac{\text{no. cells with trypan blue uptake}}{\text{total no. cells counted}} \right]$$

Fluorescence Anisotropy Measurements

Fluorescence anisotropy and intensity were measured with an MPF-44B Perkin-Elmer spectrofluorophotometer equipped with Polacoat polaroid polarizers and a thermostatically controlled cuvette holder attached to a Fisher Model 90 Refrigerated bath. Temperature was maintained by circulating water-methanol (1:1) through the cuvette chamber. The excitation wavelength used was 360 nm and emission wavelength of 426 nm with slits 5 nm each along with a filter cutoff of 390 nm. Fluorescence polarization (P) and anisotropy (r_s) is obtained from fluorescence measurements via the equations:

$$P = \frac{I_{v,v} - I_{v,h} (I_{h,v}/I_{h,h})}{I_{v,v} + I_{v,h} (I_{h,v}/I_{h,h})}$$

$$r_s = \frac{I_{v,v} - I_{v,h} (I_{h,v}/I_{h,h})}{I_{v,v} + 2I_{v,h} (I_{h,v}/I_{h,h})} = \frac{2P}{3-P}$$

where $I_{v,v}$ is the corrected fluorescence intensity with the polarizers

parallel (excitation and emission polarizers set both at 0°) and $I_{v,h}$ is the corrected fluorescence intensity with the polarizers horizontal (excitation polarizer set at 0° and emission polarizer at 90°). The factor in parenthesis, $I_{h,v}/I_{h,h}$ is the transmission efficiency correction factor of the emission monochromator both parallel and perpendicular to the grooves of the grating. The corrected fluorescence intensity was determined by subtracting the intensity of polarized light measured with unlabeled control cells from the intensity observed with the labeled cells. For each of the intensity measurements a 20 second integration is taken. For each experimental anisotropy, three independent readings were performed and averaged.

For the different cell lines, anisotropy measurements were performed at 25°C . In performing the temperature scan studies, the initial temperature was 4°C with an incremental increase of 4°C until 40°C was reached. The temperature was monitored inside the cuvette with an YSI thermistor probe.

From the fluorescence anisotropy (r_s) measurements the apparent microviscosity ($\bar{\eta}$) with units of Poise was calculated from the expression

$$\bar{\eta} = \frac{2.4 r_s}{0.362 - r_s}$$

as shown by Shinitzky and Barenholz (1978) and discussed in Review of the Related Literature. The order parameter values were calculated according to the procedure of Van Blitterswijk et al. (1981):

$$S = \left(\frac{4}{3} \frac{r_s}{0.362} - 0.28 \right)^{1/2}.$$

For the temperature scans, Arrhenius plots of $\log r_s$ versus $1/\text{tem-}$

perature ($^{\circ}$ K) were performed and analyzed for non-linear break points.

Monensin Treatment and (3 H) Acetate Labeling of Fibroblasts

Confluent fibroblasts (GM 3440, normal adult) were incubated with 1 μ M monensin (in ethanol, Calbiochem) in 10 ml culture medium for 18 hrs. Equal volumes of ethanol were added to cells not incubated with monensin according to Saito et al. (1984). Along with this, all the cells were incubated with (3 H) sodium acetate (New England Nuclear, specific activity of 685 mCi/mM). 50.0 μ Ci was used in 10 ml growth medium.

The amount of lipid was quantitated as described below by high performance silica gel G thin-layer chromatography (HPTLC). Radioactivity was determined by scraping each band of interest, transferring the samples into scintillation vials adding 5ml of Aquasol (New England Nuclear) and counting in a Beckman LS 1800 Scintillation Counter. External standards were established in the scintillation counter memory to determine the amount of quenching and counting efficiency; thus, from the actual counts per minute (cpm) the disintegration per minute (dpm) are reported.

Lipid Isolation and Quantitation

Confluent cells in 75 cm² culture flasks were washed with 5 ml cold PBS (4 $^{\circ}$ C, pH 7.2, calcium and magnesium free) three times and harvested with a home-made rubber policeman. Total lipids were then extracted from the cells three times with 2 ml each of chloroform-methanol (2:1, v/v). The samples were then dried under nitrogen

(99.99% pure) and redissolved in chloroform and applied to a Unisil Column (activated silicic acid, 100-200 mesh, Clarkson Chemical Co., Pa.). Unisil column was prepared according to Saito & Rosenberg (1982) using glass wool in a 5-3/4" length pasteur pipet with silicic acid added up to 2 cm and pre-washed with chloroform-methanol (2:1, v/v). Neutral lipids were eluted first from the column with chloroform (3 times with 2 ml) and then phospholipids with methanol (3 times with 2 ml) after redissolving the sample in methanol and reapplying to the column. These lipids were then dried under nitrogen (99.99% pure) and are ready to be quantitated.

The isolated neutral lipids were spotted on a 10 x 20 cm HPTLC (E. Merck, Darmstadt, Germany) plate along with 5 μ l, 10 μ l, 15 μ l, and 20 μ l of a standard neutral lipid mixture (consisting of 0.4 μ g/ μ l cholesterol, 0.06 μ g/ μ l oleic acid, 1 μ g/ μ l triglyceride and 0.8 μ g/ μ l cholesterol ester dissolved in dioxane and all chemicals obtained from Sigma). The plate was then developed in diethyl ether-hexane-acetic acid (35:65:2, v/v) until the solvent front ascends to about 4-5 cm above the bottom edge of the plate. Following development, excess solvent was evaporated in a fume hood for 15 minutes and then in a vacuum desiccator for 15 minutes. Then it was rechromatographed using diethyl ether-hexane-acetic acid (2:98:1, v/v) until the solvent front ascends to 1 cm of the top of the HPTLC plate.

After drying the plate several minutes in air, the lipids were charred for densitometry with 3% cupric acetate (w/v) in 8% phosphoric acid (v/v) solution and heated at 180°C for 15 minutes (Fewster et al., 1969) and scanned according to Macala et al. (1983) at 350

nm (slit = 0.2 nm, width = 3 nm) in a Kratos model SD 3000 spectrodensitometer (Kratos, Shoefel Instrument Corp., N.J.) attached with a Hewlett-Packard 3390A integrator (Hewlett-Packard Co., Pa.). The scan was done in the "fast" mode on the densitometer along with the settings on the integrator as follows: attenuation = 6, chart speed = 6 cm/min, peak width = 0.04 min, threshold = 5, and area rejection = 0. The lipids were then quantitated from comparison with the standard. Standard linear plots were determined for cholesterol, free fatty acid, triglycerides, and cholesterol ester separately as amount of lipid versus area under the curve and from it, the amount of sample lipid was determined.

One-fourth the amount of isolated phospholipids were also spotted on a 10 x 20 cm HPTLC plate along with 5 μ l, 10 μ l, 15 μ l, and 20 μ l of a standard phospholipid mixture (consisting of 2 μ g/ μ l sphingomyelin, 3 μ g/ μ l phosphatidylcholine, 0.1 μ g/ μ l phosphatidylserine, 0.05 μ g/ μ l phosphatidylinositol, and 0.5 μ g/ μ l phosphatidylethanolamine dissolved in dioxane and all chemicals obtained from Sigma). The plate was then developed in chloroform-methanol-water (60:35:4, v/v) until the solvent front reached to 1 cm from the top of the plate. After drying the plate for several minutes in air, the phospholipids were visualized and quantitated similarly as for neutral lipids (Macala et al., 1983; Schmitz et al., 1983, 1984; Gopelt & Resch, 1984). The scan on the densitometer was in the "slow" mode with the settings on the H-P 3390A integrator as follows: attenuation = 6, chart speed = 2 cm/min, peak width = 0.04 min, threshold = 5, and area rejection = 0.

Initially, to verify that the methanol elution from Unisil column did indeed give the phospholipids, phospholipids were plated and then sprayed with the Dittmer-Lester reagent (Dittmer & Lester, 1964) specific for phospholipid, which gave a positive blue spot for the fibroblast phospholipids. They were also visualized with iodine stain to make sure no other lipids were present. Each phospholipid was then identified by comparing it with a standard spotted alongside it and noting the distance migrated. Each neutral lipid was also identified by comparing it with a standard.

The yield of the phospholipid and neutral lipid was checked by densitometry. For example, the amount of neutral lipid isolated by chloroform elution from Unisil column was compared against neutral lipid content in total lipids and the result was approximately 95-99% of the neutral lipids were recovered, as judged via densitometry. This was also true for the phospholipids.

Ceramide was also quantitated in cultured human skin fibroblasts. The total lipids were isolated as stated previously and dried under nitrogen. The lipids were then applied to a Unisil column by dissolving in chloroform-methanol (9:1, v/v) and eluted three times with 2 ml of this chloroform-methanol (9:1, v/v) mixture. This ceramide containing fraction was then dried under nitrogen and then applied to a HPTLC plate along with 5 μ l, 10 μ l, 15 μ l, and 20 μ l of standard ceramide (0.05 μ g/ μ l in C-M 2:1) obtained from Sigma (from brain sphingomyelin) and developed in chloroform-methanol-water (60:25:8, v/v) until the solvent front reached to approximately 3-3.5 cm from the bottom edge of the plate according to Selvam and Radin (1981).

Following development, excess solvent was evaporated in a fume hood for 15 minutes and then in a vacuum desiccator for 15 minutes. Then, it was rechromatographed using chloroform-methanol-acetic acid (90:2:8, v/v) until the solvent front ascends to 1 cm of the top of the HPTLC plate. The percentage recovery of ceramide was estimated to be approximately 90-95%, as judged by HPTLC plating and densitometry of the fraction containing chloroform-methanol (9:1) eluant versus total lipid fraction. The visualization and quantification of the ceramide was done exactly as that described for neutral lipids and phospholipids. This plate was then scanned with the densitometer in the "fast" mode with the settings on the H-P 3390A integrator as follows: attenuation = 6, chart speed = 7 cm/min, peak width = 0.04 min, threshold = 5, area rejection = 0.

Fatty Acid Analysis of Phospholipids and Cholesterol Ester

The phospholipids were isolated as described in the previous section. They were then plated onto a 10 x 20 cm plate (prewashed in the developing solvent system of chloroform-methanol-water [60:35:4, v/v]) and developed as before. Afterwards, the plate was air dried for a few minutes and visualized with iodine. Appropriate phospholipids were marked along with blank regions and the iodine was evaporated under nitrogen. It was determined using standard phosphatidylcholine that the best way to keep unsaturated fatty acids from being degraded is to evaporate the iodine immediately with nitrogen, and, not in a vacuum desiccator. The marked spots were then scraped and dissolved in methanol and sonicated for 30 seconds. The individual

lipids were then applied to a pasteur pipet, containing glass wool, and collected in 13 x 100 mm test tubes. The tubes were centrifuged to pellet any silica gel that may have been carried through with the methanol. The supernatant containing the phospholipid of interest was then placed into teflon capped 1/2 dram vials (Supelco, Inc., Bellefonte, Pa.) and then dried under nitrogen. The fatty acids were derivatized to their methyl esters by using either MeOH-HCl (0.5 N, Supelco) according to Zanetta et al. (1972) or BF₃-MeOH (14% w/v, Supelco) according to Morrison and Smith (1964).

With respect to the MeOH-HCl (0.5 N) as the derivatizing agent, 0.5 ml was added to the teflon capped vials and the vials were flooded with nitrogen for a few seconds, to replace the air, and the vials were then tightly capped. The vials were placed in a Multi-Blok Heater (Lab-Line Instruments, Inc., Melrose Park, IL) at 100°C for 20 hrs. After the said period of heating, the vials were cooled to room temperature and the fatty acyl methyl esters were extracted twice with 0.5 ml of hexane. The hexane was dried and a final volume of 50 µl hexane was added, and, 5 µl of this was subjected to gas chromatography.

Similar to MeOH-HCl, 0.5 ml of BF₃-MeOH was added to the teflon capped vials and the vials were placed under nitrogen for a few seconds. For all phospholipids, except sphingomyelin, the samples were heated at 100°C for 15 minutes. Sphingomyelin containing samples were heated at 100°C for 75 min. After cooling to room temperature, the fatty acid methyl esters were extracted twice with 0.5 ml hexane and dried under nitrogen. Afterwards, 50 µl of hexane was added, and, 5 µl of this injected into the gas chromatograph.

The fatty acids of cholesterol esters were examined similar to that of phospholipids. Neutral lipids from fibroblasts were extracted as described in the previous section. These were then spotted on an HPTLC plate (prewashed in the solvent system of ether-hexane-acetic acid [2:98:1]) and developed as described previously. Afterwards, the plate was air dried for a few minutes and visualized with iodine. The cholesterol ester bands were marked, along with the appropriate blank, and the iodine was evaporated under nitrogen. The marked spots were then scraped and dissolved in chloroform and sonicated for 30 seconds. These then were applied to a pasteur pipet containing glass wool and collected in 13 x 100 mm tubes. The tubes were centrifuged (500 xg, 5 min) to pellet any silica gel that may have been present after passing through with chloroform. The supernatant containing cholesterol ester was placed in a 1/2 dram teflon capped vial and dried under nitrogen. Then the fatty acids from cholesterol esters were derivatized with $\text{BF}_3\text{-MeOH}$ (14% w/v, 0.5 ml/vial) at 100°C for 75 min. After cooling, the fatty acid methyl esters were extracted twice with 0.5ml hexane and dried under nitrogen. A final volume of 50 μl was added to the dried lipids, and, 5 μl of this was injected into the gas chromatograph.

The fatty acid methyl esters were analyzed using a Perkin-Elmer 990 Gas Chromatograph equipped with a flame ionization detector. The prepacked column was obtained from Supelco, Inc. containing 5% Ov-210 on Supelcoport. The conditions used for gas-liquid chromatography are summarized in Table 6.

The peaks obtained were identified using authentic standards

TABLE 6.--Conditions for Gas Liquid Chromatography
Using a Perkin-Elmer Model 990 G-C

Condition	Value
Column Temperature:	
Initial	90°C
Final	200°C
Temperature Program Rate	4°C/min
Manifold Temperature	200°C
Injector Temperature	240°C
Gas Flow Rates (All gases of Zero Grade)	
Hydrogen	30 ml/min
Air	300 ml/min
Nitrogen	7.5 ml/min
Sample volume injected	5 μ l
Attenuation	8
Cool Rate	fast
Hewlett Packard 3390A Integrator:	
Attenuation	2
Chart Speed	0.3 cm/min
Peak Width	0.04 min
Threshold	1
Area Rejection	0

obtained from Sigma or Supelco. The weight percentage of each fatty acid was determined with respect to an external standard obtained from Supelco (Supelco Standard F containing 12% C14:0, 4% C16:0, 7% C18:0, 14% C20:0, 25% C22:0, and 47% C24:0). Cholesterol ester fatty acids were analyzed with the G-C attached to a Hewlett-Packard integrator, which predetermined the areas; whereas, phospholipid fatty acids were analyzed with a Fisher Recordall Series 5000 Chart recorder (0.01 volts, 1 cm/min chart speed) from which the area of each individual peak was obtained by taking the product of height x base at half height.

Hydrogenation

For an unidentifiable peak in the fatty acids of cholesterol esters, the fatty acid methyl esters were subjected to platinum reduction using Adam's catalyst (Pt₂O) according to the method of Christie (1982). All of fatty acid methyl esters in hexane, as obtained above, were taken and dried under nitrogen. To this sample, 150 μ l of methanol (anhydrous) was added along with 1 mg of Adams' catalyst in a sealed pasteur pipet. The sample was then placed in a hydrogenation bottle and connected to a two-way tap reservoir of hydrogen. The sample was alternatively evacuated and flushed with hydrogen three or four times to remove any air, and then was vigorously shaken for two hours at a hydrogen pressure of 21 psi. After this time, the catalyst turned black; and the methanol containing reduced fatty acid methyl esters was transferred to another sealed pasteur pipet and an additional 100 μ l of methanol was added. From this, the fatty acid methyl esters

were extracted twice with 400 μ l hexane and placed into teflon capped vials. This was then dried under nitrogen and a final volume of 50 μ l hexane was added, of which, 5 μ l was injected into the gas chromatograph for identification.

CHAPTER IV

RESULTS

Fluorescence of DPH Incorporation into Cells

A time course study was performed on normal and Gaucher diseased fibroblasts at 25°C and it was noted that the steady-state fluorescence anisotropy value was constant up to the times investigated (Fig. 7). The fluorescence intensity was linear up to one hour for both normal and diseased cells (Fig. 8). The viability of the cells was also checked, using the trypan blue exclusion test, and almost 95-99 percent of all the cells were viable up to 1 hr. In order to check that the DPH probe was incorporated into the fibroblasts, an emission spectrum of the labeled and unlabeled cells (excitation wavelength = 360 nm) was performed for the different cell lines and the spectra showed the incorporation of probe into the cell membranes with a relative emission maximum at 426 nm (Figs. 9-15) for the normal and Gaucher diseased cell lines. Also, excitation spectra for one of the cell lines, GM 302A, is shown in Fig. 10 (emission wavelength = 426 nm). Culture media's intrinsic autofluorescence was also checked and it was noted there was some probe incorporated into the media but not to a significant degree that would interfere with the subsequent anisotropy measurements. It can be noted that the labeled cells

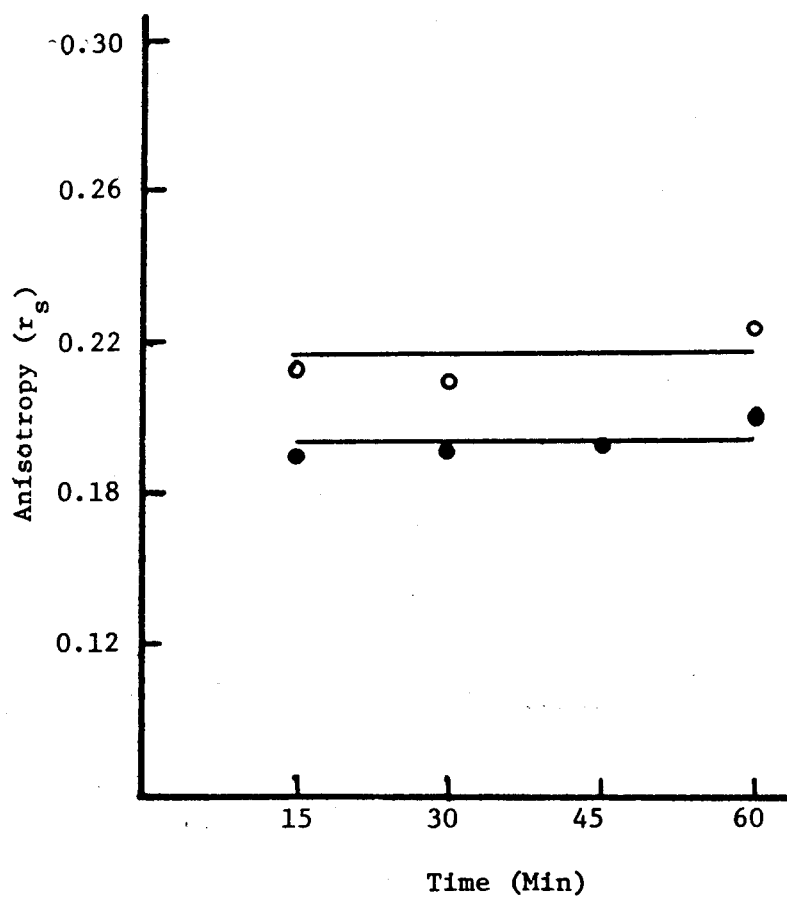


Fig. 7. Time course study of fluorescence anisotropy of Normal, NmiF (●), and Gaucher, InG 1247 (○), fibroblasts.

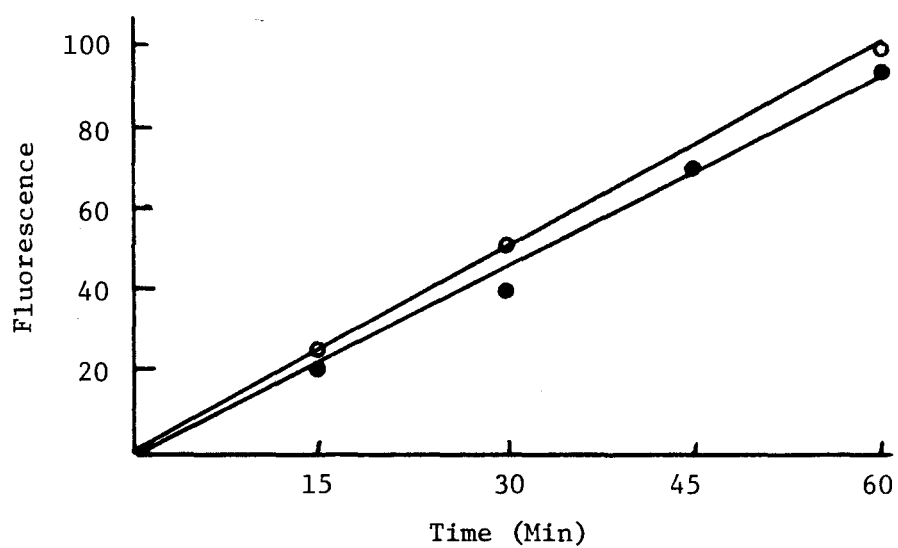


Fig. 8. Relative fluorescence intensity (arbitrary units) versus time of incubation with DPH for normal, NmlF (●), and Gaucher, InG 1247 (○), fibroblasts.

Fig. 9. Emission spectra of DPH in normal infant fibroblasts (GM 302A). Curve (a) depicts fibroblasts labeled with DPH and curve (c) non-labeled cells at the same sensitivity of the fluorometer. Curve (b) is the same as for (c) except at a higher gain (30x). Excitation wavelength was 360 nm.



Fig. 10. Excitation spectra of DPH in normal infant fibroblasts (GM 302A). Emission wavelength was 426 nm.

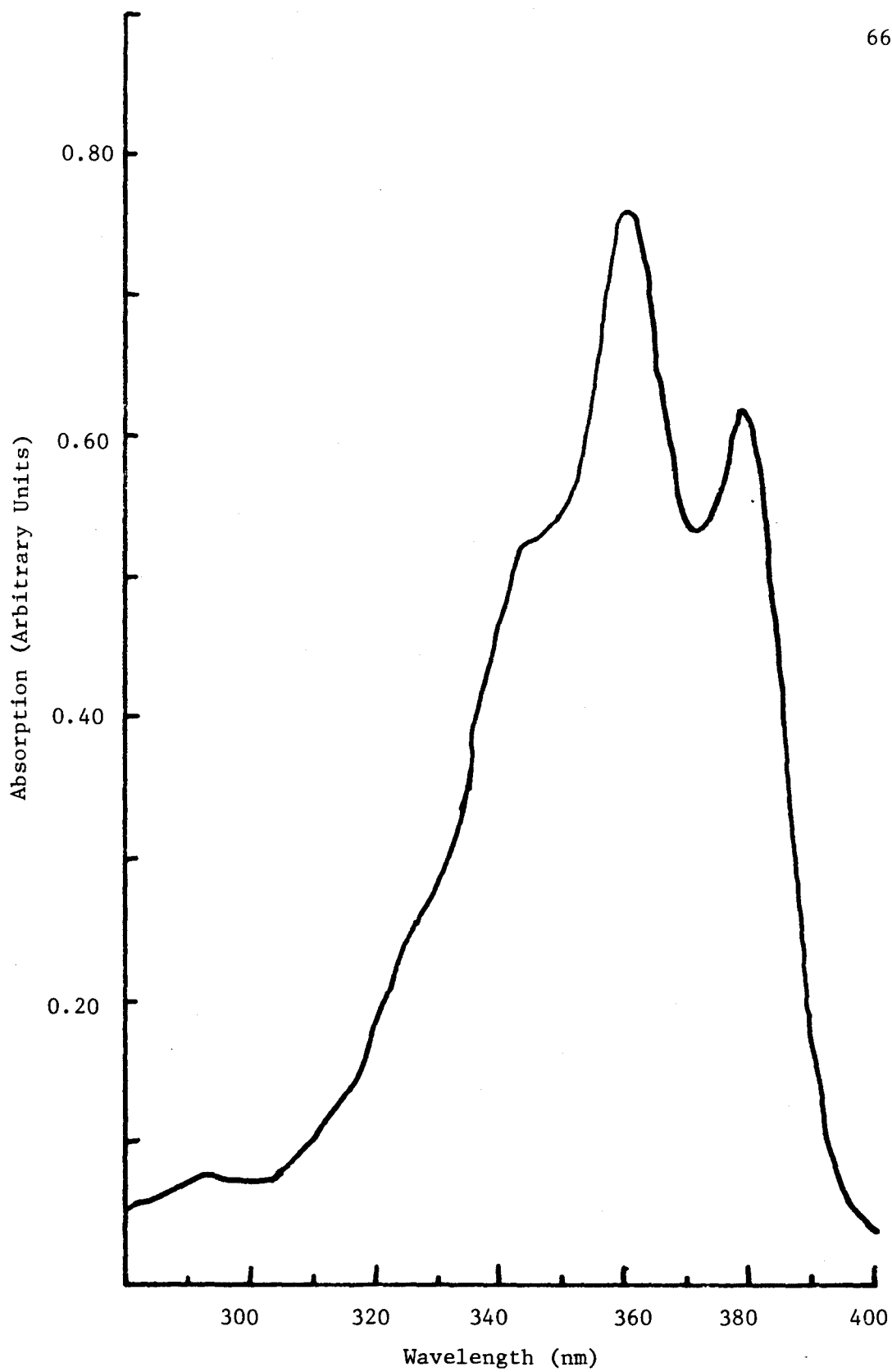


Fig. 11. Emission spectra of DPH in type 1 infant Gaucher fibroblasts (GM 4394). Curve (a) depicts fibroblasts labeled with DPH and curve (c) non-labeled cells at the same sensitivity of the fluorometer. Curve (b) is the same as for (c) except at a higher gain. Excitation wavelength was 360 nm.

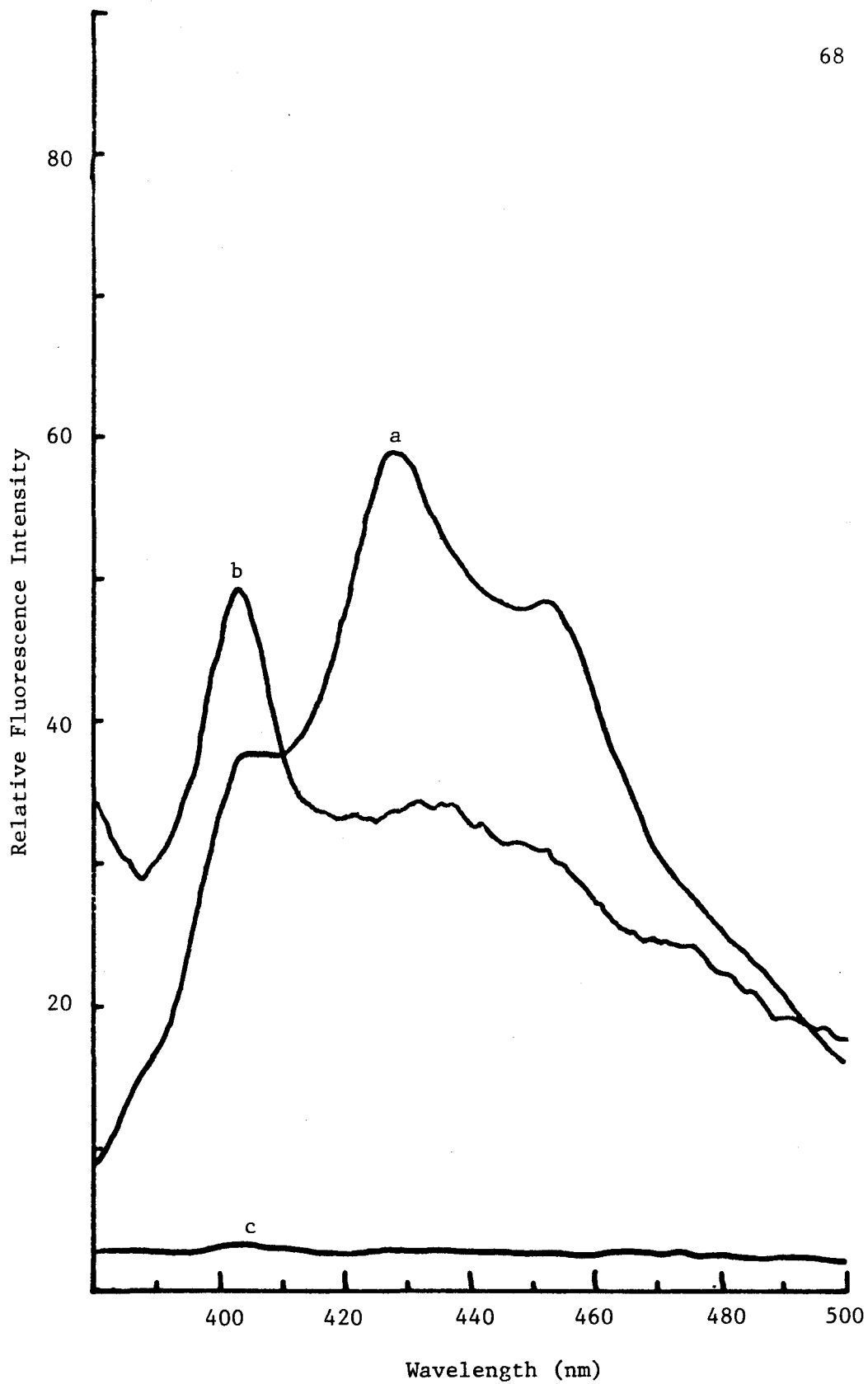


Fig. 12. Emission spectra of DPH in type 2 infant Gaucher fibroblasts (InG 1247). Curve (a) depicts fibroblasts labeled with DPH and curve (c) non-labeled cells at the same sensitivity of the fluorometer. Curve (b) is the same as for (c) except at a higher gain. Excitation wavelength was 360 nm.

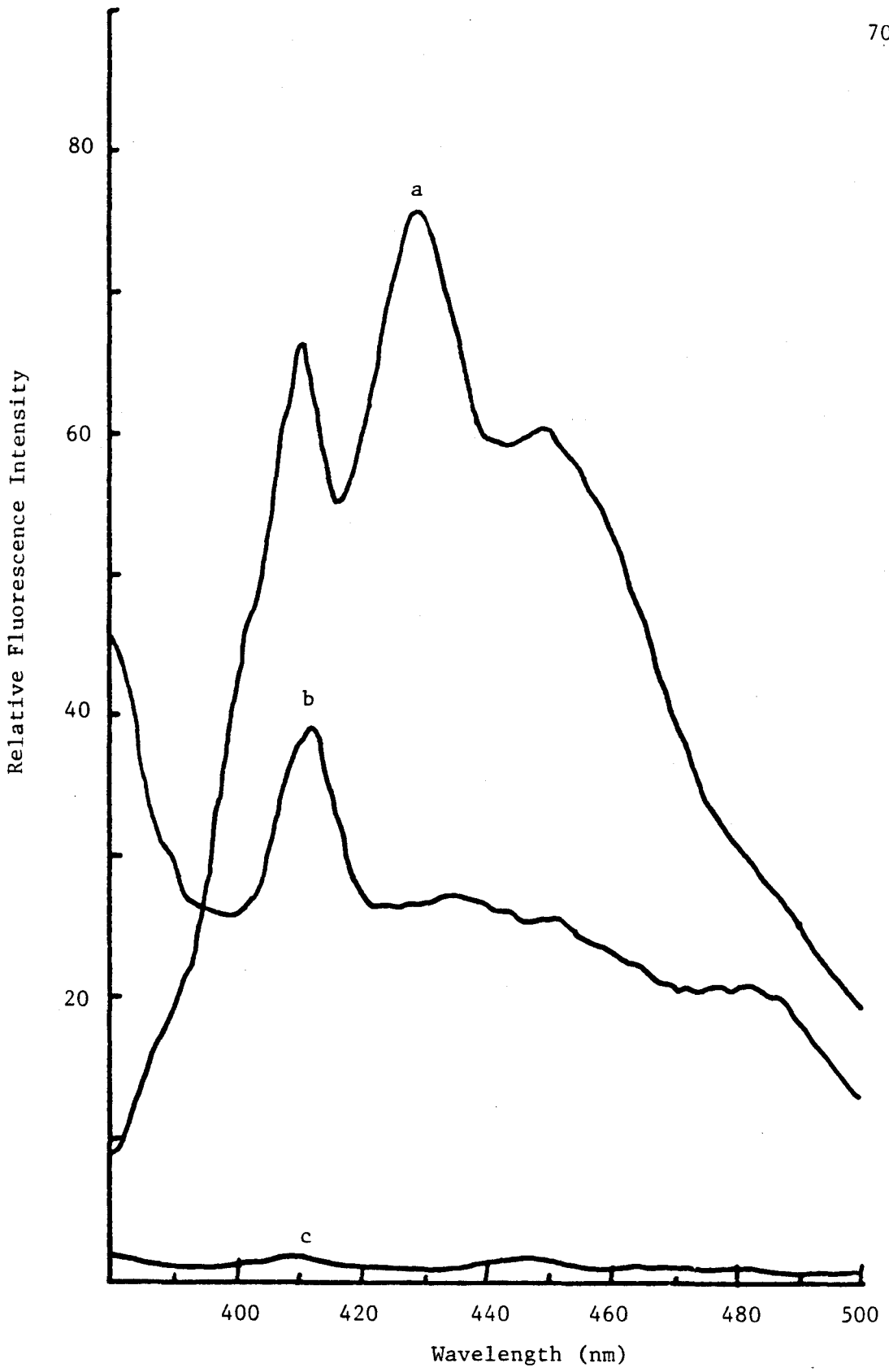


Fig. 13. Emission spectra of DPH in type 3 juvenile Gaucher fibroblasts (JuvG). Curve (a) depicts fibroblasts labeled with DPH and curve (c) non-labeled cells at the same sensitivity of the fluorometer. Curve (b) is the same as for (c) except at a higher gain. Excitation wavelength was 360 nm.

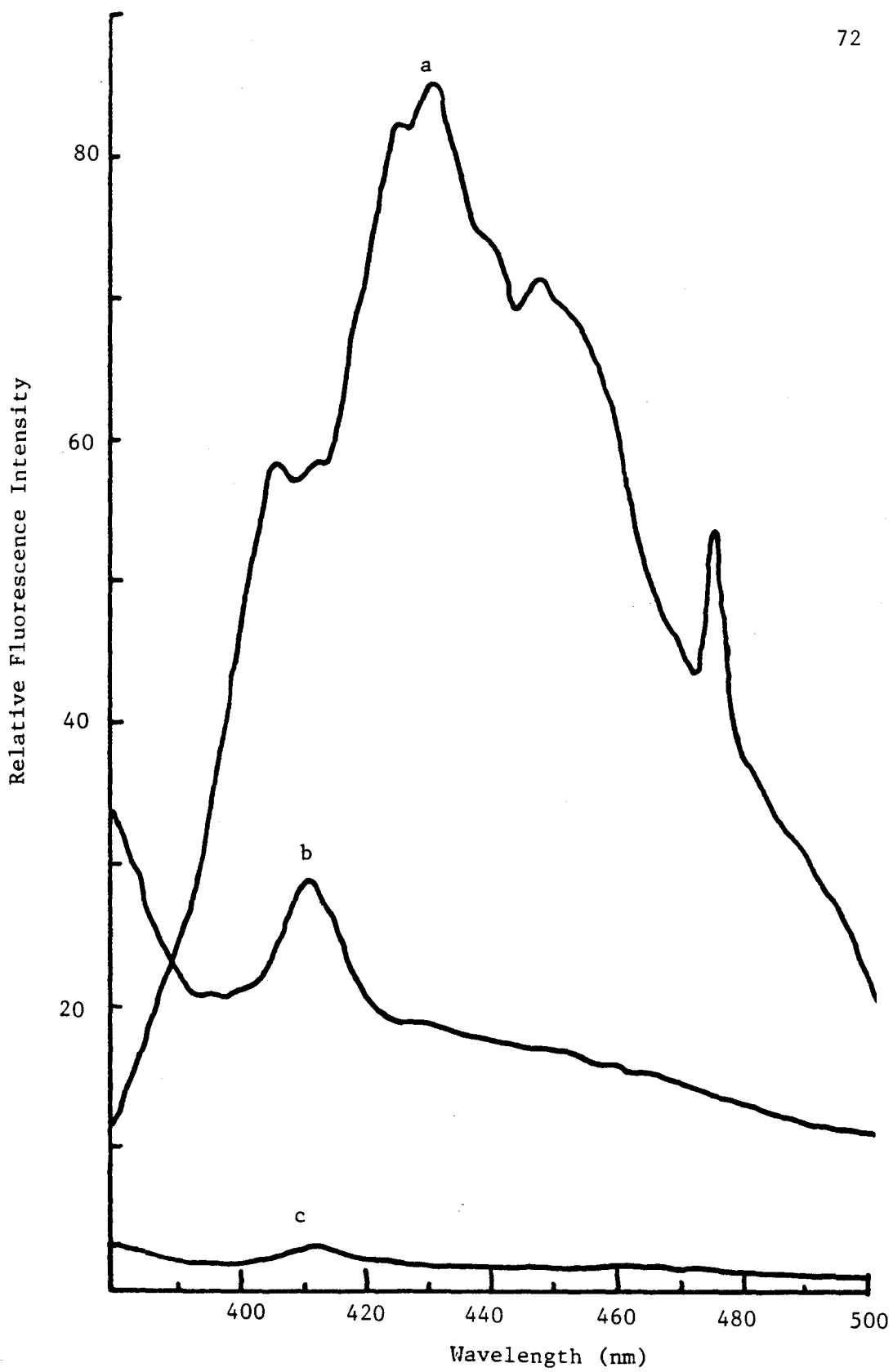


Fig. 14. Emission spectra of DPH in normal adult fibroblasts (GM 3440). Curve (a) depicts fibroblasts labeled with DPH and curve (c) non-labeled cells at the same sensitivity of the fluorometer. Curve (b) is the same as for (c) except at a higher gain. Excitation wavelength was 360 nm.

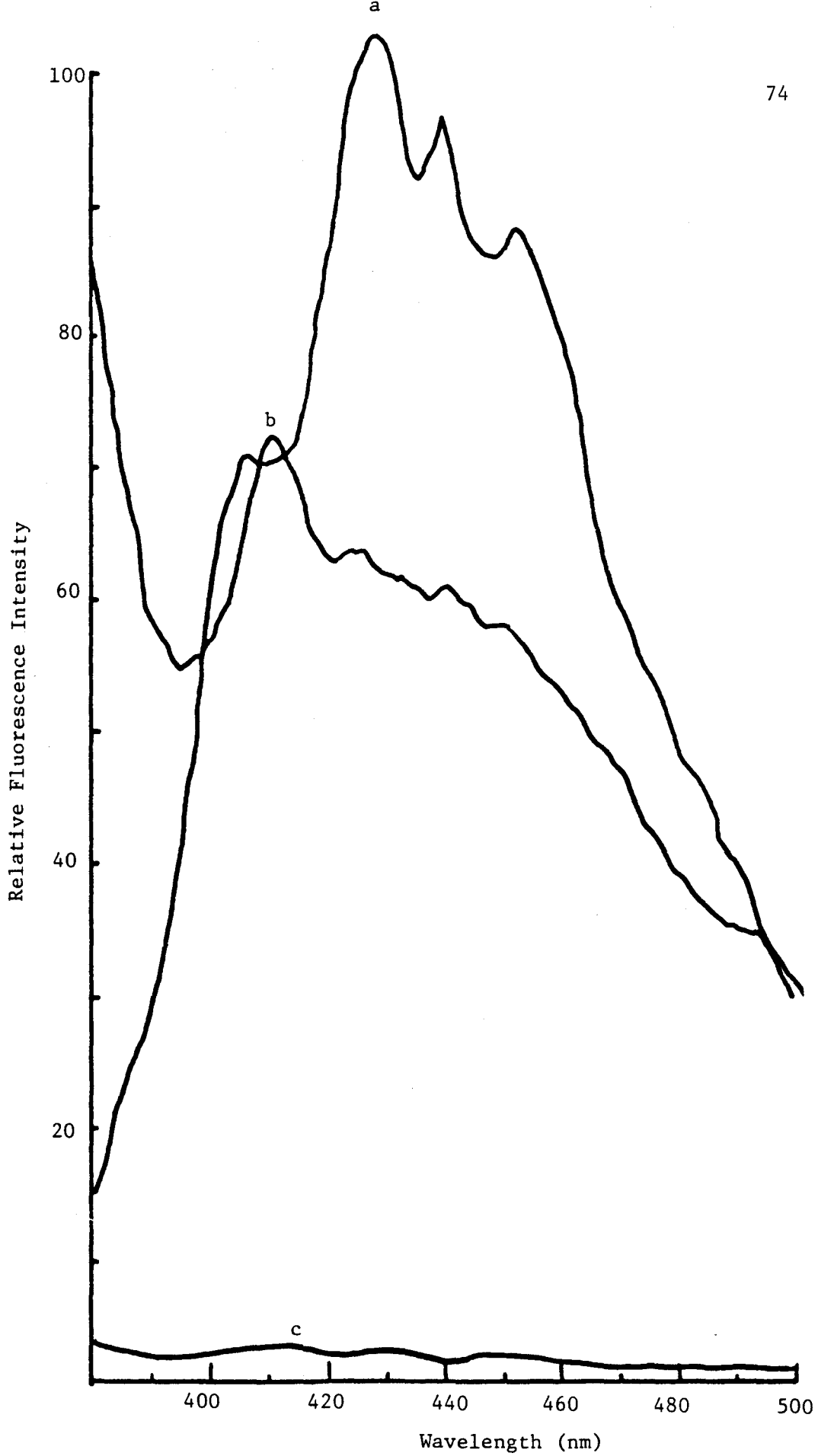
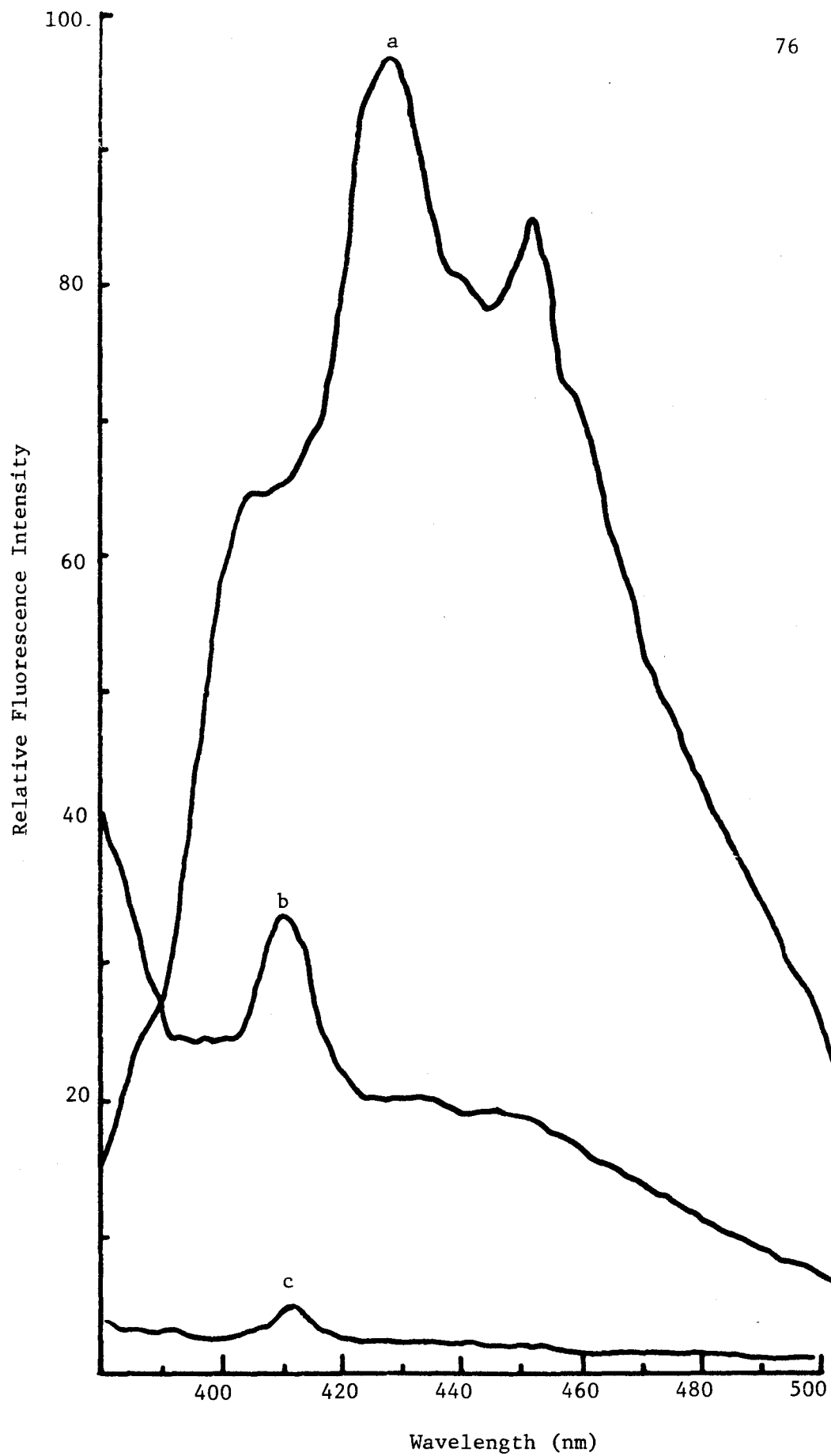


Fig. 15. Emission spectra of DPH in type 1 adult Gaucher fibroblasts (AdG 1470). Curve (a) depicts fibroblasts labeled with DPH and curve (c) non-labeled cells at the same sensitivity of the fluorometer. Curve (b) is the same as for (c) except at a higher gain. Excitation wavelength was 360 nm.



have greater than 20-30 times the intensity as compared to non-labeled cells.

Fluorescence Anisotropy of Normal and Diseased Cells

Table 7 shows the steady-state polarization and anisotropy, measurements for the various cell lines at 25°C. This table also has calculated average values for the apparent membrane microviscosity ($\bar{\eta}$), limiting fluorescence anisotropy (r_{∞}), and the lipid order parameter (S) from the steady-state fluorescence anisotropy values as shown in Materials and Methods, and Review of the Related Literature. It can be seen that as compared to normal infant fibroblasts, type 2 and type 3 Gaucher cells had significantly increased anisotropy values. Also, from the order parameter and apparent microviscosity, it can be concluded that there was decreased membrane fluidity for the neuronopathic (acute and subacute) forms of Gaucher disease. In the infant form of type 1 disease investigated, there was no significant difference in anisotropy, and thus membrane fluidity, from normal cells. As compared to normal adult fibroblast membranes, type 1 Gaucher cells exhibited a variability of data with respect to anisotropy measurements and thus membrane fluidity. On the average, type 1 Gaucher cells exhibit no difference in membrane fluidity as compared to normal cells; however, for one of the cell lines (AdG 1470), there was significant increase in anisotropy value as compared to normal cells. This difference in steady-state fluorescence anisotropy in the various type 1 Gaucher cells could be reflecting the heterogeneity found among adult non-neuronopathic forms of Gaucher

TABLE 7.--Fluorescence Polarization (P), Anisotropy (r_s), Membrane Viscosity ($\bar{\eta}$), Limiting Anisotropy (r_∞), and Order Parameter (S) of Normal and Gaucher Diseased Fibroblasts at 25°C

	P	r_s	$\bar{\eta}$ (Poise)	r_∞	S
Nml Infant					
GM 302A (n=3)	0.251 \pm .007	0.182 \pm .006	2.43	0.143	0.628
Type 1 Infant					
GM 4394 (n=3)	0.263 \pm .012	0.192 \pm .009	2.71	0.156	0.656
Type 2 Infant					
a. InG 1247 (n=5)	0.303 \pm .016**	0.225 \pm .013**	3.94	0.200	0.743
b. GM 877 (n=3)	0.311 \pm .019*	0.231 \pm .016*	4.23	0.208	0.758
Type 3 Juvenile					
JuvG (n=3)	0.294 \pm .006*	0.216 \pm .005*	3.55	0.188	0.721
Nml Adult					
a. GM 3440 (n=4)	0.270 \pm .015	0.198 \pm .012	2.90	0.164	0.673
b. NmlF (n=3)	0.279 \pm .010	0.205 \pm .008	3.13	0.173	0.692
Type 1 Adult					
a. AdG 119a (n=3)	0.262 \pm .006	0.191 \pm .004	2.68	0.155	0.654
b. AdG 1470 (n=4)	0.301 \pm .010***	0.223 \pm .009***	3.85	0.197	0.738

Each value represents mean \pm standard deviation, n represents the number of separate determinations.

*P<0.01

**P<0.001 as compared with normal infant

***P<0.01 as compared with normal adult using Student's two-tailed t test.

disease. Note, there also existed a difference between the normal adult and infant cell lines, where there was a significant increase of fluidity in normal infants as compared to normal adults.

Figures 16 and 17 show the effect of increasing temperature on fluorescence anisotropy values for normal and diseased cells and it can be seen, as a general result, that as the temperature increases, the anisotropy value decreases. Therefore, the membrane fluidity increases with increasing temperature for all membranes. As the first figure shows, type 2 and type 3 Gaucher cells, which had a significant difference from normal infant cells with respect to anisotropy values at 25°C, also exhibited a difference in fluidity at all the temperatures. Each point on the curve represents an average of two different experiments at the specified temperature. The determination for type 2 Gaucher cells was done using both the cell lines InG 1247 and GM 877; for type 3 Gaucher cells, the cell line labeled Juv G was used. This figure then shows that at all temperatures between 4-40°C, there was decreased fluidity of type 2 and type 3 Gaucher cells. This conclusion also holds true for the type 1 Gaucher cell line (AdG 1470) which had a significant difference from normal adult cells with respect to anisotropy value at 25°C. Therefore, there was decreased membrane fluidity in type 1 Gaucher fibroblasts at all temperatures between 4-40°C. From these temperature studies, one can evaluate if there are any bulk lipid phase transitions by looking at the Arrhenius plots of $\log(\text{anisotropy})$ versus $1/\text{temperature}$. This is as shown in figures 18 and 19. Figure 18 shows that there were no identifiable breaks in the Arrhenius plots of normal infant fibroblasts, type 2 and type

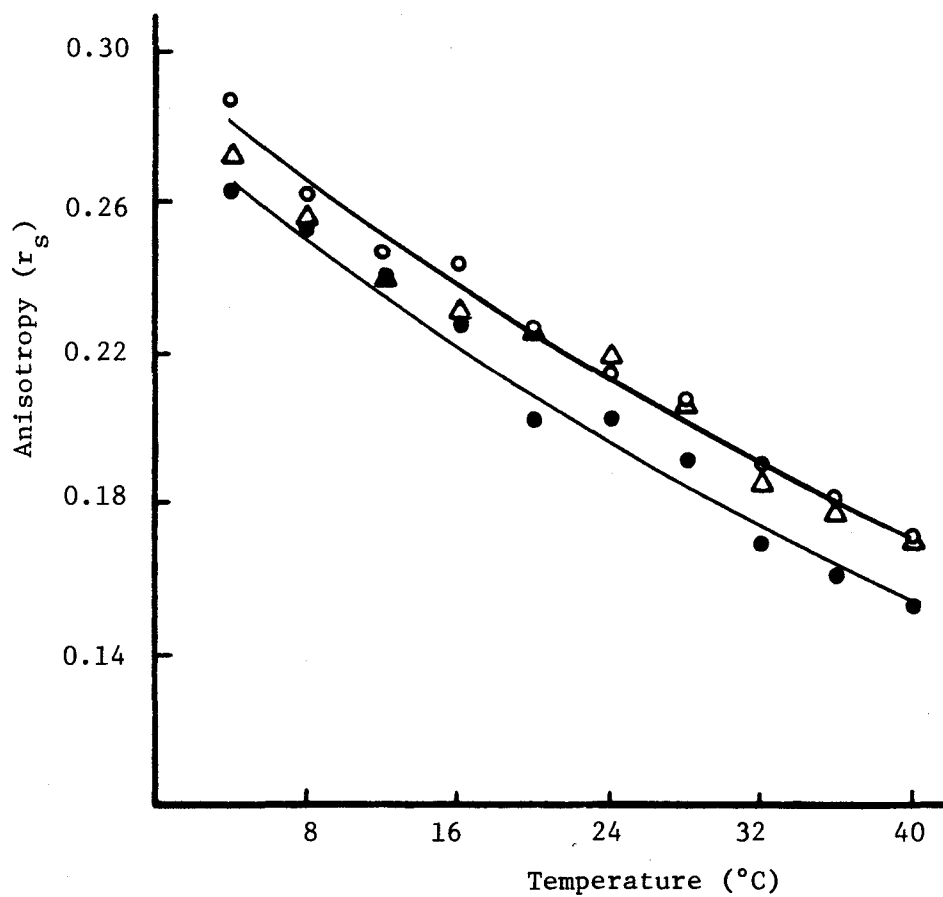


Fig. 16. Temperature dependence of anisotropy of DPH in normal infant (\bullet) and Gaucher diseased fibroblasts--type 2 (\circ) and type 3 (Δ). Each point is the average of two separate temperature scans.

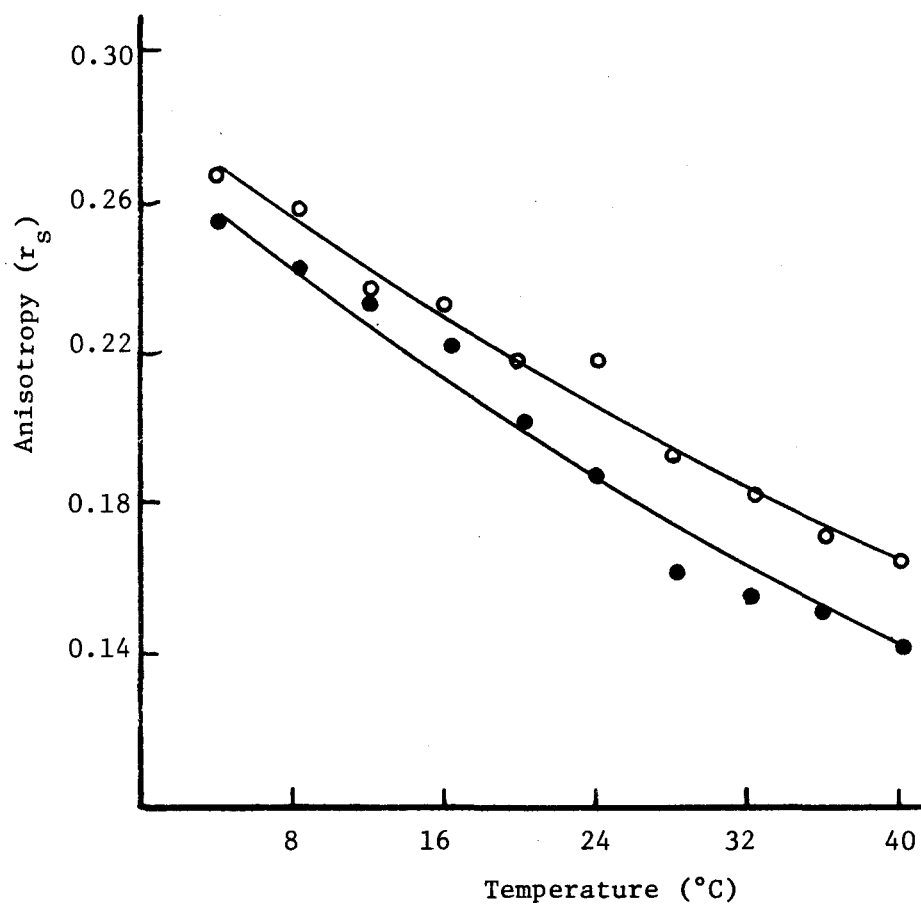


Fig. 17. Temperature dependence of anisotropy of DPH in normal adult (\bullet) and type 1 adult Gaucher diseased fibroblasts (\circ). Each point is the average of two separate experiments.

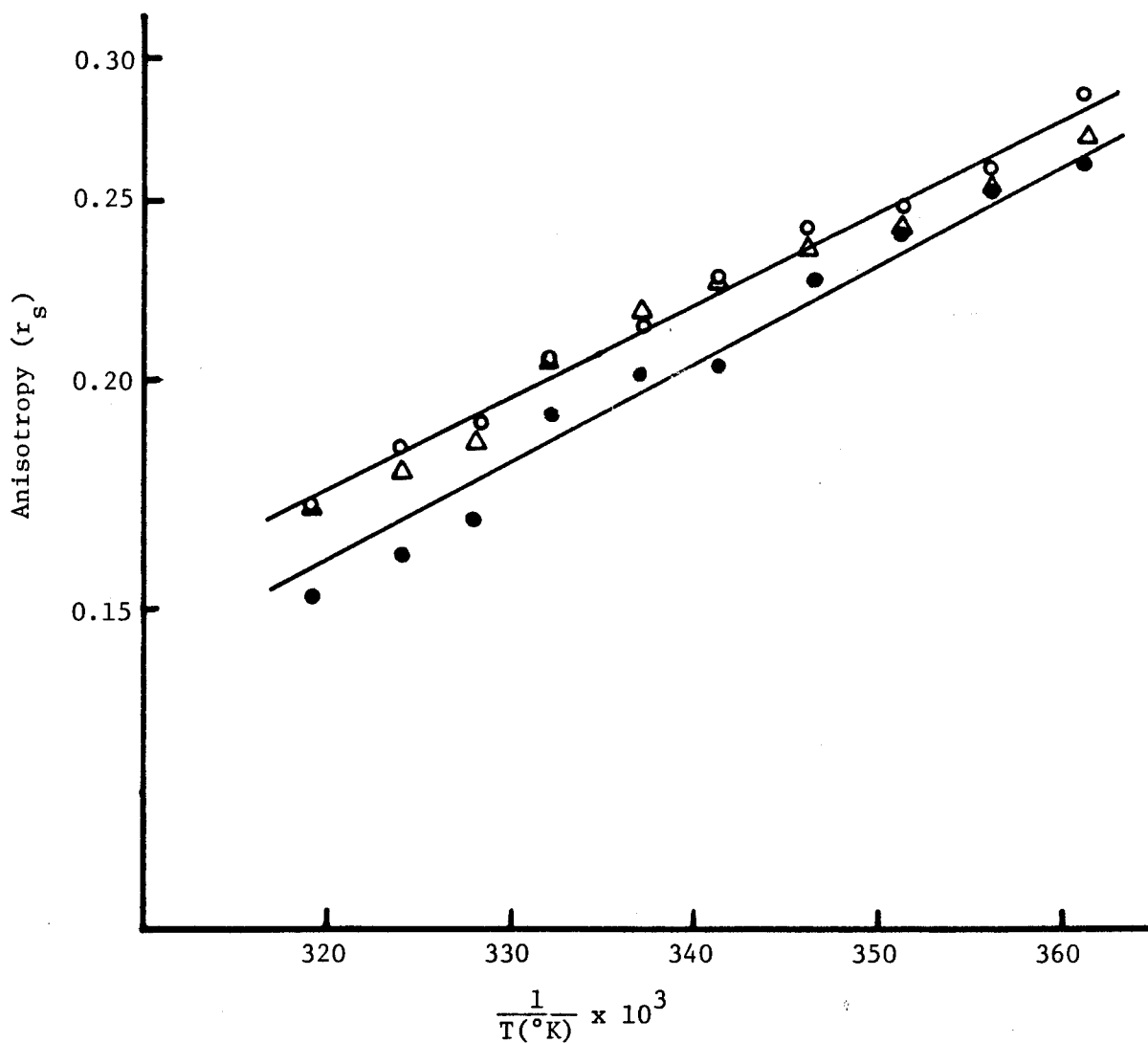


Fig. 18. Arrhenius plots of DPH in normal infant (●) and Gaucher diseased fibroblasts--type 2 (○) and type 3 (Δ). Presented as $\log r_s$ versus $1/T$. Each point is the average of two separate experiments.

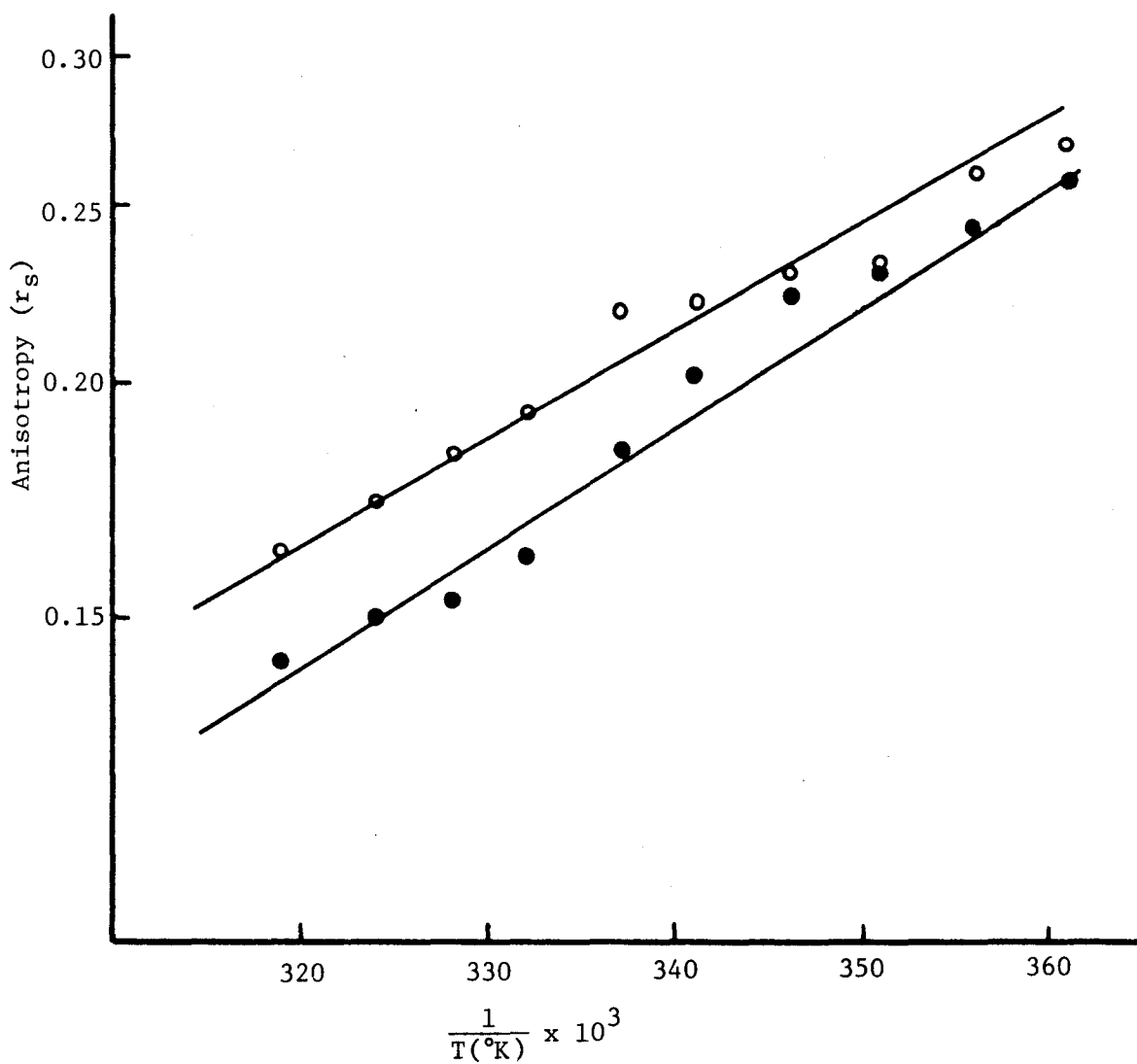


Fig. 19. Arrhenius plots of DPH in normal adult (●) and type 1 Gaucher diseased fibroblasts (○). Presented as $\log r_s$ versus $1/T$. Each point is the average of two separate experiments.

3 Gaucher cells; thus implying that, between 4-40°C, there were no bulk lipid phase transitions in fibroblast membranes as judged by steady-state fluorescence anisotropy using the probe DPH.

The slope $\left(\frac{d(\log r_s)}{d(1/T)}\right)$, as derived from linear least square fit

(Table 8), and the intercept on the ordinate for the Arrhenius curve for normal infant fibroblasts were different from that of type 2 and type 3 Gaucher cells. Figure 19 shows that using normal adult cells (GM 3440) and type 1 Gaucher cells (AdG 1470) there were no bulk lipid phase transitions. Again, the slope and the ordinate intercept were different in normal adult cells as compared with type 1 Gaucher cells.

Neutral Lipid Content of Normal and Diseased Cells

Figure 20 shows the HPTLC plate obtained using the separation system listed in Materials and Methods. From this, the total amounts of cholesterol, free fatty acid, triglycerides, and cholesterol ester were determined. It is to be noted that once the area was obtained for each spot for the standard, a standard curve was determined for total area versus amount of lipid spotted and linear least square fit was used to determine the best fit, and from it the sample amount was determined. A densitometric pattern for one of the lanes is given in the same figure. Each neutral lipid is expressed as $\mu\text{g}/\text{mg}$ of protein. As can be seen from Table 9, there were no differences between normal and Gaucher cells with respect to cholesterol and free fatty acid content. There was a considerably decreased amount of cholesterol ester in all three types of Gaucher disease fibroblasts as compared with normal fibroblasts. It seems that type 1 Gaucher

TABLE 8.--Slope, Ordinate Intercept, and Correlation Coefficient
 Derived from Arrhenius Plots of Log (Fluorescence Anisotropy)
 versus [Temperature ($^{\circ}$ K)]⁻¹

Cell Type	Slope	Intercept	Corr. Coeff.
Nml Infant	-2.68	0.0059	0.99
Type 2 Infant	-2.40	0.0051	0.99
Type 3 Juvenile	-2.30	0.0048	0.97
Nml Adult	-2.98	0.0065	0.99
Type 1 Adult	-2.44	0.0052	0.98

Fig. 20. HPTLC chromatogram of neutral lipids isolated from fibroblasts.

- (a) Lanes 1-4, 5-20 μ l standard neutral lipid mixtures (see Methods). Lane 5, sample from normal adult fibroblasts (GM 3440). Lane 6, sample from type 1 adult Gaucher diseased fibroblasts (AdG 1470). Lane 7, sample from normal infant fibroblasts (GM 302A). Lane 8, sample from type 1 infant Gaucher diseased fibroblasts (GM 4394). Symbols used: A, cholesterol; B, free fatty acid; C, triglyceride; D, cholesterol ester.
- (b) Densitometric scan of lane 7 in (a). Symbols defined as above.

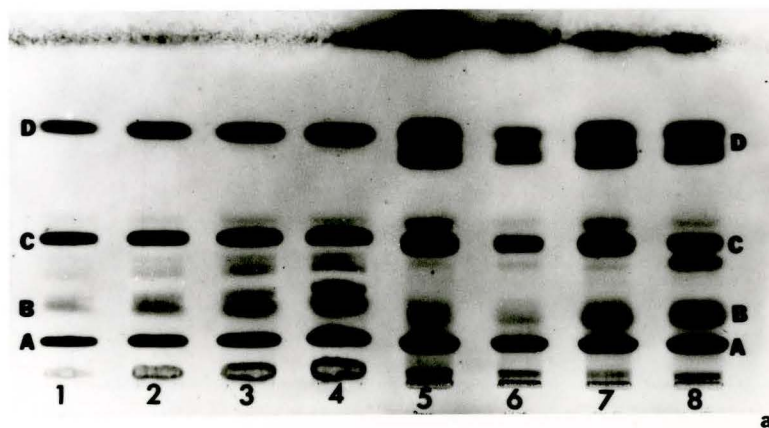
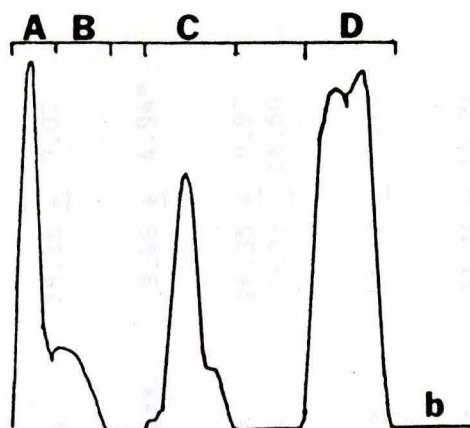


TABLE 9.--Neutral Lipid Composition of Normal and Gaucher Diseased Fibroblasts

	Cholesterol	Fatty Acid	Triglycerides	Cholesterol Ester
Nml Infant				
GM 302A (n=3)	39.63 \pm 15.75	1.52 \pm 0.58	35.09 \pm 4.24	28.38 \pm 9.02
Type 1 Infant				
GM 4394 (n=3)	29.39 \pm 12.20	1.07 \pm 0.69	14.22 \pm 6.31**	9.46 \pm 4.94*
Type 2 Infant				
a. InG 1247 (n=3)	35.12 \pm 19.42	1.19 \pm 1.16	21.75 \pm 16.65	14.35 \pm 9.97
b. GM 877 (n=3)	66.12 \pm 20.85	1.64 \pm 0.84	29.64 \pm 19.44	10.92 \pm 11.60
Type 3 Juvenile				
JuvG (n=3)	44.66 \pm 27.52	0.62 \pm 0.37	32.77 \pm 15.52	13.13 \pm 6.75
Nml Adult				
GM 3440 (n=4)	35.62 \pm 13.41	0.99 \pm 0.95	32.04 \pm 18.07	22.24 \pm 14.91
Type 1 Adult				
a. AdG 119a (n=2)	20.36 - 22.45	0.16 - 0.18	9.22 - 12.34	1.91 - 3.86
b. AdG 1470 (n=3)	37.39 \pm 23.53	0.62 \pm 0.65	12.20 \pm 6.77	9.71 \pm 1.89

Each neutral lipid is expressed as $\mu\text{g}/\text{mg}$ of protein. Each value represents mean \pm standard deviation.

* $P < 0.05$, ** $P < 0.01$ as compared with normal infant using Student's two-tailed t test.

n represents the number of separate determinations.

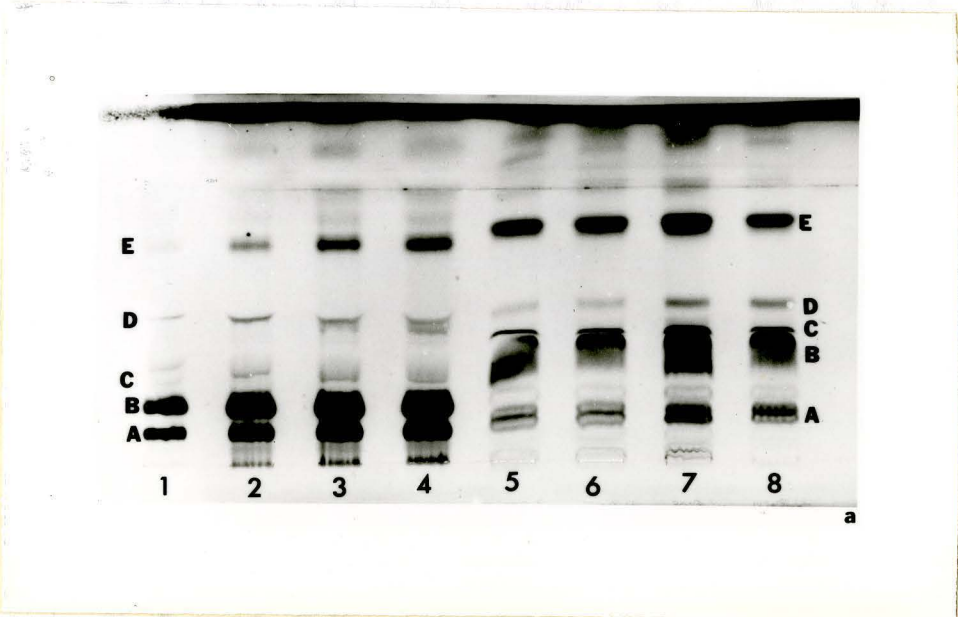
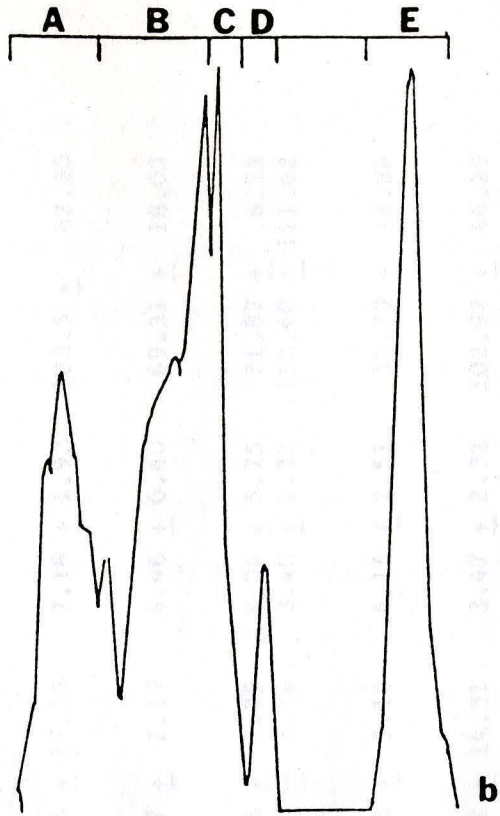
cells had a much more decreased content of cholesterol ester content as compared to type 2 and type 3 Gaucher fibroblasts. It is also interesting to note that only in type 1 Gaucher disease cells there was also a decrease in the triglyceride content as compared to normal cells; whereas, both type 2 and type 3 Gaucher cells had triglyceride content within the normal range. With respect to the type 1 Gaucher infant cell line (GM 4394), there was a significant decrease in both the triglyceride and cholesterol ester content as compared to normal.

Phospholipid Content of Normal and Diseased Cells

Figure 21 shows the HPTLC plate of phospholipids obtained using the separation system listed in Materials and Methods. It can be seen that the major lipids in fibroblasts were sphingomyelin, phosphatidylcholine, phosphatidylserine, phosphatidylinositol, and phosphatidylethanolamine. From the standards spotted, standard least-linear curves (total area versus amount of lipid) were determined, and from it the amount of unknown lipids quantitated. A densitometric pattern for one of the lanes is shown in the same figure. The results for the phospholipid content for various cell lines are summarized in Table 10. As can be seen from this table, there seemed to be no difference between normal and Gaucher cells with respect to phosphatidylserine, phosphatidylinositol, and phosphatidylethanolamine. As compared to normal infant cells, type 1 Gaucher infant cells did not have an altered sphingomyelin content; however, there seemed to be a trend for decreased phosphatidylcholine content. Type 2 Gaucher cells had, on the average, a decreased amount of sphingomyelin and phospho-

Fig. 21. HPTLC chromatogram of phospholipids isolated from fibroblasts.

- (a) Lanes 1-4, 5-20 μ l standard phospholipid mixtures (see Methods). Lanes 5 and 6, samples from normal adult fibroblasts (GM 3440). Lane 7, sample from normal infant fibroblasts (GM 302A). Lane 8, sample from type 1 adult Gaucher diseased fibroblasts (AdG 1470). Symbols used: A, sphingomyelin; B, phosphatidylcholine; C, phosphatidylserine; D, phosphatidylinositol; E, phosphatidylethanolamine.
- (b) Densitometric scan of lane 7 in (a). Symbols defined as above.



the phospholipid composition of 1/2g of protein. Mean value represents mean \pm standard deviation. Control and low-dose dexamethasone values did not differ significantly by Student's two-tailed t test. Deficiency of the most common phospholipids (PC, phosphatidylcholine) (PC), phosphatidylethanolamine (PE), phosphatidylserine (PS), phosphatidylinositol (PI), phosphatidylglycerol (PG), and sphingomyelin (SM) is represented by number of spots in parentheses.

TABLE 10.--Phospholipid Composition of Normal and Gaucher Diseased Fibroblasts

	SPM	PC	PS	PI	PE
Nml Infant					
GM 302A (n=3)	101.62 \pm 32.56	257.37 \pm 72.00	24.54 \pm 18.13	7.18 \pm 1.93	103.5 \pm 62.30
Type 1 Infant					
GM 4394 (n=3)	90.70 \pm 6.71	126.30 \pm 55.30	10.47 \pm 2.17	4.46 \pm 0.60	69.31 \pm 18.03
Type 2 Infant					
a. InG 1247 (n=3)	24.39 \pm 4.62	122.93 \pm 48.82	11.35 \pm 7.05	8.04 \pm 5.75	71.87 \pm 6.33
b. GM 877 (n=3)	82.24 \pm 8.32	116.47 \pm 51.09	12.10 \pm 6.76	3.40 \pm 1.32	152.40 \pm 111.62
Type 3 Juvenile					
Juv G (n=3)	43.18 \pm 21.89	172.60 \pm 101.62	20.15 \pm 5.16	5.14 \pm 2.51	53.79 \pm 16.86
Nml Adult					
GM 3440 (n=3)	100.59 \pm 37.90	212.23 \pm 33.52	13.42 \pm 14.31	3.47 \pm 2.32	102.97 \pm 46.29
Type 1 Adult					
a. AdG 119a (n=2)	19.92 - 33.9	65.5 - 81.6	12.5 - 21.52	3.84 - 10.8	20.76 - 56.80
b. AdG 1470 (n=3)	108.45 \pm 70.57	208.37 \pm 58.28	37.46 \pm 39.98	10.85 \pm 7.24	128.84 \pm 45.29

Each Phospholipid expressed as $\mu\text{g}/\text{mg}$ of protein. Each value represents mean \pm standard deviation. Control and Gaucher phospholipid values did not differ significantly by Student's two-tailed t test. Definition of symbols: SPM, sphingomyelin; PC, phosphatidylcholine; PS, phosphatidylserine; PI, phosphatidylinositol; PE, phosphatidylethanolamine. n represents the number of separate determinations.

tidylcholine content as compared to normal infant cells. In type 3 Gaucher cells, there was no change in phosphatidylcholine content; however, there seemed to be decreased amounts of sphingomyelin. It is interesting to note that the phospholipid content of both normal adult and normal infants were approximately the same. As compared to normal adult cell lines, one of the cell lines (AdG 119a) had decreased amounts of sphingomyelin and phosphatidylcholine; whereas, the AdG 1470 cell line had approximately the same phospholipid composition as that of normal cells. This variability in type 1 cells could possibly be due to the heterogeneity that is found among this disease.

Ceramide Content of Normal and Diseased Cells

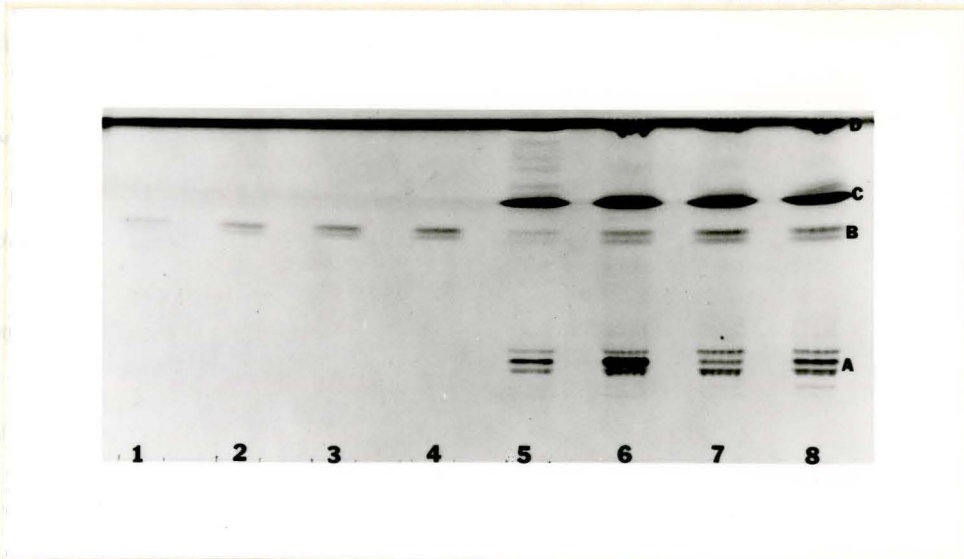
Figure 22 shows the HPTLC plate of ceramide obtained using the separation system listed in the Materials and Methods. From this technique, we were able to quantitate the ceramide content of normal and Gaucher diseased fibroblasts. It can be seen from Table 11 that as compared to normal infant cells, types 1, 2, and 3 Gaucher cells had approximately the same content of ceramide. This also held true for type 1 adult Gaucher cells as compared to normal adult fibroblasts. Ceramide content in cells was 1/10 to 1/50 the concentration of cholesterol levels.

Effect of Monensin on Normal Fibroblast Lipids

Table 12 shows the effect of monensin on neutral lipids, phospholipids, and ceramide as compared to control cells (methodology described as previously). This table describes both the total amounts of each lipid as well as the counts observed after labeling with (^3H)

Fig. 22. HPTLC chromatogram of ceramide containing lipid fraction, isolated from fibroblasts. Lanes 1-4, 5-20 μ l standard ceramide (see Methods). Lane 5, sample from type 1 adult Gaucher diseased fibroblasts (AdG 1470). Lanes 6-8, samples from type 3 juvenile Gaucher diseased fibroblasts (JuvG). Symbols used: A, phospholipids; B, ceramide; C, cholesterol; D, cholesterol ester (migrating with the solvent front).

TABLE 1. Composition of ...
...
...



...
...
...

TABLE 11.--Ceramide Composition of Normal and Gaucher Diseased Fibroblasts

	Ceramide
Nml Infant GM 302A (n=3)	2.75 \pm 1.66
Type 2 Infant GM 877 (n=3)	1.17 \pm 0.81
Type 3 Juvenile JuvG (n=3)	2.73 \pm 0.49
Nml Adult GM 3440 (n=3)	0.98 \pm 0.08
Type 1 Adult AdG 1470 (n=3)	2.33 \pm 1.62

Amount of ceramide expressed as $\mu\text{g}/\text{mg}$ of protein. Each value represents mean \pm standard deviation. Control and Gaucher ceramide values did not differ significantly by Student's two-tailed t test. n represents number of separate determinations.

TABLE 12.--Effect of Monensin on Normal Fibroblast (GM 3440) Lipids

	Total Lipid ($\mu\text{g}/\text{mg}$ of protein)		Radioactivity (dpm/mg of protein)	
	M+	M-	M+	M-
Neutral Lipids				
Cholesterol	60.94 \pm 7.42	76.67 \pm 12.24	14313 \pm 4004**	2948 \pm 844
Free Fatty Acids	2.65 \pm 0.46*	1.70 \pm 0.38	10341 \pm 799*	3663 \pm 1185
Triglycerides	39.55 \pm 3.44	50.64 \pm 11.26	61834 \pm 12726	38700 \pm 12892
Cholesterol Ester	4.15 \pm 2.18**	14.91 \pm 3.84	482 \pm 111**	3275 \pm 790
Phospholipids				
Sphingomyelin	65.13 \pm 6.85	78.33 \pm 29.12	12723 \pm 3234	11125 \pm 2947
Phosphatidylcholine	136.23 \pm 6.67*	224.13 \pm 44.41	137013 \pm 7730**	55424 \pm 13277
Phosphatidylserine	14.99 \pm 1.33**	4.76 \pm 2.28	10909 \pm 1214**	5012 \pm 1880
Phosphatidylinositol	5.16 \pm 0.65	4.83 \pm 2.56	1259 \pm 298*	627 \pm 248
Phosphatidylethanolamine	235.33 \pm 52.14	247.52 \pm 67.81	18657 \pm 3074**	7677 \pm 1716
Ceramide	0.45 \pm 0.20	0.41 \pm 0.07	44.94 \pm 17.33	46.32 \pm 15.00

Each value represents mean of three separate trials \pm standard deviation. M+ represents monensin treated cells; whereas, M- represents non-monensin treated cells.

*P<0.05; **P<0.01 as compared with non-monensin treated cells using Student's two-tailed t test.

acetate for 18 hours in the same cells labeled with either monensin (in ethanol) or without monensin (but an equal amount of ethanol).

With respect to total lipids, there was a significant decrease in the amount of cholesterol ester and phosphatidylcholine content in monensin treated cells. There was significant increase in the free fatty acid and phosphatidylserine content of monensin treated fibroblasts. The amounts of other lipids in monensin treated cells were comparable to that of non-monensin treated cells. In relation to incorporation of (³H) acetate into neutral lipids, there was decreased incorporation of the label into cholesterol ester; whereas, there was increased incorporation into cholesterol, free fatty acids, and triglycerides. The incorporation of the tritiated label was increased in phosphatidylcholine, phosphatidylserine, phosphatidylinositol and phosphatidylethanolamine; whereas, there was no change in sphingomyelin. Similar to sphingomyelin, ceramide did not have an altered incorporation of the label when treated with monensin. Some of the values in Table 12 differ from the previous tables since even the controls are treated with ethanol.

Phospholipid and Cholesterol Ester Fatty Acid Analysis

The fatty acid methyl esters of individual lipids were determined as described in Materials and Methods. Table 13 shows the fatty acid composition of phosphatidylcholine of fibroblasts of normal and diseased subjects. As can be seen from this table, the major saturated fatty acids for phosphatidylcholine were C14:0, C16:0, C18:0, and C22:0, whereas, the unsaturated fatty acids were mainly C16:1, C18:1,

TABLE 13.--Fatty Acid Composition of Phosphatidylcholine of Fibroblasts

Fatty Acid	(Weight %)				
	Adult		Infant		
	GM 3440 (Nml)	AdG 1470 (Type 1)	GM 302A (Nml)	InG 1247 (Type 2)	GM 877 (Type 2)
14:0	1.3	0.8	2.7	3.4	2.7
16:0	24.6	26.4	39.7	25.7	29.6
16:1	4.7	5.8	1.7	7.8	3.6
18:0	25.3	25.0	26.7	22.9	19.4
18:1	30.9	25.3	16.5	25.8	24.9
18:2	1.3	0.7	0.9	1.9	1.1
18:3	1.3	0.7	1.5	1.6	1.3
20:4	9.8	13.3	9.5	8.3	2.7
22:0	0.8	2.3	0.5	2.4	2.0
24:0	- ^a	-	-	-	10.0

^aTrace amounts.

the same; this was also true for type 2 Gaucher cells (InG 1247) as compared with normal infants. In GM 877, type 2 Gaucher cells, there was increase in amounts of C24:0 as compared to normal cells.

Table 14 shows the fatty acid composition of phosphatidyl-ethanolamine of the various cell lines. It can be seen in this table that there was increased amount of C18:1 in normal adult fibroblast as compared with type 1 Gaucher cells. Whereas, there was considerable increased amount of C16:0, C18:0 and decreased amount of C18:1 and C20:4 in normal cells as compared with type 2 Gaucher cells (InG 1247). In another type 2 Gaucher cell line, GM 877, there was decreased amount of C18:1 and decreased amount of C18:0 as compared with normal infant cells. It should also be noted that the fatty acid composition of phosphatidylethanolamine was different from that of phosphatidylcholine.

Table 15 shows the fatty acid composition of sphingomyelin of the various fibroblastic cell lines. Type 1 Gaucher fibroblasts sphingomyelin had a decreased amount of C16:0 and an increased amount of C18:0 and C22:0 as compared to normal adult sphingomyelin fatty acids. Sphingomyelin from Type 2 Gaucher fibroblast (InG 1247) had a considerable increased amount of C16:1 and C24:0 and a decreased amount of C16:0 and C18:0 as compared to normal. In another type 2 Gaucher cell line, GM 877, there was an increase in amount of C16:1 and some decrease in C18:0. It is also to be noted that there was a difference between normal adult and infant cells with respect to their sphingomyelin fatty acid content. And also, the fatty acid composition

TABLE 14.--Fatty Acid Composition of Phosphatidylethanolamine of Fibroblasts

Fatty Acid	(Weight %)				
	Adult		Infant		
	GM 3440 (Nml)	AdG 1470 (Type 1)	GM 302A (Nml)	InG 1247 (Type 2)	GM 877 (Type 2)
14:0	- ^a	-	1.9	-	2.4
16:0	9.3	6.6	19.7	-	18.0
16:1	0.8	-	-	1.4	2.4
18:0	27.9	36.0	42.6	28.9	32.2
18:1	23.6	14.2	15.5	23.5	30.0
18:2	-	-	4.5	3.2	1.9
18:3	-	-	-	5.2	1.3
20:4	38.4	43.2	9.2	29.5	8.8
Other	-	-	6.7	8.3	3.0

^aTrace amounts.

TABLE 15.--Fatty Acid Composition of Sphingomyelin of Fibroblasts

Fatty Acid	(Weight %)				
	Adult		Infant		
	GM 3440 (Nm1)	AdG 1470 (Type 1)	GM 302A (Nm1)	InG 1247 (Type 2)	GM 877 (Type 2)
16:0	52.8	23.7	48.7	27.2	49.2
16:1	2.7	- ^a	-	31.3	13.9
18:0	18.8	42.6	18.1	4.4	10.9
18:1	10.5	4.2	-	-	-
22:0	15.2	29.5	13.8	9.8	9.3
24:0	-	-	19.4	27.4	16.7

^aTrace amounts.

of sphingomyelin was different from that of phosphatidylcholine and phosphatidylethanolamine.

Table 16 shows the fatty acid composition of phosphatidylserine of various fibroblastic cell lines. It can be seen from the table that type 1 and type 2 Gaucher fibroblast phosphatidylserine fatty acids had an increased amount of C14:0, C16:0, C16:1, and C18:1 as compared to normal adult; whereas, there was decreased amounts of C18:0 and C20:4. Table 17 shows the fatty acid composition of phosphatidylinositol and it can be seen that there was an increased amount of C16:0, C16:1, and C18:1, whereas, there was decreased amount of C14:0 and C18:0 in type 2 Gaucher cells.

The fatty acids of cholesterol esters were also analyzed for normal and Gaucher diseased cell lines. Table 18 shows that the major saturated fatty acids for cholesterol ester were C14:0, C16:0, and C18:0, and the major unsaturated fatty acids were C16:1, C18:1, C18:2, and C18:3. As compared to normal adult cells, type 1 Gaucher cells (AdG 1470) had a dramatic increase in the amount of C14:0 and a reduction of C18:1. As compared with normal infant cholesterol ester fatty acid, type 1 infant Gaucher cells had a relative increase in C16:0, and C18:1. Type 2 infant Gaucher cells had an increased amount of C16:0, C16:1, C18:0 and C18:1. Type 3 juvenile Gaucher cells had an increased amount of C18:1 and C18:2.

In Table 18 it is also shown that there was an unidentified peak in cholesterol ester from normal cell lines which was not observed in all three types of Gaucher disease. Hydrogenation on the fatty acid methyl esters of normal infant cholesterol ester was performed

TABLE 16.--Fatty Acid Composition of Phosphatidylserine of Fibroblasts

Fatty Acid	(Weight %)				
	Adult		Infant		
	GM 3440 (Nml)	AdG 1470 (Type 1)	GM 302A (Nml)	InG 1247 (Type 2)	GM 877 (Type 2)
14:0	- ^a	3.2		-	-
16:0	-	14.1	n.d. ^b	29.6	18.4
16:1	-	5.8		1.9	11.6
18:0	49.0	32.4		24.7	34.2
18:1	5.0	14.4		25.6	13.5
20:4	45.0	30.1		18.2	22.3

^aTrace amounts.

^bn.d. denotes not determined.

TABLE 17.--Fatty Acid Composition of Phosphatidylinositol of Fibroblasts

Fatty Acid	(Weight %)			
	Adult		Infant	
	GM 3440 (Nm1)	AdG 1470 (Type 1)	GM 302A (Nm1)	InG 1247 (Type 2)
14:0	- ^a	n.d. ^b	19.5	-
16:0	-		7.0	39.6
16:1	-		-	6.0
18:0	50.0		60.2	36.3
18:1	2.4		-	4.3
20:4	47.6		13.2	13.7

^aTrace amounts.

^bn.d. denotes not determined.

TABLE 18.--Fatty Acid Composition of Cholesterol Ester of Fibroblasts

Fatty Acid	(Weight %)					
	Adult		Infant			
	GM 3440 (Nm1)	AdG 1470 (Type 1)	GM 302A (Nm1)	GM 4394 (Type 1)	InG 1247 (Type 2)	JuvG (Type 3)
14:0	1.9	26.7	10.2	15.1	11.9	15.2
16:0	23.5	21.9	16.2	21.3	24.7	11.5
16:1	7.3	1.4	2.4	5.9	7.3	4.3
18:0	16.8	26.3	23.6	21.5	31.3	22.5
18:1	39.4	4.9	10.2	21.5	17.9	21.2
18:2	2.7	9.7	10.7	14.1	6.8	25.2
18:3	2.9	9.2	- ^a	0.5	-	-
Other	6.5	-- ^b	26.7	--	--	--

^aTrace amounts.

^bNot detectable.

to check if this unidentified fatty acid had any double bonds. Hydrogenation yielded a peak in the C24:0 region. Thus, it is most likely that cholesterol ester of normal fibroblasts have a unique unsaturated fatty acid, C24 (number of double bonds unidentifiable), which is not found in Gaucher Disease.

Membrane Fluidity and Correlation with Various Lipid Ratios

Table 19 shows the cholesterol/phospholipid (mole/mole) and cholesterol/sphingomyelin (mole/mole) ratio for individual cell lines, along with the fluorescence anisotropy values. It can be seen that there was an increase in the aforementioned lipid ratios of cells from type 2 and type 3 Gaucher disease, along with significant decrease in fluidity; whereas, for type 1 infant cells, there was no alteration in membrane fluidity, along with relatively little change in the relevant lipid ratios. With respect to normal adult cells, type 1 adult Gaucher cells exhibited a variability of data with respect to membrane fluidity as well as the lipid ratios. In the cell line AdG 119a, there was no altered membrane fluidity; however, there seemed to be an increase in cholesterol/phospholipid and cholesterol/sphingomyelin ratios. With respect to the cell line AdG 1470, which had an increased anisotropy (decreased membrane fluidity), there was no increased cholesterol/phospholipid or cholesterol/sphingomyelin ratio encountered. Sphingomyelin/phosphatidylcholine as well as sphingomyelin/phospholipid ratios were also determined and no correlation with the fluidity measurements could be observed. It is interesting to note that even though there was decreased fluidity in normal adult fibro-

TABLE 19.--Fluorescence Anisotropy Values with Relevant Lipid Ratios

	r_s	C/PL	C/SPM	SPM/PL	SPM/PC
Nml Infant					
GM 302A	0.182 \pm .006	0.164	0.78	0.206	0.395
Type 1 Infant					
GM 4394	0.192 \pm .009	0.166	0.64	0.301	0.718
Type 2 Infant					
a. InG 1247	0.225 \pm .013	0.300	2.88	0.102	0.198
b. GM 877	0.231 \pm .016	0.361	1.61	0.224	0.706
Type 3 Juvenile					
JuvG	0.216 \pm .005	0.300	2.06	0.146	0.250
Nml Adult					
a. GM 3440	0.198 \pm .012	0.164	0.70	0.232	0.474
b. Nml F	0.205 \pm .008	n.d.	n.d.	n.d.	n.d.
Type 1 Adult					
a. AdG 119a	0.191 \pm .004	0.260	1.60	0.166	0.373
b. AdG 1470	0.223 \pm .009	0.152	0.68	0.220	0.520

Definition of symbols:

C/PL, $\frac{\text{Cholesterol (mol)}}{\text{Phospholipid (mol)}}$; C/SPM, $\frac{\text{Cholesterol (mol)}}{\text{Sphingomyelin (mol)}}$; SPM/PL, $\frac{\text{Sphingomyelin (mol)}}{\text{Phospholipid (mol)}}$;

SPM/PC, $\frac{\text{Sphingomyelin (mol)}}{\text{Phosphatidylcholine (mol)}}$.

Each ratio is the ratio of the means.

blasts as compared with normal infant fibroblasts, there was no alteration in the cholesterol/phospholipid or cholesterol/sphingomyelin ratios.

CHAPTER V

DISCUSSION

Relevance of Membrane Fluidity

DPH Incorporation

Cultured human skin fibroblasts have a measurable membrane fluidity via steady-state fluorescence anisotropy using the fluorescent hydrocarbon probe DPH. DPH gets incorporated into fibroblast membranes and gives characteristic excitation and emission spectra with a relative excitation maximum at 360 nm and emission maximum at 426 nm. The lipid-probe molar ratio is calculated to be approximately 10^4 - 10^5 , which is well above the range to avoid energy transfer and excimer formation between probe molecules; this is since Kawato et al. (1977) have recommended a lipid-probe molar ratio of at least 10^3 to avoid these fluorescence phenomenon. It can also be seen in this study that fibroblasts have an intrinsic fluorescence which is similar in all the cell lines (normal and Gaucher) investigated. The emission and excitation spectra are similar for both normal and diseased fibroblasts. They are also comparable to spectra obtained by other investigators on fibroblasts as well as other types of cells (Shinitzky & Inbar, 1974; Van Blitterswijk et al. 1977; Lakowicz & Sheppard, 1981; Schroeder et al., 1984).

It is believed that once DPH gets incorporated into biological

membranes, it aligns itself parallel to the fatty acyl chains in the middle of the bilayer (Lentz et al., 1976a,b). In intact cells, the fluorescent probe gets incorporated not only in plasma membranes, but also in cytoplasmic membranes. The exact amount of probe into each membrane component is not known at this moment. However, it is believed that in short term incubation (few minutes), fluorescence parameters of DPH characterize the plasma membrane; whereas, long term incubation (up to 90 minutes) characterize both the plasma membrane and intracellular membrane lipid characteristics (Pagano, et al., 1977; Bouchy et al., 1981). It is possible to calculate plasma membrane fluidity in intact cells labeled with DPH by selective quenching, nonradiative energy transfer, of the fluorescence emitted from the plasma membrane after tagging the cell with an impermeable membrane electron acceptor such as 2,4,6-trinitrobenzene sulfonate (TNBS) (Grumberger et al., 1982).

Fluorescence Anisotropy

In this study, the objective was to determine the membrane fluidity of physiological viable Gaucher cells and to compare them to normal fibroblasts and relate this to the lipid abnormalities which occur. As can be seen from Figure 7, the fluorescence anisotropy of both normal and diseased cells remain relatively constant for the times investigated implying that once the probe gets incorporated into the lipid pools, the average distance between the embedded DPH molecules is high enough to avoid intermolecular transfer of excitation energy (Shinitzky & Inbar, 1974, 1976). It also implies that for

all the times investigated, the compartmentalization of DPH in plasma membrane as well as the cytoplasmic membranes is approximately the same in the cell. It can also be concluded that the probe incorporation in normal and diseased cells is approximately the same in each compartment since there is no change in fluorescence anisotropy measurements with respect to time of incubation of DPH, taking into account the freely diffusing property of DPH (Shinitzky & Barenholz, 1978).

There are several methods which can be used to measure the fluorescence anisotropy of intact cells. One of the ways in which one can measure the anisotropy of intact cells is to treat the cells with the fluorescent probe and then detach them from the surface of the flask with EDTA or trypsin (Fuchs et al., 1975; DeLaat, et al., 1977; Haggerty et al., 1978) and then use the suspension for fluidity measurements. It is possible that this may impair the lipid-protein interactions within the cell membrane. Therefore, another method has been set up for cultured cells where fluorescence polarization can be determined for cells attached to a glass substratum (DeLaat et al., 1977). Measurements of neuroblastoma cells with this methodology suggest that EDTA and trypsin detachment decrease the apparent membrane fluidity. The problem with this type of measurement seems to be that it does not correct for scattering which might occur due to the cells on the glass substratum. In this study, trypsinization treatment for detaching the cells was chosen since we wanted to compare the average fluorescence anisotropy of Gaucher fibroblasts with that of normal cells. Even though this might give an apparent fluidity

measurement, it is useful for comparison. Along with this, it is suspected that DPH in most biological membranes gives information regarding lipid-lipid interaction and, thus, trypsin treatment which destroys lipid-protein interactions may not have a significant effect on the fluidity measurements (Van Blitterswijk et al., 1977, 1981; Pottel et al, 1983).

In relation to the discussion above, steady-state fluorescence measurements were performed on several fibroblastic cell lines from both normal and Gaucher disease subjects. At 25°C, as compared with normal infant cells (GM 302A), type 1 Gaucher cells (GM 4394) did not exhibit any difference in the fluorescence anisotropy value; thus, no change in microviscosity or order parameter was seen. In contrast to this, type 2 Gaucher cells (InG 1247 and GM 877) and type 3 Gaucher cells (JuvG) had a significant increase in the fluorescence anisotropy values and, thus, an increase in the apparent microviscosity as well as order parameter. As compared with normal adult fibroblasts, type 1 Gaucher cells exhibited a variability of data. One of the cell lines, AdG 119a, did not exhibit any difference in the fluorescence anisotropy value; whereas, AdG 1470 did have a significantly increased fluorescence anisotropy value and thus the apparent microviscosity and order parameter were increased.

Cholesterol/Phospholipid and Cholesterol/Sphingomyelin Ratios

The decreased fluidity in type 2 and type 3 Gaucher disease cells also correlated well with the increased cholesterol/phospholipid and cholesterol/sphingomyelin ratios. With respect to type 1 infant

Gaucher cells, there was no altered membrane fluidity as well as no change in the aforementioned lipid ratios. This finding of altered membrane fluidity correlating with altered cholesterol/phospholipid ratio agrees well with several investigators (Pottel et al., 1983; Shinitzky & Barenholz, 1978; Owen et al., 1982). The correlation of altered membrane fluidity with cholesterol/sphingomyelin ratio has not been presented previously. This correlation, however, seems justified in the sense that Patton (1970) has theoretically proposed a tight association between cholesterol and sphingomyelin in various biological membranes. The tight association between cholesterol and sphingomyelin has been shown to occur in model membranes (Barenholz & Thompson, 1980). Also, Van Blitterswijk et al. (1981) have correlated an increased fluidity with a decreased cholesterol/phospholipid ratio and, when this lipid ratio was constant, this was attributed to a decrease in sphingomyelin/total phospholipid ratio. These authors have also suggested that cholesterol is the primary important parameter and sphingomyelin is the secondary important factor determining structural order in biomembranes. Association of cholesterol and sphingomyelin also seems important in acanthocytes (which have decreased fluidity) as shown by Barenholz et al. (1981). These authors treated acanthocytes and normal erythrocyte membranes with cholesterol oxidase and noted that the fluidity of normal and diseased cells was approximately the same. This was then interpreted to mean that membrane fluidity is dependent upon normal interactions of cholesterol with phospholipids (especially sphingomyelin and phosphatidylcholine).

The association between cholesterol/phospholipid and choles-

terol/ sphingomyelin ratios to membrane fluidity in adult type 1 Gaucher cells did not follow the same pattern as that for the infant cells. For one of the cell lines which had no alteration in membrane fluidity as compared to normal adult cells, there seemed to have been some increase in the relevant lipid ratios. Whereas, for the type 1 Gaucher cell line which had a significant increase in the fluorescence anisotropy measurement, there was no change in the lipid ratios. This could be explained in several ways. One explanation for the cell line AdG 119a having a constant anisotropy value with an increased cholesterol/phospholipid ratio could be that these cells have adapted their lipid concentration and phospholipid fatty acid such as to attain a "homeoviscous" state. This homeoviscous adaptation phenomenon has been observed in murine fibroblasts (LM cells) where alteration in phospholipid polar headgroups led to alteration in fatty acid content of the phospholipids and along with this, no change in membrane fluidity occurred (Schroeder, 1978).

It is useful to note that there was a significant difference between the steady-state fluorescence anisotropy value between normal infant fibroblasts and normal adult fibroblasts. The data presented in Table 7 show that normal infant fibroblasts had an increased membrane fluidity, since there was a decreased value of fluorescence anisotropy. The decreased membrane fluidity of aged cells has been investigated previously in red blood cells by monitoring the electron paramagnetic resonance spectra of fatty acid spin labels incorporated into the membranes (Shiga et al., 1979). In this study by Shiga, et al., there was decreased membrane fluidity in aged human erythro-

cytes and it is suggested that this was in part due to lipid/protein ratio, the modified protein-lipid interaction and/or the influences of diminished ATP content. There was no change in cholesterol/phospholipid ratio observed. As another example of decreased membrane fluidity of aging membranes, Nagy et al. (1983) have shown by electron spin resonance, using modified stearic acid as a probe of synaptosomal membranes of rat brain cortex, that there is significantly decreased fluidity in older rat brain synaptosomes. Therefore, in this study, it is not surprising to find decreased fluidity in fibroblast membranes from adults as compared with normal infant cells. As can be seen from Table 19, there was no difference in the lipid ratios for normal adult and infant cells. The reason for the altered fluidity could possibly be altered lipid-protein interactions, amount of ATP changes (Shiga et al., 1979) or altered fatty acids of phospholipids. It is also to be noted that there was no passage effect observed in the evaluation of membrane fluidity of fibroblasts and is consistent with the findings of Haggerty et al. (1978). It is believed that fibroblasts have a limited lifetime in culture and they "age" with increasing passage. However, this "aging" did not contribute significantly to alter the membrane fluidity (Table 20).

Temperature Scans and Arrhenius Plots

Along with the changes observed in fluorescence anisotropy and membrane fluidity of different fibroblastic cell lines at 25°C, temperature studies also revealed the same results as that for 25°C. As compared with normal infant fibroblasts, type 2 and type 3 Gaucher

TABLE 20.--Passaging of Fibroblasts and Its Effect on Fluorescence Anisotropy (r_s)

GM 3440 & Nml F (Nml Adult)		GM 302A (Nml Infant)	
Passage Number	r_s	Passage Number	r_s
13	0.287	17	0.259
14	0.259	18	0.247
14	0.277	19	0.247
17	0.256		
33	0.269		
34	0.279		
37	0.289		

cells had an increased fluorescence anisotropy values between 4-40°C. For the type 1 adult cell line which had an increased value of anisotropy at 25°C temperature scan study revealed the same phenomena occurring between 4-40°C. It is interesting to note that as the temperature increases, the fluorescence anisotropy decreases--which agree well with the observation that as the temperature increases, membrane fluidity increases as well.

From the temperature scans and anisotropy values, Arrhenius plots ($\log r_s$ versus $1/\text{temperature } [^{\circ}\text{K}]$) were determined for normal and diseased cells. As could be determined from the Arrhenius plots, there were no phase transitions detectable in either normal or Gaucher diseased fibroblast membranes. This result is in accordance with that of Haggerty et al. (1978). It is not clear from literature which type of Arrhenius plots reveal the maximum information--e.g., $\log r_s$, $\log \bar{n}$, $\log P$ or $\log \left(\frac{r}{r^0} - 1\right)^{-1}$ versus $1/T$ (Shinitzky & Barenholz, 1974; Fuchs et al., 1975; Haggerty et al., 1978; Shinitzky & Barenholz, 1978; Bottema et al., 1983; Berlin & Sainz, 1984; Nagatomo et al., 1984). In this report, $\log r_s$ versus $1/T$ curves were plotted and no phase transitions could be detected. $\log \bar{n}$, $\log P$, and $\log \left(\frac{r}{r^0} - 1\right)$ were also used in the ordinate value for Arrhenius plots and, again, no phase transitions could be detected. The possible reason for not detecting any phase transition, and thus lipid phase separation could be that DPH gives some average information of the molecular heterogenous bilayer (Shinitzki & Barenholz, 1978). Also, Ladbroke et al. (1968) have shown that cholesterol diminishes and eventually abolishes the endothermic lipid phase transition of phos-

pholipids. Concentration of 10 mole percentage cholesterol eliminates the pre-transition of phosphatidylcholines. In biological membranes, therefore, cholesterol could be interacting with phospholipid fatty acyl chains in such a way as to abolish phase transition (Barenholz et al., 1981). It also seems worth to note that cholesterol and phospholipids are probably interacting in a similar fashion in both normal and Gaucher diseased cells such as to give no lipid phase transitions between 4-40°C.

The differences of slopes in Arrhenius plots of normal from Gaucher diseased fibroblasts probably implies that the flow activation energy of lipids in membranes is different (Shinitzky & Barenholz, 1978). The change in the intercept of normal versus Gaucher cells reflects the fact that Gaucher cells have an increased microviscosity at all temperatures between 4-40°C.

As an interesting further study, it would be useful to study the fluidity of various fibroblast membranes from normal cells and compare this to membranes from Gaucher fibroblasts. In particular, attention must be given to plasma membrane fluidity since much of the intact cell membrane fluidity arises from these membranes. Also, lysosomal membrane fluidity should be discerned since Gaucher disease is a lysosomal membranous enzymopathy. Lipid composition of plasma membranes and lysosomal membranes must also be investigated and correlated with membrane fluidity measurements. The fluidity measurements should also be carried out in several related lysosomal enzymopathy of sphingolipids to determine if there are membrane abnormalities in these diseases and if any correlations occur.

Relevance of Neutral Lipid, Phospholipid,
and Ceramide Composition of Fibroblasts

It has been reported by Saito and Rosenberg (1984a) that Gaucher disease fibroblasts do not have an increased accumulation of glucosylceramide as compared with normal cells (1.23 ± 0.08 nmole/mg of protein for Gaucher cells, 1.11 ± 0.48 nmole/mg of protein for normal infant cells). However, there is some alteration of higher neutral glycosphingolipids as well as gangliosides in Gaucher cells. Until recently, the quantity of other lipids in Gaucher diseased fibroblasts (neutral lipids, phospholipids, and ceramide) has not been investigated. Abnormalities in phospholipid have been suggested by Barton and Rosenberg (1974) and cholesterol content in one of the cell lines from Gaucher disease has been determined by Warren et al. (1976) as discussed previously.

Neutral Lipid Composition

Table 9 shows the neutral lipid analysis for normal and Gaucher diseased cells. Neutral lipids were analyzed by high performance thin-layer chromatography and densitometry. The developing solvent system used has not been reported previously and it was able to discern between cholesterol, free fatty acids, triglycerides, and cholesterol ester. From this methodology, the amount of each neutral lipid was determined. As compared with normal infant fibroblasts, type 1 Gaucher cells had significantly decreased values of triglycerides and cholesterol ester; whereas, there was no difference with respect to the cholesterol and free fatty acid content. Type 2 infant cells had approximately the same content of cholesterol, free fatty acid, and

triglycerides; whereas, there may have been some decrease in the cholesterol ester content (not statistically significant). Type 3 cells had a similar neutral lipid content as that of type 2 fibroblasts. Normal adult cells did not exhibit any difference, in neutral lipid content, from normal infant cells. Type 1 adult cells had decreased triglyceride and cholesterol ester content as compared to normal adult. This finding that cholesterol ester may be decreased in all three types of Gaucher cells, and triglyceride decreased in type 1 Gaucher disease has not been reported previously. Therefore, even though there is decrease in activity of only one enzyme (β -glucosidase) in Gaucher disease which leads to abnormal glycosphingolipid content, there are other lipid abnormalities which can also occur. This is similar to Niemann-Pick disease, type D, in which there is deficiency of lysosomal sphingomyelinase which leads to increased accumulation of the phospholipid sphingomyelin in the spleen as well as other tissues; along with this, cholesterol, cholesterol ester, total phospholipids and bis-(mono-acylglyceryl) phosphate are also increased above the normal range (Rao & Spence, 1977).

Phospholipid Composition

The major phospholipids in fibroblasts were sphingomyelin, phosphatidylcholine, phosphatidylserine, phosphatidylinositol and phosphatidylethanolamine as represented in Table 10. As compared with normal infant fibroblasts, there seemed to be somewhat decreased amounts of phosphatidylcholine in type 1 cells. Type 2 cells possibly had both a decreased amount of sphingomyelin and phosphatidylcholine.

Type 3 cells had on the average, decreased amounts of sphingomyelin. With respect to normal adult cells, type 1 adult cells exhibited a variability of data. AdG 119a seemed to have decreased amounts of sphingomyelin and phosphatidylcholine; whereas, there was no difference in the phospholipid content of AdG 1470 as compared with normal adult cells.

The decrease in sphingomyelin, phosphatidylcholine and cholesterol ester of Gaucher cells could possibly be due to the fact that since there is deficiency of the lysosomal enzyme β -glucosidase in Gaucher diseased fibroblasts, there may be a compensatory increase in the other lysosomal enzymes such as sphingomyelinase, phospholipases and cholesterol esterase. It has been suggested by Rapoport and Ginns (1984) and Besley and Moss (1984) that there is an increase in activity of lysosomal sphingomyelinase in the cells of patients with Gaucher disease. It is also possible that neutral sphingomyelinases (non-lysosomal) could have an increased activity, thereby, leading to increased degradation of membrane sphingomyelin. However, Sutrina and Chen (1984) have shown that in normal cellular metabolism of plasma membrane-associated sphingomyelin, majority of it is hydrolyzed by lysosomal sphingomyelinases and a minor fraction is degraded by non-lysosomal neutral sphingomyelinases. It is possible, with respect to decreased phosphatidylcholine content in Gaucher diseased cells, that plasma membrane phospholipases could be altered such as to have increased activity. It is also possible that the synthesis of phosphatidylcholine in Gaucher cells is inhibited, since there is decreased amount of sphingomyelin; and thus, the direct enzyme-mediated

transfer of phosphorylcholine from sphingomyelin to diglyceride does not occur (Spence et al., 1983). The increased activity in cholesterol esterase could be due to the general compensatory increase in enzymes. If it is the case that lysosomal sphingomyelinase, phospholipases, and cholesterol esterase are relatively increased in Gaucher diseased cells this would then imply that there is a tight association between β -glucosidase and the aforementioned enzymes. The fact that there is also decreased amounts of triglycerides in type 1 Gaucher disease could be that there is some type of β -glucosidase isozyme deficiency or a presence of a factor which is stimulating the activity of triglycerol lipase.

Ceramide Composition

The data obtained that the content of ceramide is virtually the same in normal and Gaucher diseased fibroblasts implies that the activity of lysosomal ceramidase is probably not altered in diseased cells. It is also to be noted that the levels of ceramide could be important in cell homeostasis (Kannagi et al., 1982) similar to cholesterol, and thus a constant level has to be established. It seems interesting that ceramide, a precursor to all the glycosphingolipids, is constant in Gaucher cells; whereas, glycosphingolipids are increased in Gaucher cells (Saito & Rosenberg, 1984a). This constant ceramide level in Gaucher cells are most likely occurring due to increase synthesis of ceramide from sphingosine and fatty acids. Thus, even though the catabolic pathway of glucosylceramide is decreased, the anabolic starting substrate, ceramide, is tightly controlled.

Effects of Monensin

The finding that monensin treated normal cells give rise to decreased cholesterol ester and phosphatidylcholine leads one to suspect that monensin could serve as a chemical modifier which gives rise to effects similar to Gaucher disease. This is since monensin leads to increased glucosylceramide (Saito et al., 1984) and decreased cholesterol ester and phosphatidylcholine in normal fibroblasts. These lipid abnormalities do not arise from increased lysosomal enzyme activities since it is believed that lysosomal functions are inhibited by monensin by increased pH (Tartakoff, 1983). It is possible that the activity of acyl coenzyme A:cholesterol O-acyltransferase (ACAT), which catalyzes the formation of cholesterol ester from cholesterol and fatty acyl coenzyme A (Chang & Doolittle, 1983), is decreased. This then would lead to decreased cholesterol ester and increased fatty acids. The (³H) acetate labeling data agrees well with the decreased ACAT activity hypothesis. The increased incorporation of labeled acetate in cholesterol possibly implies that the activity of 3-hydroxy-3-methylglutaryl coenzyme A (HMG-CoA) reductase, which leads to increased cholesterol synthesis in the cells (Chang, 1983), is increased. Also, other lipids had increased label incorporation possibly due to stimulation of other microsomal enzymes.

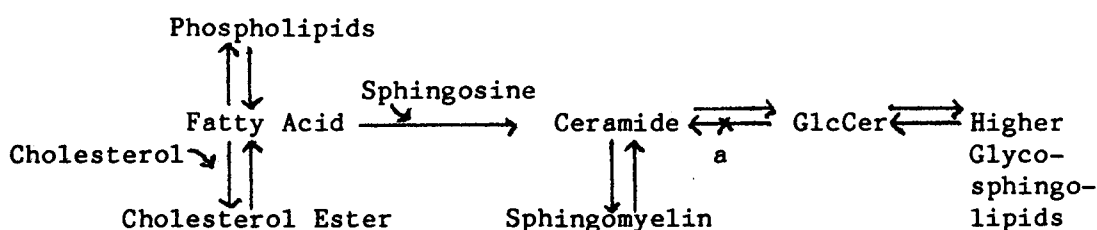
In relation to decreased phosphatidylcholine content and increased label in this phospholipid, it is possible that monensin, which is a cationophore increasing sodium levels in fibroblasts and possibly calcium levels, increases activity of membrane-bound phospholipases and, thus, increased phospholipid degradation occurs. This

is similar to accelerated phospholipid degradation, which occurs in ischemic liver disease due to increased activity of membrane-bound phospholipases activated by Ca^{2+} increase (Chien et al., 1978). The increased incorporation of (^3H) acetate label into phospholipids could be possible if monensin induces microsomal enzyme activity. The possible reason for increased phosphatidylserine content in monensin treated cells could be that the activity of microsomal phosphatidylethanolamine serine transferase, which catalyzes a calcium-dependent exchange between L-serine and the ethanolamine moiety or phosphatidylethanolamine (Esko & Raetz, 1983), increases considerably. The relative stability of ceramide with respect to monensin treatment again implies that even though glucosylceramide and higher glycosphingolipids are increased, the starting substrate is highly regulated.

Fatty Acid Composition

Not only are there differences observed in the quantity of neutral lipids and phospholipids in Gaucher disease, but there are some differences in the fatty acid components of phospholipids, especially sphingomyelin, and cholesterol ester. It has been shown by Kudoh et al. (1983) that if [stearoyl-1- ^{14}C] sphingomyelin is introduced into normal cultured skin fibroblasts, it is degraded in lysosomes to [^{14}C] stearoyl-sphingosine and [^{14}C] stearic acid. This free fatty acid then enters a fatty acid pool for synthesis of the major lipids found in cultured skin fibroblasts. These lipids are identified to be phospholipids, including phosphatidylcholine and sphingomyelin, cholesterol ester, ceramide, and the ganglioside GM_3 (Kudoh & Wenger,

1982). It has been shown by Warren et al. (1976) that Gaucher cells glucosylceramide fatty acids have an increase in C16:0 and C18:0 and a decrease in C20:0 and C22:0. From this, it is possible that ceramide, phospholipids, and cholesterol ester in cultured skin fibroblasts utilize fatty acids from a common pool; and when the pool is depleted, such as in Gaucher disease where more fatty acid are used up to maintain a normal level of ceramide and an increased quantity of glycosphingolipids, there will be alteration in fatty acid composition of related lipids. The association of abnormalities in glycosphingolipid, sphingomyelin and cholesterol ester fatty acids could be summarized diagrammatically as follows:



In normal fibroblasts, glucosylceramide is catabolised in a normal fashion (pathway a) and thus enough fatty acid is available in the "pool" for incorporation into other lipids. However, in contrast, Gaucher diseased fibroblasts have decreased catabolism of glucosylceramide and thus the fatty acid pool is disturbed, leading to alterations in glucosylceramide, sphingomyelin, cholesterol ester and phospholipid fatty acid composition. As a further study, it would therefore be useful to study fatty acid metabolism in normal and Gaucher diseased cultured skin fibroblasts.

The finding that the cholesterol ester in Gaucher fibroblasts

do not have the unsaturated C24 fatty acid implies, again, that the metabolism of fatty acids is different from that of normal cells. This fatty acid was not observed by Goldstein et al. (1975) in normal cultured skin fibroblasts. The only C24 unsaturated fatty acid in cholesterol ester has been identified as C24:4 in pork testis by Holman and Hofstetter (1965). Thus, it is possible that normal fibroblasts have the ability to synthesize C24:4; whereas, Gaucher cells cannot synthesize this polyunsaturated fatty acid.

CHAPTER VI

SUMMARY

Membrane fluidity measurements, via steady-state fluorescence anisotropy of 1,6-diphenyl-1,3,5-hexatriene, were performed on cultured human skin fibroblasts from normal and hereditary lysosomal β -glucosidase deficient (Gaucher disease) subjects. At 25°C, type 2 and type 3 neuronopathic Gaucher diseased fibroblasts displayed decreased membrane fluidity as compared with normal fibroblasts. Type 1 non-neuronopathic Gaucher cells exhibited variability. Of the three cell lines with the type 1 (non-neuronopathic) variety of Gaucher disease, only one had decreased membrane fluidity as compared with normal fibroblasts. Abnormality in membrane fluidity of the diseased cells was correlated with an increase in cholesterol/phospholipid and cholesterol/sphingomyelin ratios.

Temperature scan studies of fluorescence anisotropy, between 4-40°C, on normal and Gaucher diseased fibroblasts gave the same results as at 25°C. From the temperature scans, Arrhenius plots were constructed to determine bulk lipid phase transitions. As could be determined from the Arrhenius plots, there were no phase transitions detectable over this range in either normal or Gaucher diseased fibroblast membranes.

Neutral lipid, phospholipid and ceramide composition of normal

and Gaucher diseased fibroblasts were determined. The major neutral lipids were observed to be cholesterol, free fatty acid, triglyceride and cholesterol ester. Types 1, 2 and 3 Gaucher diseased fibroblasts exhibited a significant decrease in cholesterol ester as compared with appropriate controls. Type 1 Gaucher cells also had a lower content of triglyceride. Analysis of the fatty acids in cholesterol esters of normal and Gaucher diseased cells was performed, and it was determined that there was a major difference between the normal and the diseased cells.

The major phospholipids of cultured skin fibroblasts were sphingomyelin, phosphatidylcholine, phosphatidylserine, phosphatidylinositol and phosphatidylethanolamine. As compared with normal infant cells, there seemed to be a decreased content of phosphatidylcholine in type 1 Gaucher cells and, in type 2 Gaucher cells, possibly a decreased amount of sphingomyelin and phosphatidylcholine. Type 3 Gaucher cells had a remarkably decreased amount of sphingomyelin. Type 1 adult Gaucher cells exhibited variability. Fatty acid analysis of individual phospholipids were also performed, and it was determined that there was a significant difference in fatty acid composition of diseased cells--especially sphingomyelin. The content of ceramide was virtually the same in normal and Gaucher diseased fibroblasts.

Normal cultured skin fibroblasts were treated with the carboxylic monovalent cationophore monensin to determine its effect on neutral lipid, phospholipid and ceramide composition. Treatment with monensin decreased the amount of cholesterol ester and phosphatidylcholine, and increased the content of free fatty acid and phosphatidyl-

serine. When the cells were also labeled with [^3H] acetate, there was increased incorporation of the label into all lipids except into cholesterol ester, where it was decreased, and sphingomyelin and ceramide, where the incorporation was relatively constant. The pattern due to monensin treatment seems to be similar to that observed in Gaucher disease.

The findings that membrane fluidity and various lipids, including glycosphingolipids, are altered in Gaucher disease indicates that even though there is hereditary deficiency of only one lysosomal enzyme, β -glucosidase, this leads to more generalized membrane effects. These pronounced metabolic effects are seen in altered membrane fluidity and neutral lipid, phospholipid and fatty acid composition of Gaucher diseased fibroblasts.

BIBLIOGRAPHY

- Balint, J. A., Spitzer, H. L., and Kyriakides, E. C. (1963) Studies of red-cell stromal lipids in Tay-Sachs Disease and other lipidoses. J. Clin. Invest. 42:1661-1668.
- Barenholz, Y. and Thompson, T. E. (1980) Sphingomyelins in bilayers and biological membranes. Biochim. Biophys. Acta 604:129-158.
- Barenholz, Y., Yechiel, E., Cohen, R. and Deckelbaum, R. J. (1981) Importance of cholesterol-phospholipid interaction in determining dynamics of normal and abetalipoproteinemia red blood cell membrane. Cell Biophys. 3:115-126.
- Barroin, A., Thomas, D. D., Osborne, B., and Devaux, P. F. (1977) Saturation transfer electron paramagnetic resonance on membrane-bound proteins. I-Rotational diffusion of rhodopsin in the visual receptor membrane. Biochem. Biophys. Res. Commun. 78:442-447.
- Barton, N. W. and Rosenberg, A. (1974) Metabolism of glucosyl [³H] ceramide by human skin fibroblasts from normal and glucosylceramidotic subjects. J. Biol. Chem. 250:3966-3971.
- Berlin, E. and Sainz, E. (1984) Fluorescence polarization order and phase transitions in lipids and lipoproteins. Biochim. Biophys. Acta 794:49-55.
- Besley, G. T. N. and Moss, S. E. (1983) Studies on sphingomyelinases and β -glucosidase activities in Niemann-Pick Disease variants. Phosphodiesterase activities measured with natural and artificial substrates. Biochim. Biophys. Acta 752:54-64.
- Beverstock, G. C. and Pearson, P. L. (1981) Membrane fluidity measurements in peripheral cells from Huntington's Disease patients. J. Neurol. Neurosurg. Psych. 44:684-689.
- Borochoy, H., Zahler, P., Wilbrandt, W. and Shinitzky, M. (1977) The effect of phosphatidylcholine to sphingomyelin mole ratio on the dynamic properties of sheep erythrocyte membrane. Biochim. Biophys. Acta 470:382-388.
- Bottema, C. D. K., McLean-Bowen, C. A. and Parks, L. W. (1983) Role of sterol structure in the thermotropic behavior of plasma

membranes of Saccharomyces cerevisiae. Biochim. Biophys. Acta 734:235-248.

- Bouchy, M., Donner, M. and Andre, J. C. (1981) Evolution of fluorescence polarization of 1,6-diphenyl-1,3,5-hexatriene (DPH) during the labelling of living cells. Exp. Cell. Res. 133:39-46.
- Brady, R. O. and Barranger, J. A. (1983) Glucosylceramide lipidosis: Gaucher's Disease. In The Metabolic Basis of Inherited Disease. J. B. Stanbury, J. B. Wyngaarden, D. S. Fredrickson, J. L. Goldstein, and M. S. Brown, Eds. 5th ed. New York: McGraw-Hill, pp. 842-856.
- Brady, R. O., Kanfer, J. N. and Shapiro, D. (1965) Metabolism of glucocerebroside. II. Evidence of an enzymatic deficiency in Gaucher's Disease. Biochem. Biophys. Res. Commun. 18: 221-225.
- Cantor, C. R. and Schimmel, P. R. (1980) Biophysical Chemistry. Part II: Techniques for the Study of Biological Structure and Function. Vol. II. San Francisco: W. H. Freeman and Company, pp. 525-537.
- Castuma, C. E. and Brenner, R. R. (1983) Effect of fatty acid deficiency on microsomal membrane fluidity and cooperativity of the UDP-glucuronyltransferase. Biochim. Biophys. Acta 729:9-16.
- Chang, T.-Y. (1983) Mammalian HMG-CoA reductase and its regulation. In The Enzymes. P. D. Boyer, Ed. Vol. XVI, 3rd ed. New York: Academic Press, pp. 491-521.
- Chang, T.-Y. and Dolittle, G. M. (1983) Acyl coenzyme A: Cholesterol O-acyltransferase. In The Enzymes. P. D. Boyer, Ed. Vol. XVI, 3rd ed. New York: Academic Press, pp. 523-539.
- Chapman, D. (1983) Biomembrane fluidity: The Concept and its development. In Membrane Fluidity in Biology. R. C. Aloia, Ed. Vol. 2. New York: Academic Press, pp. 5-42.
- Chatterjee, S., Sekerke, C. S. and Kwiterovich, P. O., Jr. (1976) Alterations in cell surface glycosphingolipids and other lipid classes of fibroblasts in familial hypercholesterolemia. Proc. Natl. Acad. Sci. U.S.A. 73:4339-4343.
- Chen, W. W., Moser, A. B. and Moser, H. W. (1981) Role of lysosomal acid ceramidase in the metabolism of ceramide in human skin fibroblasts. Arch. Biochem. Biophys. 208:444-455.

- Chien, K. R., Abrams, J., Serroni, A., Martin, J. T. and Farber, J. L. (1978) Accelerated phospholipid degradation and associated membrane dysfunction in irreversible, ischemic liver cell injury. J. Biol. Chem. 253:4809-4817.
- Christie, W. W. (1982) Lipid Analysis. 2nd ed. New York: Pergamon Press, p. 61.
- Cooper, R. A., Diloy-Puray, M., Lando, P. and Greenberg, M. S. (1972) An analysis of lipoproteins, bile acids, and red cell membranes associated with target cells and spur cells in patients with liver disease. J. Clin. Invest. 51:3182-3192.
- Cooper, R. A., Durocher, J. R. and Leslie, M. H. (1977) Decreased fluidity of red cell membrane lipids in abetalipoproteinemia. J. Clin. Invest. 60:115-121.
- Cooper, R. A., Leslie, M. H., Fischkoff, S., Shinitzky, M. and Shattil, S. J. (1978) Factors influencing the lipid composition and fluidity of red cell membranes in vitro: Production of red cells possessing more than two cholesterol per phospholipid. Biochemistry 17:327-331.
- Daniels, L. B. and Glew, R. H. (1982) β -Glucosidase assays in the diagnosis of Gaucher's Disease. Clin. Chem. 28:569-577.
- Dawson, G., Matalon, R. and Dorfman, A. (1972) Glycosphingolipids in cultured human skin fibroblasts. I. Characterization and metabolism in normal fibroblasts. J. Biol. Chem. 247:5944-5950.
- DeLaat, S. W., Van der Saag, P. T. and Shinitzky, M. (1977) Microviscosity modulation during the cell cycle of neuroblastoma cells. Proc. Natl. Acad. Sci. U.S.A. 74:4458-4461.
- Desnick, R. J. (1982) Gaucher Disease: A century of delineation and understanding. Prog. Clin. Biol. Res. 95:1-30.
- Desnick, R. J., Grabowski, G. A., Dinur, T., Fabbro, D., Goldblatt, J. and Gatt, S. (1982) Gaucher Disease: A membranous enzymopathy. Prog. Clin. Biol. Res. 97:193-215.
- Dittmer, J. C. and Lester, R. L. (1964) A simple, specific spray for the detection of phospholipids on thin-layer chromatograms. J. Lipid Res. 5:126-127.
- Esko, J. D. and Raetz, C. R. H. (1983) Synthesis of phospholipids in animal cells. In The Enzymes. P. D. Boyer, Ed. Vol. XVI, 3rd ed. New York: Academic Press, pp. 207-253.

- Farias, R. N., Bloj, B., Morero, R. D., Sineriz, F. and Trucco, R. E. (1975) Regulation of allosteric membrane-bound enzymes through changes in membrane lipid composition. Biochim. Biophys. Acta 415:231-251.
- Fewster, M. E., Burns, B. J. and Mead, J. F. (1969) Quantitative densitometric thin-layer chromatography of lipids using copper acetate reagent. J. Chromatogr. 43:120-126.
- Fuchs, P., Parola, A., Robbins, P. W. and Blout, E. R. (1975) Fluorescence polarization and viscosities of membrane lipids of 3T3 cells. Proc. Natl. Acad. Sci. U.S.A. 72:3351-3354.
- Gatt, S., Dinur, T. and Desnick, R. J. (1982) Studies on human acid β -glucosidase and the nature of the molecular defect in type 1 Ashkenazi Gaucher Disease. Prog. Clin. Biol. Res. 95: 315-331.
- Gilmore, R., Cohn, N. and Glaser, M. (1979a) Fluidity of LM cell membranes with modified lipid compositions as determined with 1,6-diphenyl-1,3,5-hexatriene. Biochemistry 18:1042-1049.
- Gilmore, R., Cohn, N. and Glaser, M. (1979b) Rotational relaxation times of 1,6-diphenyl-1,3,5-hexatriene in phospholipids isolated from LM cell membranes. Effects of phospholipid polar head-group and fatty acid composition. Biochemistry 18: 1050-1056.
- Ginns, E. I., Brady, R. O., Pirruccello, S., Moore, C., Sorrell, S., Furbish, F. S., Murray, G. J., Tager, J. and Barranger, J. A. (1982) Mutations of glucocerebrosidase: Discrimination of neurologic and non-neurologic phenotypes of Gaucher's Disease. Proc. Natl. Acad. Sci. U.S.A. 79:5607-5610.
- Ginns, E. I., Tegelaers, F. P. W., Barneveld, R., Galjaard, H., Reuser, A. J. J., Brady, R. O., Tager, J. M. and Barranger, J. A. (1983) Determination of Gaucher's Disease phenotypes with monoclonal antibody. Clin. Chim. Acta 131:283-287.
- Golan, D. E., Alecio, M. R., Veatch, W. R. and Rando, R. R. (1984) Lateral mobility of phospholipid and cholesterol in the human erythrocyte membrane: Effects of protein-lipid interactions. Biochemistry 23:332-339.
- Goldstein, J. L., Dana, S. E., Faust, J. R., Beaudet, A. L. and Brown, M. S. (1975) Role of lysosomal acid lipase in the metabolism of plasma low density lipoprotein. Observations in cultured fibroblasts from a patient with Cholesteryl Ester Storage Disease. J. Biol. Chem. 256:8487-8495.

- Goppelt, M. and Resch, K. (1984) Densitometric quantitation of individual phospholipids from natural sources separated by one-dimensional thin-layer chromatography. Anal. Biochem. 140: 152-156.
- Grant, C. W. M. (1983) Lateral phase separations and the cell membrane. In Membrane Fluidity in Biology. R. C. Aloia, Ed. Vol. 2. New York: Academic Press, pp. 131-150.
- Grunberger, D., Haimovitz, R. and Shinitzky, M. (1982) Resolution of plasma membrane lipid fluidity in intact cells labelled with diphenylhexatriene. Biochim. Biophys. Acta 688:764-774.
- Haggerty, D. F., Kalra, V. K., Popjak, G., Reynolds, E. E. and Chiappelli, F. (1978) Fluorescence-polarization measurements on normal and mutant human skin fibroblasts. Arch. Biochem. Biophys. 181:51-62.
- Hartree, E. F. (1972) Determination of protein: A modification of the Lowry method that gives a linear response. Anal. Biochem. 48:422-427.
- Herring, F. G., Tatischeff, I. and Weeks, G. (1980) The fluidity of plasma membranes of Dictyostelium discoideum. The effects of polyunsaturated fatty acid incorporation assessed by fluorescence depolarization and electron paramagnetic resonance. Biochim. Biophys. Acta 602:1-9.
- Hildenbrand, K. and Nicolau, C. (1979) Nanosecond fluorescence anisotropy decay of 1,6-diphenyl-1,3,5-hexatriene in membranes. Biochim. Biophys. Acta 553:365-377.
- Ho, M. W. and O'Brien, J. S. (1971) Gaucher's Disease: Deficiency of "acid" β -glucosidase and reconstitution of enzyme activity in vitro. Proc. Natl. Acad. Sci. U.S.A. 68:2810-2813.
- Holman, R. T. and Hofstetter, H. H. (1965) The fatty acid composition of the lipids from bovine and porcine reproductive tissues. J.A.O.C.S. 42:540-544.
- Houslay, M. D. and Stanley, K. K. (1982) Dynamics of Biological Membranes. Influence on Synthesis, Structure and Function. New York: John Wiley and Sons.
- Jain, M. K. and Wagner, R. C. (1980) Introduction to Biological Membranes. New York: John Wiley and Sons, pp. 78-81.
- Kannagi, R., Nudelman, E. and Hakomori, S.-I. (1982) Possible role of ceramide in defining structure and function of membrane glycolipids. Proc. Natl. Acad. Sci. U.S.A. 79:3470-3474.

- Kawato, S., Kinoshita, K., Jr. and Ikegami, A. (1977) Dynamic structure of lipid bilayers studied by nanosecond fluorescence techniques. Biochemistry 16:2319-2324.
- Kawato, S., Kinoshita, K., Jr. and Ikegami, A. (1978) Effect of cholesterol on the molecular motion in the hydrocarbon region of lecithin bilayers studied by nanosecond fluorescence techniques. Biochemistry 17:5026-5031.
- Kinoshita, K., Jr., Kawato, S., and Ikegami, A. (1977) A theory of fluorescence polarization decay in membranes. Biophys. J. 20:289-305.
- Kitajima, Y. and Thompson, G. A., Jr. (1977) Self-regulation of membrane fluidity. The effects of saturated normal and methoxy fatty acid supplementation on Tetrahymena membrane physical properties and lipid composition. Biochim. Biophys. Acta 468:73-80.
- Kudoh, T., Velkoff, M. A. and Wenger, D. A. (1983) Uptake and metabolism of radioactively labeled sphingomyelin in cultured skin fibroblasts from controls and patients with Niemann-Pick Disease and other lysosomal diseases. Biochim. Biophys. Acta 754:82-92.
- Kudoh, T. and Wenger, D. A. (1982) Diagnosis of metachromatic leukodystrophy, Krabbe Disease, and Farber Disease after uptake of fatty acid-labeled cerebroside sulfate into cultured skin fibroblasts. J. Clin. Invest. 70:89-97.
- Kuske, T. T. and Rosenberg (1972) Quantity and fatty acyl composition of the glycosphingolipids of Gaucher spleen. J. Lab. Clin. Med. 80:523-529.
- Ladbrooke, B. D., Williams, R. M. and Chapman, D. (1968) Studies on lecithin-cholesterol-water interactions by differential scanning calorimetry and x-ray diffraction. Biochim. Biophys. Acta 150:333-340.
- Lakowicz, J. R. and Sheppard, J. R. (1981) Fluorescence spectroscopic studies of Huntington fibroblast membranes. Am. J. Hum. Genet. 33:155-165.
- Lentz, B. R., Barenholz, Y. and Thompson, T. E. (1976a) Fluorescence depolarization studies of phase transitions and fluidity in phospholipid bilayers. I. Single component phosphatidylcholine liposomes. Biochemistry 15:4521-4528.

- Lentz, B. R., Barenholz, Y. and Thompson, T. E. (1976b) Fluorescence depolarization studies of phase transitions and fluidity in phospholipid bilayers. 2. Two-component phosphatidylcholine liposomes. Biochemistry 15:4529-4537.
- Macala, L. J., Yu, R. K. and Ando, S. (1983) Analysis of brain lipids by high performance thin-layer chromatography and densitometry. J. Lipid Res. 24:1243-1250.
- Malkiewicz-Wasowicz, B., Gamst, O. and Stromme, J. H. (1977) The influence of changes in the phospholipid pattern of intact fibroblasts on the activities of four membrane-bound enzymes. 482:358-369.
- Morrison, W. R. and Smith, L. M. (1964) Preparation of fatty acid methyl esters and dimethylacetals from lipids with boron fluoride-methanol. J. Lipid Res. 5:600-608.
- Mueller, O. T. and Rosenberg, A. (1977) β -glucoside hydrolase activity of normal and glucosylceramidotic cultured human skin fibroblasts. J. Biol. Chem. 252:825-829.
- Mueller, O. T. and Rosenberg, A. (1979) Activation of membrane-bound glucosylceramide: β -glucosidase in fibroblasts cultured from normal and glucosylceramidotic human skin. J. Biol. Chem. 254:3521-3525.
- Nagatomo, T., Sasaki, M. and Konishi, T. (1984) Differences in lipid composition and fluidity of cardiac sarcolemma prepared from newborn and adult rabbits. Biochem. Med. 32:122-131.
- Nagy, K., Simon, P. and Zs.-Nagy, I. (1983) Spin label studies on synaptosomal membranes of rat brain cortex during aging. Biochem. Biophys. Res. Commun. 117:688-694.
- Neufeld, N. D. and Corbo, L. M. (1984) Membrane fluid properties of cord blood mononuclear leukocytes: Association with increased insulin receptors. Pediatr. Res. 18:773-778.
- Nilsson, O. and Svennerholm, L. (1982) Accumulation of glucosylceramide and glycosylsphingosine (psychosine) in cerebrum and cerebellum in infantile and juvenile Gaucher Disease. J. Neurochem. 39:709-718.
- Oldfield, E. and Chapman, D. (1972) Dynamics of lipids in membranes: Heterogeneity and the role of cholesterol. FEBS Letters 23: 285-297.
- Owen, J. S., Bruckdorfer, K. R., Day, R. C. and McIntyre, N. (1982) Decreased erythrocyte membrane fluidity and altered lipid composition in human liver disease. J. Lipid Res. 23:124-132.

- Pagano, R. E., Ozato, K. and Ruysschaert, J.-M. (1977) Intracellular distribution of lipophilic fluorescent probes in mammalian cells. Biochim. Biophys. Acta 465:661-666.
- Patton, S. (1970) Correlative relationship of cholesterol and sphingomyelin in cell membranes. J. Theor. Biol. 29:489-491.
- Peters, S. P., Coyle, P., Coffee, C. J., Glew, R. H., Kuhlenschmidt, M. S., Rosenfeld, L. and Lee, Y. C. (1977) Purification and properties of a heat-stable glucocerebrosidase activating factor from control and Gaucher spleen. J. Biol. Chem. 252: 563-573.
- Pottel, H., Van der Meer, W. and Herreman, W. (1983) Correlation between the order parameter and the steady-state fluorescence anisotropy of 1,6-diphenyl-1,3,5-hexatriene and an evaluation of membrane fluidity. Biochim. Biophys. Acta 730:181-186.
- Rao, B. G. and Spence, M. W. (1977) Niemann-Pick Disease Type D: Lipid analyses and studies on sphingomyelinases. Ann. Neurol. 1:385-392.
- Rappeport, J. M. and Ginns, E. I. (1984) Bone-marrow transplantation in severe Gaucher's Disease. N. Engl. J. Med. 311:84-88.
- Saito, M., Mueller, O. T. and Rosenberg, A. (1982) Multiple forms of human skin fibroblast β -glucosidase and their activation by fibroblast monosialoglycosphingolipids. Prog. Clin. Biol. Res. 95:385-403.
- Saito, M. and Rosenberg, A. (1982) Glycolipids and their developmental patterns in chick thigh and leg muscles. J. Lipid Res. 23:3-8.
- Saito, M. and Rosenberg, A. (1984a) The fate of glucosyl ceramide (glucocerebroside) in genetically impaired (lysosomal - glucosidase deficient) Gaucher Disease diploid human fibroblasts. Submitted for publication.
- Saito, M. and Rosenberg, A. (1984b) Unpublished observations.
- Saito, M., Saito, M. and Rosenberg, A. (1984) Action of monesin, a monovalent cationophore, on cultured human fibroblasts: Evidence that it induces high cellular accumulation of glucosyl- and lactosylceramide (gluco- and lactocerebroside). Biochemistry 23:1043-1046.
- Schmitz, G., Assmann, G. and Bowyer, D. E. (1984) A quantitative densitometric method for the rapid separation and quantitation of the major tissue and lipoprotein lipids by high-performance thin-layer chromatography. J. Chromatogr. 307:65-79.

- Schmitz, G., Jabs, H.-U. and Assmann, G. (1983) Densitometry of phosphatidylcholine and sphingomyelin in high-density lipoproteins. Clin. Chem. 29:1435-1437.
- Schroeder, F. (1978) Isothermal regulation of membrane fluidity in murine fibroblasts with altered phospholipid polar head group. Biochim. Biophys. Acta 511:356-376.
- Schroeder, F., Goetz, I. E. and Roberts, E. (1984) Membrane anomalies in Huntington's Disease fibroblasts. J. Neurochem. 43:526-539.
- Seelig, A. and Seelig, J. (1977) Effect of a single cis double bond on the structure of a phospholipid bilayer. Biochemistry 16:45-50.
- Selvam, R. and Radin, N. (1981) Quantitation of lipids by charring on thin-layer plates and scintillation quenching: Application to ceramide determination. Anal. Biochem. 112:338-345.
- Shafit-Zagardo, B., Devine, E. A. and Desnick, R. J. (1980) Electrophoretic separation of neutral and acid β -glucosidase isozymes in human tissues. Biochim. Biophys. Acta 614:459-65.
- Shafit-Zagardo, B., Devine, E. A., Smith, M., Arredondo-Vega, F. and Desnick, R. J. (1981) Assignment of the gene for acid β -glucosidase to human chromosome 1. Am. J. Hum. Genet. 33:564-575.
- Shaw, J. M., Henry, J. E., Shaw, K. V., and Konigsberg, I. R. (1983) Order measurements in plasma membranes from duchenne dystrophy fibroblasts. Biochim. Biophys. Acta 733:1-14.
- Shiga, T., Maeda, N., Suda, T., Kon, K. and Sekiya, M. (1979) The decreased membrane fluidity of in vivo aged, human erythrocytes. A spin label study. Biochim. Biophys. Acta 553:84-95.
- Shinitzky, M. and Barenholz, Y. (1974) Dynamics of the hydrocarbon layer in liposomes of lecithin and sphingomyelin containing dicetylphosphate. J. Biol. Chem. 249:2652-2654.
- Shinitzky, M. and Barenholz, Y. (1978) Fluidity parameters of lipid regions determined by fluorescence polarization. Biochim. Biophys. Acta 515:367-394.
- Shinitzky, M. and Inbar, M. (1974) Difference in microviscosity induced by different cholesterol levels in the surface membrane lipid layer of normal lymphocytes and malignant lymphoma cells. J. Mol. Biol. 85:603-615.

- Shinitzky, M. and Inbar, M. (1976) Microviscosity parameters and protein mobility in biological membranes. Biochim. Biophys. Acta 433:133-149.
- Shinitzky, M. and Yuli, I. (1982) Lipid fluidity at the submacroscopic level: Determination by fluorescence polarization. Chem. Phys. Lipids 30:261-282.
- Smith, R. L. and Oldfield, E. (1984) Dynamic structure of membranes by deuterium NMR. Science 225:280-288.
- Spence, M. W., Clarke, J. T. R. and Cook, H. W. (1983) Pathways of sphingomyelin metabolism in cultured fibroblasts from normal and sphingomyelin lipidosi subjects. J. Biol. Chem. 258: 8595-8600.
- Spiegel, S., Schlessinger, J. and Fishman, P. H. (1984) Incorporation of fluorescent gangliosides into human fibroblasts: Mobility, fate, and interaction with fibronectin. J. Cell Biol. 99: 699-704.
- Stubbs, C. D. (1983) Membrane fluidity: Structure and dynamics of membrane lipids. Essays in Biochem. 19:1-39.
- Stubbs, C. D., Tsang, W. M., Belin, J., Smith, A. D. and Johnson, S. M. (1980) Incubation of exogenous fatty acids with lymphocytes. Changes in fatty acid composition and effects on the rotational relaxation time of 1,6-diphenyl-1,3,5-hexatriene. Biochemistry 19:2756-2762.
- Stubbs, C. D., Kinoshita, K., Jr., Munkonge, F., Quinn, P. J. and Ikegami, A. (1984) The dynamics of lipid motion in sarcoplasmic reticulum membranes determined by steady-state and time resolved fluorescence measurements on 1,6-diphenyl-1,3,5-hexatriene and related molecules. Biochim. Biophys. Acta 775:374-380.
- Stubbs, C. D. and Smith, A. D. (1984) The modification of mammalian membrane polyunsaturated fatty acid composition in relation to membrane fluidity and function. Biochim. Biophys. Acta 779:89-137.
- Sudo, M. (1977) Brain glycolipids in infantile Gaucher's Disease. J. Neurochem. 29:379-381.
- Sutrina, S. L. and Chen, W. W. (1984) Lysosomal involvement in cellular turnover of plasma membrane sphingomyelin. Biochim. Biophys. Acta 793:169-179.

- Suzuki, K. (1982) Glucosylceramide and related compounds in normal tissues and in Gaucher Disease. Prog. Clin. Biol. Res. 95: 219-230.
- Suzuki, K. and Suzuki, Y. (1983) Galactoceramide lipidosis: Globoid cell leukodystrophy (Krabbe's Disease). In The Metabolic Basis of Inherited Disease. J. B. Stanbury, J. B. Wyngaarden, D. S. Fredrickson, J. L. Goldstein, and M. S. Brown, Eds. 5th ed. New York: McGraw-Hill, pp. 842-856.
- Svennerholm, L., Dreborg, S., Erikson, A., Groth, C. G., Hillborg, P. O., Hakansson, G., Nilsson, O. and Tibblin, E. (1982) Gaucher Disease of the Norrbottnian Type (type III). Phenotypic manifestations. Prog. Clin. Biol. Res. 95:67-94.
- Tartakoff, A. M. (1983) Perturbation of vesicular traffic with the carboxylic ionophore monensin. Cell 32: 1026-1028.
- Thulburn, K. R. (1981) The use of N-(9-anthroyloxy) fatty acids as fluorescent probes for biomembranes. In Fluorescent Probes. G. S. Beddard and M. A. West, Eds. New York: Academic Press, pp. 113-141.
- Vaccaro, A. M., Muscillo, M. and Suzuki, K. (1983) Effect of hydrogenation of glucosyl- and galactoceramide on their enzymatic hydrolysis. Clin. Chim. Acta 131:1-13.
- Van Blitterswijk, W. J., Emmelot, P., Hilkmann, H. A. M., Oomenmeulemans, E. P. M. and Inbar, M. (1977) Differences in lipid fluidity among isolated plasma membranes of normal and leukemic lymphocytes and membranes exfoliated from their cell surface. Biochim. Biophys. Acta 467:309-320.
- Van Blitterswijk, W. J., Van Hoeven, R. P. and Van der Meer, B. W. (1981) Lipid structural order parameters (reciprocal of fluidity) in biomembranes derived from steady-state fluorescence polarization measurements. Biochim. Biophys. Acta 644: 323-332.
- Van Hoeven, R. P., Van Blitterswijk, W. J. and Emmelot, P. (1979) Fluorescence polarization measurements on normal and tumour cells and their corresponding plasma membranes. Biochim. Biophys. Acta 551:44-54.
- Vance, D. E., Krivit, W. and Sweeley, C. C. (1969) Concentrations of glucosyl ceramides in plasma and red cells in Fabry's Disease, a glycolipid lipidosis. J. Lipid Res. 10:188-192.
- Warren, K. R., Schafer, I. A., Sullivan, J. C., Petrelli, M. and Radin, N. S. (1976) The effects of N-hexyl-O-glucosyl sphingo-

sine on normal cultured human fibroblasts: A chemical model for Gaucher's Disease. J. Lipid Res. 17:132-138.

Wenger, D. A. and Olson, G. C. (1981) Heterogeneity in Gaucher Disease. In Lysosomes and Lysosomal Storage Diseases. J. W. Callahan and J. A. Lowden, Eds. New York: Raven Press, pp. 157-171.

Zanetta, J. P., Breckenridge, W. C. and Vincendon, G. (1972) Analysis of monosaccharides by gas-liquid chromatography of the O-methyl glycosides as trifluoroacetate derivatives. Application to glycoproteins and glycolipids. J. Chromatogr. 69:291-304.

Zannoni, C., Arcioni, A., and Cavatorta, P. (1983) Fluorescence depolarization in liquid crystals and membrane bilayers. Chem. Phys. Lipids 32:179-250.

APPROVAL SHEET

The dissertation submitted by Ravi Salgia has been read and approved by the following committee:

Abraham Rosenberg, Ph.D., Director
Professor, Biochemistry and Biophysics and Director
of the Division of Developmental and Pathological
Neurochemistry
Loyola University Stritch School of Medicine

Glyn Dawson, Ph.D.
Professor, Pediatrics and Biochemistry
University of Chicago

Allen Frankfater, Ph.D.
Associate Professor, Biochemistry and Biophysics
Loyola University Stritch School of Medicine

Robert G. Kemp, Ph.D.
Professor and Chairman, Biological Chemistry and Structure
Chicago Medical School

Mariko Saito, Ph.D.
Instructor, Biochemistry and Biophysics and Surgery
Loyola University Stritch School of Medicine

The final copies have been examined by the director of the dissertation and the signature which appears below verifies the fact that any necessary changes have been incorporated and that the dissertation is now given final approval by the Committee with reference to content and form.

The dissertation is therefore accepted in partial fulfillment of the requirements for the degree of Doctor of Philosophy.

March 15, 1985
Date

Abraham Rosenberg
Director's Signature